Mathematisches Forschungsinstitut Oberwolfach

Report No. 09/2012

DOI: 10.4171/OWR/2012/09

Advanced Computational Engineering

Organised by
Olivier Allix, Cachan
Carsten Carstensen, Berlin
Jörg Schröder, Essen
Peter Wriggers, Hannover

February 12th – February 18th, 2012

Abstract. The finite element method is the established simulation tool for the numerical solution of partial differential equations in many engineering problems with many mathematical developments such as mixed finite element methods (FEMs) and other nonstandard FEMs like least-squares, nonconforming, and discontinuous Galerkin (dG) FEMs. Various aspects on this plus related topics ranging from order-reduction methods to isogeometric analysis has been discussed amongst the pariticpants form mathematics and engineering for a large range of applications.

Mathematics Subject Classification (2000): 46N40, 65L60, 65M60, 65N30, 73V05, 74S05, 76M10.

Introduction by the Organisers

The finite element method is now an established simulation tool for the solution of partial differential equations that are related to the models in many engineering problems. It has an enormous range of applicability including elasticity, visco-elasto-plasticity, contact, fluid mechanics, heat conduction, acoustics, and electromagnetism. As the range of applications has grown it has become increasingly apparent that special features of each model can be exploited to improve the performance and robustness of the finite element method (FEM). This has led to many mathematically interesting developments including mixed FEMs and other nonstandard FEMs like least-squares, non-conforming, and discontinuous Galerkin (dG) FEMs. Their use often aims at improved or robust discretizations that are superior to standard FEMs in many numerical simulations in solid, structural, and fluid mechanics and electromagnetics.

Discontinuous Galerkin (dG) schemes are more flexible than standard finite element formulations. Here the trial and test functions are piecewise polynomial functions that are not required to be continuous across element boundaries which leads to an increase in the number of unknowns. Nonetheless the extra flexibility can be advantageous for up-winding, for adaptivity, for overcoming locking, and for the design of simple schemes for fourth order problems. At present, the convergence analysis for dG FEMs has been carried out for simple model problems, but the corresponding analysis for more complicated problems was in the focus of the discussion amongst the participants. This was shown in recent results reported by Jay Gopalakrishnan who discussed a discrete inf-sup condition and showed superb applications to wave propagation in heterogeneous materials. Antonio Huerta made a comparative study of continuous and discountinuous Galerkin formulations that lead to some surprising results and thus proved the urge of further research in this area. Furthermore Eun-Jae Park gave an overview on the latest developments on hybrid dG and mixed FEM for problems with multiple scales.

While edge elements have proved very useful in electromagnetics applications, it was shown that they can also be applied to elasticity and flow problems using special weak forms. this was discussed in depth in the presentation by Joachim Schöberl who reviewed new classes of elements for elasticity and flow problems based on *curl* and *div div* spaces. This generated great interest, especially, since the related discretization schemes are accompanied by fast iterative solvers. Nevertheless significant questions remain about the best choice of elements and penalty parameters, a posteriori estimates and the robustness of the various schemes to non-conforming mesh adaptation.

Besides principle applications and the empirical investigation of the performance in practical real-life applications, the mathematical understanding of the non-standard FEMs was progressed during the meeting. Mira Schedensack presented comparison results which complemented earlier work by Dietrich Braess. For the simplest model problem, three different FEMs are equivalent in their performance up to multiplicative constants and up to data oscillations. Dietmar Gallistl discussed the optimality of adaptive mesh-refining strategies for the Stokes equations using a pseudo-stress formulation, while Hella Rabus pointed out the robustness in the optimality of non-conforming adaptive FEMs in elasticity; all three were Leibniz fellows. Finally, Thirupathi Gudi illustrated the medius analysis for fourth-order plate problems with mathematical arguments from the a priori and a posteriori error analysis.

In the whole it was impressive to note how much mixed finite element technologies have recently progressed by combining the deep knowledge of the properties of the mathematical spaces with technological aspects such as e.g. integration rules and element shapes.

The application of conforming and non-conforming mixed FEMs to finite strain problems with hyperelastic materials were discussed by Ferdinando Aurricchio. He illustrated many challenges related to the design of finite element spaces in

combination with different incompressibility conditions. This has stressed pratical and mathematical challenges that constitute problems with non unique solutions.

Isogeometric analysis has gained interest over the last years since it opens up the possibility to go directly from CAD models to the analysis phase. Besides the classical NURBS based interpolations, new formulations with T-Splines and other mesh coupling techniques were explored in the talks by Robert L. Taylor and Yuri Bashilevs. Especially the application to fluid-structure interaction problems of wind turbines generated interest since this coupled modern discretizations techniques with the dynamics solution of large systems based on moving meshes. Besides being a promising new technology for science and engineering numerical simulation, the new method carries a rich mathematical structure still to be explored. Those presentations along with the one of Wolfgang Wall have documented the interest of using non-standard meshes in real industrial applications. It has been clear during the discussion that progresses in this hot topic of non-conforming meshes (precision, stability, optimality) can be made by merging the knowledge of the mathematical community with the one of the engineering science community.

Least-squares FEMs offer in general some advantages compared to other variational methods, such as, for instance, the inherent ellipticity of the governing functional or an a posteriori error estimator without additional costs. Even for equations with non-selfadjoint operators, the procedure leads to a symmetric and positive definite algebraic system, which can be solved efficiently with iterative solution strategies. Recent developments related to large strain models for hyperelastic materials were discussed for example in the talk by Alexander Schwarz. Those results can be generalized to even more complex physically nonlinear continuum mechanical problems; as e.g. quasi-incompressibility, elasto-viscoplasticity and anisotropic elasticity.

In a variety of complex applications, the discretization of the underlying boundary value problem could lead to several 100 million of unknowns. With todays demands to solve such problems in industrial and medical environments in real-time computing, one has to design reduced models for the design of process control algorithms and for the numerical simulation of processes with uncertainties. The scientific challenge is to simplify the model in such a way that certain modeling aspects are accurately described while non-relevant aspects are neglected. The question of modeling error and of output of interest are at the heart of reduction method and of progresses in uncertainty quantification. The later aspect has been particularly clear in the talk of Michael Ortiz. The certification of computation with guaranteed bounds in an uncertain context is one future topic of highest relevance in advanced engineering computation.

While there are established methods of order-reduction available in some fields (like e.g. proper orthogonal decomposition (POD) or singular value decomposition (SVD), reduced basis (RB) techniques, and Craig-Bampton methods in structural dynamics or model order reduction in differential equation systems), there exist only a very limited amount of methodologies that can be employed in order to reduce nonlinear or multi-scale problems. The lectures by Pierre Ladeveze

addressed the proper generalized decomposition (PGD) method that has advantages in engineering application and that can be combined with error analysis for domain decomposition methods. Some of the modeling approaches include multiscale models and uncertainty quantification procedures. Daniel Peterseim could provide a new analysis technique for up and down scaling effective for applications even without scale separation. All those different approaches were discussed vividly during the breaks and in the evenings. Other new methods emerge from the need to do real-time computations e.g. in computer assisted surgery, where Here Stefanie Reese and Adrien Leygue provided new insights. Especially the presentation by Adrien Leygue showed how to combine off-line with on-line computations in order to achieve real-time analysis tools. This was demonstrated by an impressive deformation analysis of a liver. Nevertheless these techniques are still in their beginnings but will open up new possibilities for many engineering and medical applications.

The interaction of mathematicians and engineers was extremely fruitful and provided definitions of new research directions. This workshop on Advanced Computational Engineering clearly demonstrated that the field is very active and currently enjoys great progress with many new important results. It became transparent during the workshop that new non-standard FEMs with higher-order approximations and a huge range of different partial differential equations have a large potential for future work. The improvement of sharp bounds for error control within adaptive methods, mathematical stability conditions – for example the nonlinear counterpart of the inf-sup condition – lead to valuable discussion amongst the participants from the different mathematical and engineering disciplines.

Workshop: Advanced Computational Engineering

Table of Contents

Abstracts

Advances in discontinuous Petrov Galerkin methods

Jay Gopalakrishnan
(joint work with Leszek Demkowicz)

This report summarizes a few recent developments in the construction and analysis of DPG (discontinuous Petrov Galerkin) methods.

To describe the DPG method in the abstract, suppose we want to approximate $u \in U$ satisfying $b(u, v) = l(v)$ for all $v \in V$. Here U is a reflexive Banach space and V is a Hilbert space under an inner product $(\cdot, \cdot)_V$, both over $\mathbb{R}$, and the forms $b(\cdot, \cdot) : U \times V \mapsto \mathbb{R}$ and $l(\cdot) : V \mapsto \mathbb{R}$ are continuous. Let $U_h \subset U$ be a finite dimensional trial subspace (where h denotes a parameter determining the finite dimension). The DPG method finds an approximate solution u_h in U_h satisfying

$$b(u_h, v) = l(v), \quad \forall v \in V_h, \tag{1}$$

where $V_h = T(U_h)$ and $T : U \mapsto V$ is defined by

$$(Tw, v)_V = b(w, v), \qquad \forall v \in V. \tag{2}$$

The test functions of the form Tw are called "optimal test functions" [6] because they attain the supremum in an inf-sup condition. These methods are interesting because by design, the discrete inf-sup condition is inherited from the exact inf-sup condition. The concept of optimal test functions resurfaces from time to time in the literature, in different forms and names, e.g., [1, 9, 13] (and also [12], as was pointed out in this workshop). Another viewpoint to understand (1) is to interpret it as a least squares Galerkin method [2] in a non-standard inner product, which points to further avenues to connect to older literature. Notwithstanding these relationships at the abstract level, the novelty in our approach is the use of a DG framework to *locally* compute the optimal test functions.

To explain this further, let us first note that the main drawback of methods of the form (1) is that it is not easy to apply the operator T in most standard variational formulations. However, for a few one-dimensional problems, and a two-dimensional linear advection problem, it is possible to calculate T in closed form, as shown in [5, 6]. The remarkable stability properties of the resulting methods motivated our further research into such methods. But it turned out to be difficult or impossible to calculate T in closed form for many physically important problems, so we abandoned this avenue for generalizations. The further development of DPG methods stemmed from the observation that in certain 'ultraweak' variational formulations, the operator T becomes local. For instance, consider a formulation with a test space V consisting of functions with continuity constraints across mesh element interfaces. It can often be reformulated, by hybridization, to yield a test space of discontinuous functions with no inter-element continuity constraints, yielding an 'ultraweak' formulation. Then, the computation of T in (2) can proceed

element by element. Although this was noticed in [6], the resulting methods were not mathematically understood completely until [7].

DPG methods based on such ultraweak formulations were developed for acoustic wave propagation in [10] and for linear elasticity in [3]. In the former [10], we found, numerically, that the method exhibits negligible phase errors (otherwise known as pollution errors) even in the lowest order case. Theoretically, we are able to prove [10] error estimates that explicitly show the dependencies with respect to the wavenumber ω, the mesh size h, and the polynomial degree p. But the current state of the theory does not fully explain the remarkably good numerical phase errors. In the latter [3], we presented two new methods for linear elasticity that simultaneously yield stress and displacement approximations of optimal accuracy in both the mesh size h and polynomial degree p. Locking-free convergence properties were established. While existing mixed methods for linear elasticity require very rich stress spaces to ensure the discrete inf-sup condition, within the DPG framework the discrete inf-sup condition is automatically obtained for any U_h. This provides a wide array of simple stress elements with corresponding stable test spaces.

A further development concerns an essential practical approximation made in implementation of DPG methods. Even if the DPG approach yields a local T, calculable element-by-element, a glance at (2) shows that an infinite dimensional problem on each mesh element needs to be solved to apply T. In practical computations, T is approximated using polynomials of some degree $r > p$ on each mesh element, where p is the degree of trial polynomials spaces. In [11], we showed that such an approximation of T does not destroy optimal convergence rates, provided that $r \geq p + N$, where N is the space dimension (two or more), for certain elliptic equations.

Among other interesting recent developments, we note [8] which proves robustness in convection-dominated diffusion, and [4] which gives a unified derivation of DPG methods for general Friedrichs' systems. More work is needed to address the gap between theoretical predictions and practical observations, especially in wave propagation. Unexploited opportunities may also lie in the design of efficient solvers using the Hermitian positive definite nature of the systems that result from DPG discretizations.

References

[1] I. Babuška, G. Caloz, and J. E. Osborn. Special finite element methods for a class of second order elliptic problems with rough coefficients. *SIAM J. Numer. Anal.*, 31(4):945–981, 1994.

[2] J. H. Bramble, R. D. Lazarov, and J. E. Pasciak. A least-squares approach based on a discrete minus one inner product for first order systems. *Math. Comp.*, 66(219):935–955, 1997.

[3] J. Bramwell, L. Demkowicz, J. Gopalakrishnan, and W. Qiu. A locking-free *hp* DPG method for linear elasticity with symmetric stresses. *Submitted*, 2011.

[4] T. Bui-Thanh, L. Demkowicz and O. Ghattas. A Unified Discontinuous Petrov-Galerkin Method and its Analysis for Friedrichs' Systems, (submitted) 2012.

[5] L. Demkowicz and J. Gopalakrishnan. A class of discontinuous Petrov-Galerkin methods. Part I: The transport equation. *Computer Methods in Applied Mechanics and Engineering*, 199:1558–1572, 2010.
[6] L. Demkowicz and J. Gopalakrishnan. A class of discontinuous Petrov-Galerkin methods. Part II: Optimal test functions. *Numerical Methods for Partial Differential Equations*, 27(1):70–105, 2011.
[7] L. Demkowicz and J. Gopalakrishnan. Analysis of the DPG method for the Poisson equation. *SIAM J Numer. Anal.*, 49(5):1788–1809, 2011.
[8] L. Demkowicz and N. Heuer, Robust DPG Method for Convection-Dominated Diffusion Problems (submitted to SIAM J. Num. Anal.) 2012.
[9] L. Demkowicz and J. T. Oden, *An adaptive characteristic Petrov-Galerkin finite element method for convection-dominated linear and nonlinear parabolic problems in one space variable*, J. Comput. Phys., 67 (1986), pp. 188–213.
[10] L. Demkowicz, J. Gopalakrishnan, I. Muga, and J. Zitelli. Wavenumber explicit analysis for a DPG method for the multidimensional Helmholtz equation. *Computer Methods in Applied Mechanics and Engineering*, 213-216:126–138, March 2012.
[11] J. Gopalakrishnan and W. Qiu. An analysis of the practical DPG method. *Submitted*, 2011.
[12] M. Ortiz. A variational formulation for convection-diffusion problems. *Internat. J. Engrg. Sci.*, 23(7):717–731, 1985.
[13] W. Wendland, *On Galerkin methods*, in Proceedings of ICIAM 95, vol. 76 (Supplement 2), Muhlenstrasse 33-34, D-13187 Berlin, Germany, 1996, Akademie-Verlag GMBH, pp. 257–260.

Stress-displacement least squares mixed finite element approximation for hyperelastic materials

Gerhard Starke
(joint work with Benjamin Müller, Alexander Schwarz, Jörg Schröder)

A mixed finite element method for nonlinear elasticity is investigated which is based on the stress-displacement first-order system least squares formulation studied in [3] and [2] for the linear case. Our approach is based on the first-order system

$$\operatorname{div} \mathbf{P} + \mathbf{f} = \mathbf{0}\,, \tag{1}$$

$$\mathbf{P}\mathbf{F}^T - \partial_{\mathbf{F}}\psi(\mathbf{C})\mathbf{F}^T = \mathbf{0}\,, \tag{2}$$

where $\mathbf{f}$ is some external source, $\mathbf{P}$ denotes the first Piola-Kirchhoff stress tensor and $\mathbf{F} = \mathbf{I} + \boldsymbol{\nabla}\mathbf{u}$ stands for the deformation gradient. Moreover, the stored energy function $\psi : \mathbb{R}^{3\times 3}_{\mathrm{sym}} \to \mathbb{R}$ is defined on the space of symmetric matrices and $\mathbf{C} = \mathbf{F}^T\mathbf{F}$ denotes the right Cauchy-Green strain tensor (we also introduce the left Cauchy-Green strain tensor $\mathbf{B} = \mathbf{F}\mathbf{F}^T$ at this point which we will use further below).

As one specific instance of hyperelasticity we consider neo-Hookean materials with a stored energy function of the form

$$\psi(\mathbf{C}) = \frac{\mu}{2}\,\operatorname{tr}\mathbf{C} + \frac{\lambda}{4}\,J^2 - \left(\frac{\lambda}{2} + \mu\right)\ln\,J$$

with $J = \det \mathbf{F}$ and Lamé parameters λ, μ (cf. Ciarlet [4, Sect. 4.10]). For this neo-Hookean stored energy function,

$$\partial_{\mathbf{F}} \psi(\mathbf{C}) \mathbf{F}^T = \mu\, \mathbf{F}\mathbf{F}^T + \left(\frac{\lambda}{2} \left(J^2 - 1\right) - \mu \right) \mathbf{I} =: \mathbf{G}(\mathbf{B})$$

holds, where the mapping $\mathbf{G}(\mathbf{B}) = \mu \mathbf{B} + (\lambda/2\,(\det \mathbf{B} - 1) - \mu)\mathbf{I}$ leaves the subspace of symmetric matrices invariant. For the Gâteaux derivative, a straightforward calculation leads to

$$\mathbf{G}'(\mathbf{B})[\mathbf{E}] = \lim_{s \to 0} \frac{\mathbf{G}(\mathbf{B} + s\mathbf{E}) - \mathbf{G}(\mathbf{B})}{s} = \mu\, \mathbf{E} + \frac{\lambda}{2}\, \det \mathbf{B} (\mathbf{B}^{-T} : \mathbf{E}) \mathbf{I}\,.$$

In particular, $\mathbf{G}'(\mathbf{I})[\mathbf{E}] = \mu\, \mathbf{E} + \lambda/2(\operatorname{tr} \mathbf{E})\mathbf{I}$ recovers the well-known strain-stress relation from linear elasticity.

The first-order system associated with this formulation is given by

$$\mathcal{R}(\mathbf{u}, \mathbf{P}) = \begin{pmatrix} \operatorname{div} \mathbf{P} + \mathbf{f} \\ \mathbf{G}'(\mathbf{I})^{-1/2} (\mathbf{P}\mathbf{F}(\mathbf{u})^T - \mathbf{G}(\mathbf{B}(\mathbf{u}))) \end{pmatrix},$$

where the scaling of the second argument is done in order to obtain uniform results in the incompressible limit analogous to the linear case (cf. [3]). The corresponding least squares formulation consists in finding $\mathbf{u} \in H^1(\Omega)^3$ and $\mathbf{P} \in H(\operatorname{div}, \Omega)^3$ such that

$$\mathcal{F}(\mathbf{u}, \mathbf{P}) = \|\mathcal{R}(\mathbf{u}, \mathbf{P})\|^2_{L^2(\Omega)}$$

is minimized subject to suitable boundary conditions for $\mathbf{u}$ on $\Gamma_D \subset \partial\Omega$ and for $\mathbf{P} \cdot \mathbf{n}$ on $\Gamma_N \subset \partial\Omega$. The solution of this nonlinear least squares problem also satisfies the variational formulation

$$(\mathcal{R}(\mathbf{u}, \mathbf{P}), \mathcal{J}(\mathbf{u}, \mathbf{P})[\mathbf{v}, \mathbf{Q}])_{L^2(\Omega)} = 0$$

for all $\mathbf{u} \in H^1_{\Gamma_D}(\Omega)^3$ and $\mathbf{P} \in H_{\Gamma_N}(\operatorname{div}, \Omega)^3$, where

$$\mathcal{J}(\mathbf{u}, \mathbf{P})[\mathbf{v}, \mathbf{Q}] = \begin{pmatrix} \operatorname{div} \mathbf{Q} \\ G'(\mathbf{I})^{-1/2} (\mathbf{Q}\mathbf{F}(\mathbf{u})^T + \mathbf{P}(\boldsymbol{\nabla}\mathbf{v})^T - \mu(\mathbf{F}(\mathbf{u})(\boldsymbol{\nabla}\mathbf{v})^T + (\boldsymbol{\nabla}\mathbf{v})\mathbf{F}(\mathbf{u})^T) \\ -\lambda\, \det(\mathbf{I} + \boldsymbol{\nabla}\mathbf{u})(\mathbf{Cof}\, (\boldsymbol{\nabla}\mathbf{u}) : \boldsymbol{\nabla}\mathbf{v}))\mathbf{I} \end{pmatrix}$$

denotes the Gateaux derivative of the first-order system operator $\mathcal{R}(\mathbf{u}, \mathbf{P})$. For the behavior of the stress-displacement least squares approach for other nonlinear models in solid mechanics, see also [7] and [6].

We report on a simple numerical experiment illustrating the feasibility of the method. More sophisticated computations involving adaptively refined triangulations will be contained in [5]. Here we study the second problem in [1] where plane strain assumptions are set and a uniform body force $\mathbf{f} = (0, \gamma)$ is applied to the unit square $\Omega = [-1, 1]^2$. As boundary conditions, $\mathbf{u} \cdot \mathbf{n} = 0$ and $(\mathbf{P} \cdot \mathbf{n}) \cdot \mathbf{t} = 0$ on the left, right and bottom are prescribed while the top is held traction-free, i.e., $\mathbf{P} \cdot \mathbf{n} = \mathbf{0}$. The case $\lambda \to \infty$ is investigated (and μ is normalized to 1) which leads to a known exact solution $\mathbf{u} \equiv \mathbf{0}$ and $\mathbf{P}(x_1, x_2) = \gamma(1 - x_2)\mathbf{I}$.

In order to estimate the critical load values where the problem loses its stability and a secondary solution occurs, the smallest eigenvalue of the system matrix $(\mathcal{J}(\mathbf{u}, \mathbf{P})[\boldsymbol{\Phi}_j], \mathcal{J}(\mathbf{u}, \mathbf{P})[\boldsymbol{\Phi}_i])$ is computed. On a triangulation with 2144 elements,

we use standard conforming piecewise quadratic functions for **u** and next-to-lowest order Raviart-Thomas (RT_1) spaces for **P**.

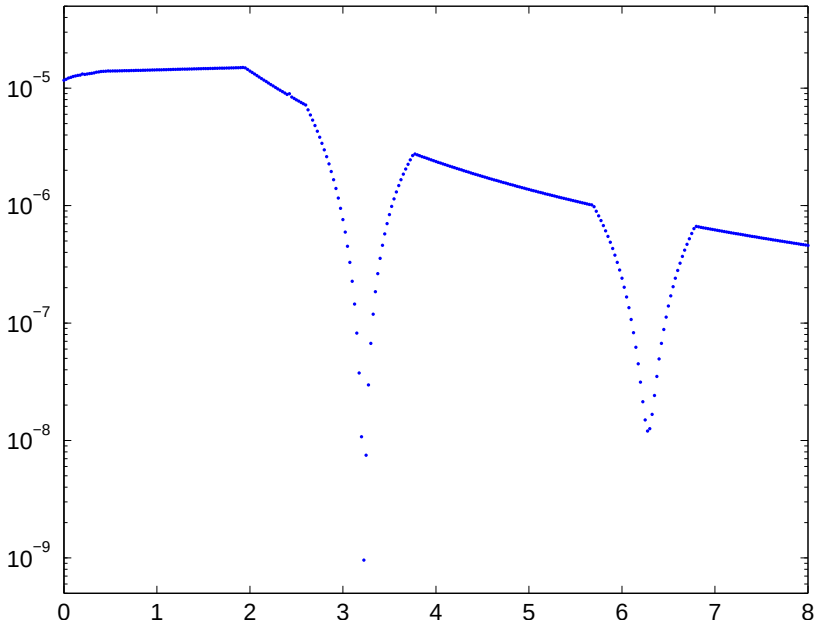

The smallest eigenvalue of the system matrix is plotted (on a logarithmic scale) against the load parameter in the range of 0 to 8 in the figure above. Critical load values are obtained at about $\gamma = 3.23$ in accordance to the results in [1] and again at $\gamma = 6.28$. It is obvious from the graph shown above that the smallest eigenvalue approaches zero at these load values and a one-dimensional null space is approximated. In the figures below the corresponding (near zero) eigenfunctions at $\gamma = 3.23$ (left) and at $\gamma = 6.28$ (right) are shown.

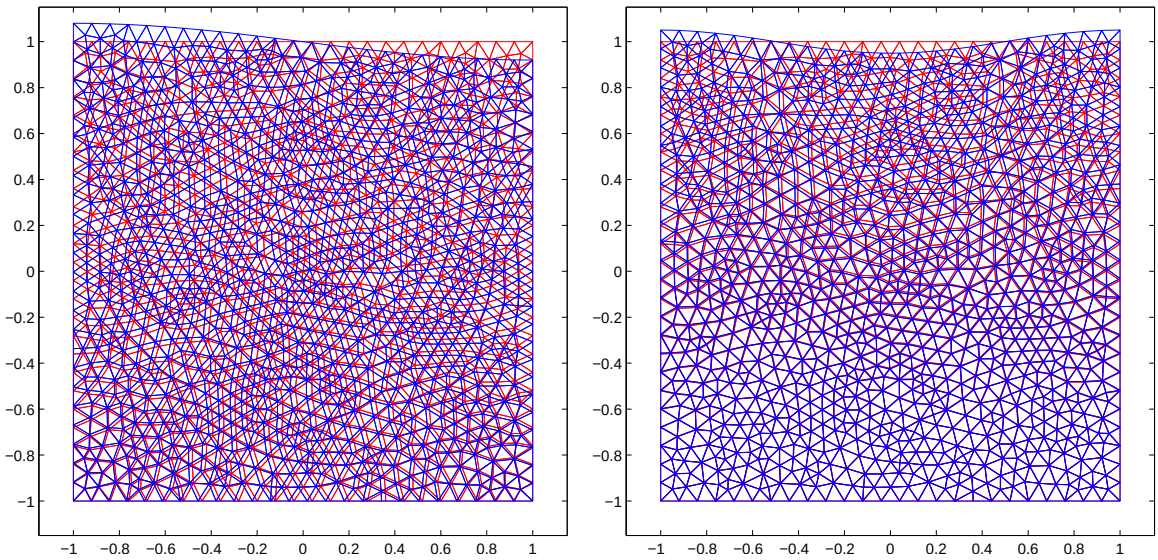

References

[1] F. Auricchio, L. B. da Veiga, C. Lovadina, and A. Reali, *The importance of the exact satisfaction of the incompressibility constraint in nonlinear elasticity: Mixed FEMs versus NURBS-based approximations*, Comput. Methods Appl. Mech. Engrg. **199** (2010), 314–323.

[2] Z. Cai, J. Korsawe, and G. Starke, *An adaptive least squares mixed finite element method for the stress-displacement formulation of linear elasticity*, Numer. Methods Partial Differential Equations **21** (2005), 132–148.
[3] Z. Cai and G. Starke, *First-order system least squares for the stress-displacement formulation: Linear elasticity*, SIAM J. Numer. Anal. **41** (2003), 715–730.
[4] P. G. Ciarlet, *Mathematical Elasticity Volume I: Three–Dimensional Elasticity*, North-Holland, Amsterdam, 1988.
[5] B. Müller, G. Starke, A. Schwarz, and J. Schröder, *Stress-displacement least squares for hyperelasticity*, (2012). In preparation.
[6] A. Schwarz, J. Schröder, and G. Starke, *Least-squares mixed finite elements for small strain elasto-viscoplasticity*, Int. J. Numer. Meth. Engrg. **77** (2009), 1351–1370.
[7] G. Starke, *An adaptive least-squares mixed finite element method for elasto-plasticity*, SIAM J. Numer. Anal. **45** (2007), 371–388.

Least-squares mixed finite elements for hyperelastic material models

Alexander Schwarz
(joint work with Jörg Schröder, Gerhard Starke, Karl Steeger)

1. Introduction

In recent years the interest in solving partial differential equations with the least-squares method has grown steadily. The resulting least-squares finite element method (LSFEM) has some theoretical advantages compared to other variational approaches. In general the LSFEM is based on a minimization principle and is not restricted to the LBB-condition. Furthermore, least-squares formulations normally provide an a posteriori error estimator without additional computational costs, which can be used for the construction of algorithms for adaptive mesh refinement. The method has been successfully applied to many fields in mechanics and mathematics; an exhaustive overview with respect to theoretical foundations and application-oriented issues can be found for example in the monograph [1]. In solid mechanics exist, amongst others, contributions towards e.g. elasticity ([2], [3], and [4]) and plasticity ([5]).

2. Least-Squares Formulation

In the present work a mixed finite element based on a geometrically nonlinear least-squares formulation in consideration of a hyperelastic material model is proposed. Basis for the element formulation is a div-grad first order system consisting of the equilibrium condition and a material law

$$\text{Div}\,\boldsymbol{P} + \boldsymbol{f} = \boldsymbol{0} \quad \text{and} \quad \boldsymbol{F}^{-1}\boldsymbol{P} - 2\rho\,\partial_{\boldsymbol{C}}\psi(\boldsymbol{C}) = \boldsymbol{0}\,, \tag{1}$$

with the first Piola-Kirchhoff stress tensor $\boldsymbol{P}$, the vector of the body forces $\boldsymbol{f}$, a free energy ψ, the right Cauchy-Green deformation tensor $\boldsymbol{C} = \boldsymbol{F}^T\boldsymbol{F}$, the deformation gradient $\boldsymbol{F} = \boldsymbol{1} + \nabla\boldsymbol{u}$, and the density ρ (in the following we assume a constant

unity density $\rho = 1$). For the considered St.Venant-Kirchhoff material the free energy is given by

$$\psi(\boldsymbol{C}) = \frac{1}{2}\lambda(\mathrm{tr}\boldsymbol{E})^2 + \mu\mathrm{tr}\boldsymbol{E}^2 = \frac{1}{2}\boldsymbol{E}\cdot\mathbb{C}\boldsymbol{E} = \frac{1}{8}(\boldsymbol{C}-\boldsymbol{1})\cdot\mathbb{C}(\boldsymbol{C}-\boldsymbol{1})\,. \tag{2}$$

Here, the Green-Lagrange strain tensor and the constitutive tensor are defined as

$$\boldsymbol{E} = \frac{1}{2}(\nabla\boldsymbol{u} + [\nabla\boldsymbol{u}]^T + [\nabla\boldsymbol{u}]^T\nabla\boldsymbol{u}) \;\text{ and }\; \mathbb{C} = \lambda\boldsymbol{1}\otimes\boldsymbol{1} + 2\mu\mathbb{I}\,. \tag{3}$$

With $\partial_{\boldsymbol{E}}\psi(\boldsymbol{C}) = 2\partial_{\boldsymbol{C}}\psi(\boldsymbol{C}) = \mathbb{C}\boldsymbol{E}$ and by multiplying $(1)_2$ with the compliance tensor $\mathbb{C}^{-1}$ we obtain the relations

$$\mathrm{Div}\,\boldsymbol{P} + \boldsymbol{f} = \boldsymbol{0} \;\text{ and }\; \mathbb{C}^{-1}\boldsymbol{F}^{-1}\boldsymbol{P} - \boldsymbol{E} = \boldsymbol{0}\,. \tag{4}$$

These residuals lead by means of quadratic L_2-norms to a least-squares functional depending on stresses and displacements

$$F(\boldsymbol{P},\boldsymbol{u}) \;=\; \frac{1}{2}\left(||\mathrm{Div}\,\boldsymbol{P} + \boldsymbol{f}||_0^2 + ||\mathbb{C}^{-1}\boldsymbol{F}^{-1}\boldsymbol{P} - \boldsymbol{E}||_0^2\right)\,. \tag{5}$$

For the minimization of the functional, the first variations with respect to the unknowns have to vanish, i.e. $\delta_{u,P}F = 0$. We obtain the first variations as

$$\begin{aligned}
\delta_u F &= \int_B (\mathbb{C}^{-1}\boldsymbol{F}^{-1}\boldsymbol{P} - \boldsymbol{E})\cdot(\mathbb{C}^{-1}\delta\boldsymbol{F}^{-1}\boldsymbol{P} - \delta\boldsymbol{E})\,dV \\
\delta_P F &= \int_B (\mathbb{C}^{-1}\boldsymbol{F}^{-1}\boldsymbol{P} - \boldsymbol{E})\cdot\mathbb{C}^{-1}\boldsymbol{F}^{-1}\delta\boldsymbol{P}\,dV + \\
&\qquad \int_B (\mathrm{Div}\boldsymbol{P} + \boldsymbol{f})\cdot\mathrm{Div}\,\delta\boldsymbol{P}\,dV\,.
\end{aligned} \tag{6}$$

The solution of the problem can be obtained, similar to the case governed by material non-linearites in [5], by the Newton method. Therefore, we have to find the minimizer $I(\boldsymbol{P},\boldsymbol{u})$ by updating of

$$\Delta I(\boldsymbol{P},\boldsymbol{u}) = \boldsymbol{K}^{-1}\boldsymbol{r} \quad\text{with}\quad \boldsymbol{K}\in\Delta\delta F \quad\text{and}\quad \boldsymbol{r}\in\delta F\,, \tag{7}$$

where $\Delta\delta F$ denotes the second variation with respect to all unknowns. The implementation as well as the interpolation of the unknowns follows similar procedures as in case of linear elasticity, see e.g. [3]. The finite element space in two dimensions for the stresses is

$$\boldsymbol{X}_h^m = \left\{\boldsymbol{P}\in H(\mathrm{div},B_e)^2 : \boldsymbol{P}|_{B_e}\in RT_m(B_e)^2\;\forall\,B_e\right\}\subset\boldsymbol{X}\,. \tag{8}$$

Thus, shape functions related to the edges of a respective triangular element B_e are applied. These vector-valued functions belong to a Raviart-Thomas space, which guarantees a conforming discretization of the required Sobolev space $H(\mathrm{div},B_e)$. The finite element space for the displacements is

$$\boldsymbol{V}_h^k = \left\{\boldsymbol{u}\in W^{1,p}(B_e)^2 : \boldsymbol{u}|_{B_e}\in P_k(B_e)^2\;\forall\,B_e\right\}\subset\boldsymbol{V}\,. \tag{9}$$

Here, standard Lagrange polynomials associated to vertices are used for the continuous approximation of the displacements. In (8) and (9) the indices m and k denote the polynomial interpolation order of the resulting mixed finite element RT_mP_k.

3. Numerical Example

In order to provide a numerical example, we consider the well-known Cook's Membrane problem. On the trapezoidal geometry with dimensions of 48×60 units $\{l\}$ the left side is assumed to be a displacement boundary and clamped. The other edges are stress boundaries. Stress-free boundary conditions are applied at the upper and lower edge. On the right edge we prescribe a maximum load of $\boldsymbol{PN} = (0,5)[N/\{l\}^2]$, which is increased in every load step by 10% of the final load. The Young's modulus is chosen as $E = 200[N/\{l\}^2]$ and Poisson's ratio as $\nu = 0.35$. In Figure 1 the material parameters and boundary conditions as well as the geometry can be found. Figure 2 shows the Cauchy stresses σ_{11} and the convergence of the vertical displacement of the top right point.

System setup:			
Right side	$\boldsymbol{PN}$	=	$(0,5)[N/\{l\}^2]$
Upper/Lower side	$\boldsymbol{PN}$	=	$(0,0)[N/\{l\}^2]$
Left side	$\boldsymbol{u}$	=	$(0,0)[\{l\}]$
Young's modulus	E	=	$200[N/\{l\}^2]$
Poisson's ratio	ν	=	0.35

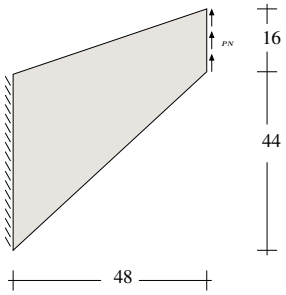

Figure 1. Material parameters, boundary conditions and geometry of Cook's Membrane.

The results are reasonable and convergent, but the performance of the cubic element is clearly superior to the performance of the quadratic element.

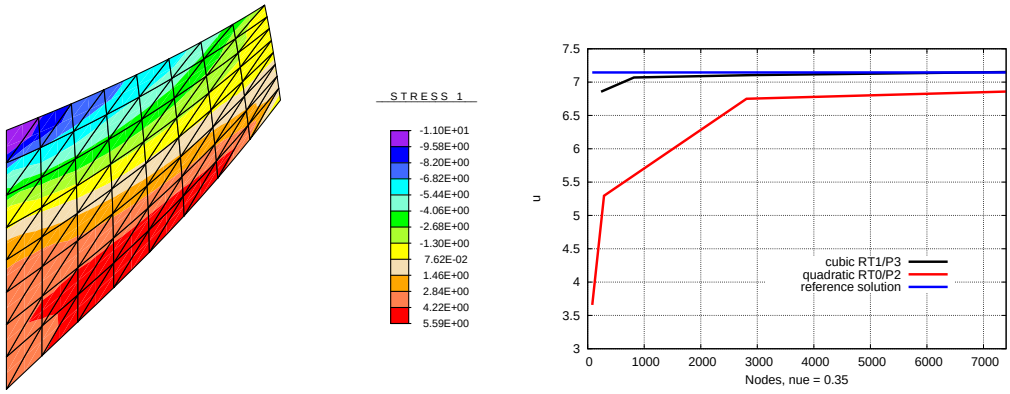

Figure 2. Cauchy stresses σ_{11} (left) and convergence of vertical displacement of the top right point (right).

References

[1] P.B. Bochev and M.D. Gunzburger, *Least-Squares Finite Element Methods*, Springer Verlag, New York (2009).

[2] Z. Cai and G. Starke, *Least-squares methods for linear elasticity*, SIAM Journal on Numerical Analysis **42** (2004), 843–859.

[3] A. Schwarz, J. Schröder and G. Starke, *A modified least-squares mixed finite element with improved momentum balance*, International Journal for Numerical Methods in Engineering **81** (2010), 286–306.

[4] G. Starke, A. Schwarz and J. Schröder, *Analysis of a modified first-order system least squares method for linear elasticity with improved momentum balance*, SIAM Journal on Numerical Analysis **49** (2011), 1006–1022.

[5] A. Schwarz, J. Schröder and G. Starke, *Least-squares mixed finite elements for small strain elasto-viscoplasticity*, International Journal for Numerical Methods in Engineering **77** (2009), 1351–1370.

A new Mixed Finite Element Formulation based on Different Approximations of the Minors of Deformation Tensors

Daniel Balzani

(joint work with Jörg Schröder, Peter Wriggers)

1. Introduction

The notion of polyconvexity in the sense of Ball [2] is fundamental in the field of nonlinear continuum mechanics, especially for hyperelastic materials since the existence of minimizers of variational problems is guaranteed. The first anisotropic polyconvex strain energy functions are introduced in [4] and recently extended to different applications, e.g. to soft biological tissues in [3]. Especially for the case of incompressibility various mixed Finite Element approaches have been introduced in the past, however, suitable formulations providing locking-free accurate solutions for coarse meshes still need attention, see e.g. [1]. Along these lines we focus in this contribution on a new mixed Finite Element formulation is derived based on different approximations of the deformation gradient, its cofactor and its determinant. These quantities are the minors of the deformation gradient and play a major role with respect to (i) the transformation of infinitesimal line-, area- and volume elements, and (ii) in the formulation of polyconvex strain energy functions.

2. Variational Basis of the Mixed Formulation

Considering a framework formulated in the deformation gradient $\mathbf{F}$ the modified Hu-Washizu functional can be written as $\Pi^{tot} = \Pi + \Pi^{ext}$, wherein the external potential is given by $\Pi^{ext} = -\int_\Omega \mathbf{x}\cdot\mathbf{f}\,dV - \int_{\partial\Omega}\mathbf{x}\cdot\mathbf{t}\,dA$ and the internal part reads

$$\Pi(\mathbf{x},\mathbf{H}^c,\theta\,,\mathbf{B},p) = \int_\Omega W(\mathbf{F},\mathbf{H}^c,\theta)\,dV + \int_\Omega p(J-\theta)\,dV + \int_\Omega \mathbf{B}\cdot(\mathrm{cof}\mathbf{F}-\mathbf{H}^c)\,dV\,.$$

Here, the independent variables are the deformation $\mathbf{x}$, a tensor field $\mathbf{H}^c$, representing the cofactor, and the scalar θ related to the volumetric dilatation. Associated with the last two quantities are the stress-like quantity $\mathbf{B}$ and the pressure-like

quantity p. The volume forces and traction forces are denoted by $\mathbf{f}$ and $\mathbf{t}$, respectively. Alternatively, the strain energy function W as a function of the deformation gradient and its minors can also be written in terms of the right Cauchy-Green tensor $\mathbf{C} = \mathbf{F}^T\mathbf{F}$, i.e. $\psi := \psi(\mathbf{C}, \mathbf{H}^c, \theta)$, which then leads to

$$\Pi(\mathbf{x}, \mathbf{H}^c, \theta\,, \mathbf{B}, p) = \int_\Omega \psi(\mathbf{C}, \mathbf{H}^c, \theta)\, dV + \int_\Omega p(J-\theta)\, dV + \int_\Omega \mathbf{B} \cdot (\mathrm{cof}\mathbf{C} - \mathbf{H}^c)\, dV\,.$$

3. Approximation

The first variation and a consistent linearization are given in [5], where it is also shown that the five-field formulation can be reduced to a pure displacement formulation by static condensation. For the approximation the ansatz spaces have to be balanced in order to obtain a robust and stable discretization. It is known in classical formulations for incompressibility that a reduced ansatz space, applied to the pressure term, could yield more suitable finite element formulations. This results for example in the well-known T2/P1 or T2/P0 formulations for triangular/tetrahedral elements. Since the volumetric term depends cubically on the components of the right Cauchy-Green tensor $\mathbf{C}$ and the cofactor cof$\mathbf{C}$ depends quadratically on the components of $\mathbf{C}$ a suitable choice for the ansatz spaces could be provided by

- a quadratic interpolation for $\mathbf{x}$,
- a linear interpolation for $\mathbf{H}^c$ and $\mathbf{B}$ and
- a constant interpolation for θ and p.

4. Numerical Examples

As a first example we consider a bending beam, cf. Fig. 1a and investigate the mesh distortion sensitivity. For this purpose different meshes are analyzed which are distorted by increasing the distortion parameter a. For the analysis a number of $n_{ele} = 12288$ elements are used for the discretization of the beam. As can be seen in Fig. 1c the proposed formulation (cofem) shows a reduced sensitivity with respect to mesh distortions than the standard displacement formulation (t2) or the F-bar approach (fbar). Furthermore, a completely unreasonable stress distribution is observed for the standard displacement formulation and the strongly distorted mesh ($a = 4.99$), see Fig. 1b (lower image), whereas the proposed formulation shows a rather smooth distribution, see Fig. 1b (upper image).

As a second example the Finite-Element convergence is studied at a Cooks-type problem, see Fig. 2a for the boundary value problem. Then the displacements of point C are analyzed for different Finite-Element discretizations. Fig. 2b,c show the displacements u_x and u_y, respectively, versus the number of elements in a logarithmic scale. It can be observed that the proposed formulation converges faster than the standard displacement formulation and the F-bar approach.

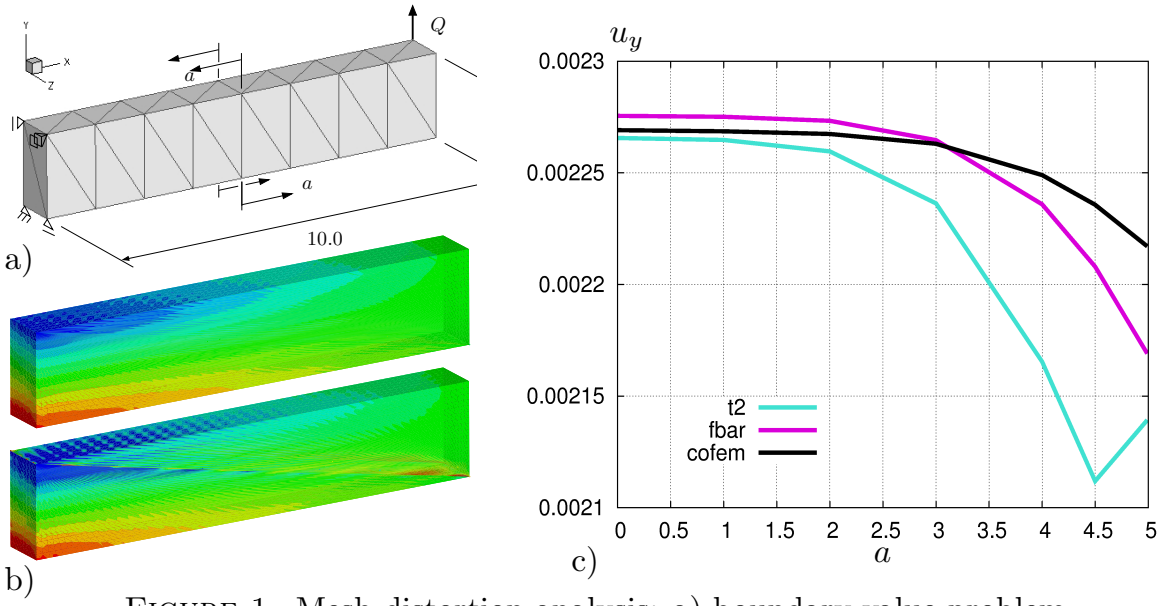

FIGURE 1. Mesh-distortion analysis: a) boundary value problem with an undeformed undistorted mesh ($a = 0$), b) the distorted mesh for $n_{ele} = 12288$ elements and a mesh distortion of $a = 4.99$ unit lengths, and c) vertical displacements of the loading point versus distortion parameter a.

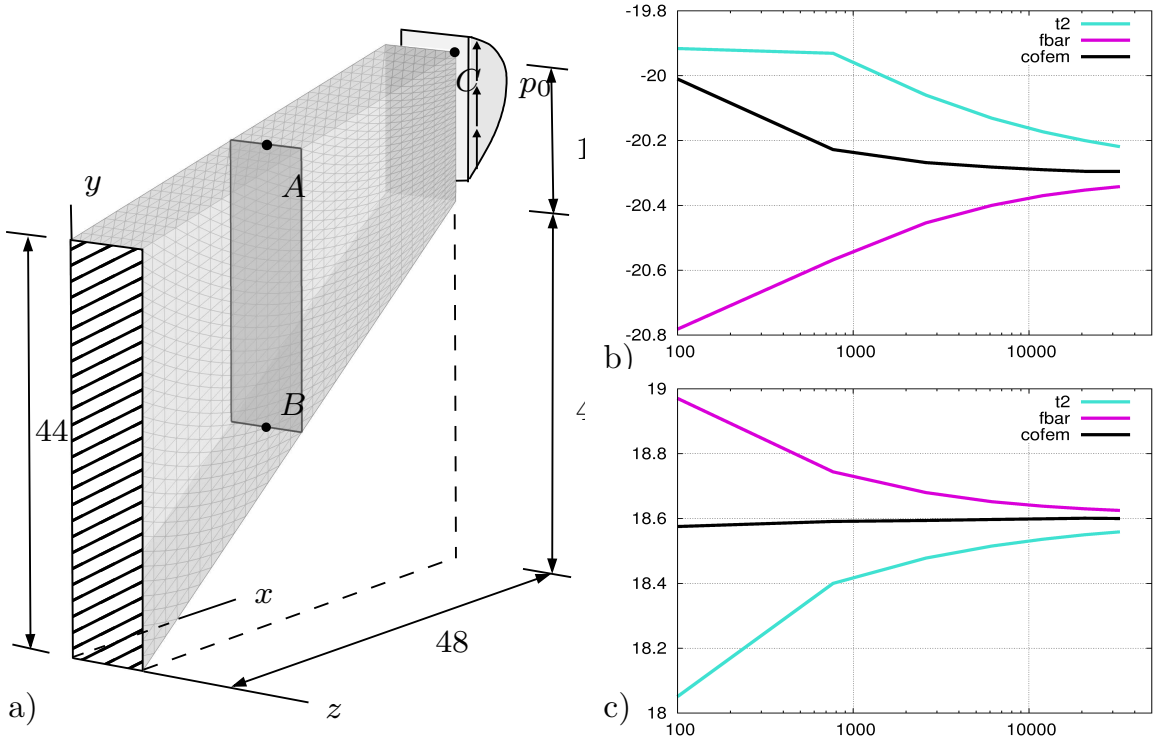

FIGURE 2. Convergence study of Cook's-type problem: a) boundary value problem, b) distribution of the displacements u_x and c) u_y versus number of elements (in a logarithmic scale).

REFERENCES

[1] Auricchio, F., Beirao de Veiga, L., Lovadina, C., and Reali, A., *A stability study of some mixed finite elements for large deformation elasticity problems*, Comp. Meth. Appl. Mech. Eng. **194** (2005), 1075–1092.

[2] Ball, J.M., *Convexity conditions and existence theorems in non-linear elasticity*, Archive for Rational Mechanics and Analysis **63** (1977), 337–403.
[3] Balzani, D., Neff, P., Schröder, J., and Holzapfel, G.A., *A polyconvex framework for soft biological tissues. Adjustment to experimental data*, International Journal of Solids and Structures **43**/20 (2006), 6052–6070.
[4] Schröder, J. and Neff, P., *Invariant formulation of hyperelastic transverse isotropy based on polyconvex free energy functions*, International Journal of Solids and Structures **40** (2003), 401–445.
[5] Schröder, J., Wriggers, P. and Balzani, D., *A new Mixed Finite Element based on Different Approximations of the Minors of Deformation Tensors*, Computer Methods in Applied Mechanics and Engineering **200** (2011), 3583–3600.

Adaptive mixed finite element methods and new hybriddiscontinuous Galerkin method

Eun-Jae Park
(joint work with Dongho Kim and Youngmok Jeon)

This short report deals with locally conservative methods and consists of two parts: first part on adaptive mixed finite element methods and second on new hybrid discontinuous Galerkin (HDG) method.

First part is based on joint work with Dongho Kim. The mixed finite element method has two important features; it conserves the mass locally and produces accurate flux even for highly nonhomogeneous media with large jumps in the physical properties. In many cases the mixed finite element method gives better approximations for the flux variable associated with the solution of a second order elliptic problem than the classical Galerkin method. Mixed finite element methods for highly nonlinear cases in divergence form were treated by the author [11, 12, 13]. There, by using the Brouwer fixed point theory, unique solvability of the approximate problem is proved and optimal order error estimates are obtained for the Raviart-Thomas mixed finite element space. This approach requires construction of a mapping which maps a ball in appropriate function spaces into itself. The choice of norms used to measure the distance from the approximation to a projection of the solution and its flux variable, plays a crucial role in proving solvability of the nonlinear algebraic equations arising from the mixed finite-element method. In order to be able to prove existence of a numerical solution, more regularity was required of the solution. This has the negative effect of precluding the use of the lowest-indexed mixed finite-element spaces (see [11, 12, 13]). In practice, one often uses the lowest order elements which are of interest for actual implementation.

In [7], we presented a priori and a posteriori mixed finite element error analysis of elliptic problems, in particular, with gradient nonlinearities in the lower order term in two and three space dimensions [11]. We take a different approach based on the Brezzi-Rappaz-Raviart framework [3, 4] rather than using the Brouwer fixed point theory. First, we derived an optimal order a priori error estimate measured in the $L^m(\Omega)$-norm in the framework of Brezzi-Rappaz-Raviart which requires of the $C^{1,1}$-regularity of the lower order term $b(x, p, \nabla p)$; we extended the theory to

allow more general $C^{1,\alpha}$ class of the function b for $0 < \alpha \leq 1$. Then, we derived reliable and efficient a posteriori error estimators in $L^m(\Omega)$ for the error control of our approximation to the nonlinear problem under consideration in two and three space dimensions using some of the ideas presented in [5].

On the other hand, Newton type methods for solving nonlinear algebraic equations arising from discretization give rise to convection-diffusion equations. In particular, in the case of the convection dominated diffusion problems, one needs to incorporate upwind method to capture internal or boundary layers. Since the mixed finite element method uses discontinuous finite elements for pressure spaces, it is natural to use upwind method for the convection term. In [6], we derived reliable and efficient error estimators. Numerical results shows that the derived error estimators are also computationally robust in terms of the diffusion parameter.

Second part is based on joint work with Youngmok Jeon [9, 10]. The new method is based on recently introduced nonconforming cell boundary element (CBE) methods [8]. The CBE method is designed in such a way that they enjoy the mass conservation at the element level and the normal component of fluxes at inter-element boundaries are continuous for unstructured triangular meshes.

A brief outline of the GCBE can be described as follows.

Step 1: Introduce a trace variable $\lambda = u|_{K_h}$ on the *skeleton*.

Step 2: Solve two elliptic equations for u_λ and u_f on each T such that

$$-\Delta u_\lambda = 0 \text{ in } T, \qquad u_\lambda = \lambda \text{ on } \partial T,$$
$$-\Delta u_f = f \text{ in } T, \qquad u_f = 0 \text{ on } \partial T$$

and set $u = u_\lambda + u_f$.

Step 3: Use the flux continuity equation at cell interfaces to obtain a global system of equations in unknowns λ only.

Our method has a flavor of the discontinuous Galerkin (DG) method. In the GCBE, generic unknowns are supported on the skeleton of a mesh as in Step 1. Step 2 is a process of generating PDE-adapted local basis which can be done in parallel. This is achieved by a DG method similar to the Baumann-Oden formulation [1] at the element level. We use completely discontinuous polynomials $P_k(T)$ for u and globally continuous polynomials $P_k(\partial T)$ for the interface variable λ. For the lowest order case, i.e., $k = 1$, we add a bubble for each T as in [2] for stability. More details on GCBE can be found in [9, 10], where some extension to the Stokes problem is discussed.

References

[1] C. E. Baumann and J. T. Oden, A discontinuous *hp* finite element method for convection-diffusion problems, Comput. Methods Appl. Mech. Engrg. 175 (1999), no. 3-4, 311–341.

[2] F. Brezzi and L.D. Marini, Bubble stabilization of discontinuous Galerkin methods, in Advances in numerical mathematics, Proc. International Conference on the occasion of the 60th birthday of Y.A. Kuznetsov, September 16-17, 2005 (W. Fitzgibbon, R. Hoppe, J. Periaux, O. Pironneau, Y. Vassilevski, Eds) Institute of Numerical Mathematics of the Russian Academy of Sciences, Moscow, (2006), 25-36.

[3] F. Brezzi, J. Rappaz, P.A. Raviart, *Finite dimensional approximation of nonlinear problems*, Numer. Math. (1980), 36, pp. 1–25.
[4] G. Caloz, J. Rappaz, "Numerical Analysis for Nonlinear and Bifurcation Problems", Handbook of Numerical Analysis (P. G. Ciarlet and J. L. Lions, eds.) Vol. V, 487–637, North-Holland, Amsterdam, 1997.
[5] C. Carstensen, *A posteriori error estimate for the mixed finite element method*, Math. Comp. vol. 66, No. 218 (1997), pp. 465–476.
[6] D. Kim and E.-J. Park, *A posteriori error estimators for the upstream weighting mixed methods for convection diffusion problems*, Computer Methods in Applied Mechanics and Engineering, Vol. 197 (2008), No. 6-8, pp. 806–820.
[7] D. Kim and E.-J. Park, *A Priori and A Posteriori Analysis of Mixed Finite Element Methods for Nonlinear Elliptic Equations*, SIAM Journal on Numerical Analysis,Vol. 48 (2010), No. 3, pp. 1186–1207.
[8] Y. Jeon and E.-J. Park, *Nonconforming cell boundary element methods for elliptic problems on triangular mesh*, Appl. Numer. Math. 58 (2008), 800-814.
[9] Y. Jeon and E.-J. Park, *A hybrid discontinuous Galerkin method for elliptic problems*, SIAM J. Numer. Anal. 48 (2010), no. 5, 1968-1983.
[10] Y. Jeon and E.-J. Park, *New locally conservative finite element methods on a rectangular mesh*, Preprint.
[11] F. A. Milner and E.-J. Park, *Mixed finite element methods for Hamilton-Jacobi-Bellman-type equations*, IMA J. Numer. Anal. Vol.16 (1996), pp. 399–412.
[12] F. A. Milner and E.-J. Park, *A mixed finite element method for a strongly nonlinear second-order elliptic problem*, *Math. Comp.* Vol.64 (1995), pp.973–988.
[13] E.-J. Park, *Mixed finite element methods for nonlinear second-order elliptic problems*, SIAM J. Numer. Anal. 32 (1995), no. 3, 865–885.

Computational competition of symmetric mixed FEM in linear elasticity

Joscha Gedicke
(joint work with Carsten Carstensen, Martin Eigel)

The numerical solution of the Navier-Lamé equation with mixed weak formulations allows a robust approximation even if the crucial Lamé parameter passes to the incompressible limit when the Poisson ratio approaches 1/2, see [5, Chapter IV §3]. In low-order displacement formulations, the well-known locking effect causes a priori error estimates to deteriorate. While there are many known stable mixed finite element methods (MFEM), the additional symmetry constraint implied for the stress tensor σ proved to be difficult to impose in numerical schemes. This has resulted in the introduction of discretisations with no or reduced symmetry incorporated in the discrete stress space [1, 8, 17]. The first MFEM which were designed especially to fulfil the stress symmetry without the need of a sub-grid are due to Arnold and Winther [3, 4, 10]. As discussed in [3], the continuity property imposed on the stress field in the conforming MFEM substantially increases complexity of the finite elements. Since (complete) continuity is not required in the mixed formulation of linear elasticity, non-conforming MFEM can be an efficient and easier to implement alternative to conforming elements.

The article [9] is devoted to the computational competition of several FEM displayed in Table 1 for the Navier-Lamé equation of linear elasticity. While the

name	convergence result
AW21	$\|\sigma - \sigma_h\|_{L^2(\Omega)} \leq Ch\|u\|_{H^2(\Omega)}$
AW15	$\|\sigma - \sigma_h\|_{L^2(\Omega)} \leq Ch\|u\|_{H^2(\Omega)}$
AW30	$\|\sigma - \sigma_h\|_{L^2(\Omega)} \leq Ch^m\|\sigma\|_{H^m(\Omega)}$ for $1 \leq m \leq 3$
AW24	$\|\sigma - \sigma_h\|_{L^2(\Omega)} \leq Ch^m\|\sigma\|_{H^m(\Omega)}$ for $1 \leq m \leq 2$
S15	$\|\sigma - \sigma_h\|_{L^2(\Omega)} \leq Ch^{m-1}\|u\|_{H^m(\Omega)}$ for $1 \leq m \leq 2$
S27	$\|\sigma - \sigma_h\|_{L^2(\Omega)} \leq Ch^{m-1}\|u\|_{H^m(\Omega)}$ for $1 \leq m \leq 3$
KS	$\|\sigma - \sigma_h\|_{L^2(\Omega)} \leq Ch\|\sigma\|_{H^1(\Omega)}$
PEERS	$\|\sigma - \sigma_h\|_{L^2(\Omega)} \leq Ch\|\sigma\|_{H^1(\Omega)}$
P_k	$\|\sigma - \sigma_h\|_{L^2(\Omega)} \leq C(\lambda)h^k\|u\|_{H^{k+1}(\Omega)}$ for $k = 1, 2, 3$
P_4	$\|\sigma - \sigma_h\|_{L^2(\Omega)} \leq Ch^4\|u\|_{H^5(\Omega)}$

TABLE 1. Theoretical convergence rates of different mixed FEM, the non-conforming KS-FEM and the conforming P_k-FEM; σ denotes the stress tensor and u the displacement. The constant C is independent of material parameters (except for P_k, $k = 1, 2, 3$) and independent of the (sufficiently small) mesh-size h.

conforming lowest-order AW30 and AW24 MFEM of Arnold and Winther [3] have 30 and 24 degrees of freedom and are based on a polynomial basis of degree 3, the non-conforming AW21 and AW15 MFEM [4] are based on a quadratic polynomial basis with 21 and 15 degrees of freedom. The recently introduced S15 and S27 MFEM due to Pechstein and Schöberl [16] are based on linear and quadratic polynomials and have 15 and 27 degrees of freedom. Of particular interest is the numerical competition of the many newly available mixed finite elements of order one up to three with traditional displacement-oriented FEM of the same orders. Since P_4 is locking free [6] in contrast to P_k, $k = 1, 2, 3$, it is included in the survey as well as the low-order MFEM of weak symmetry (PEERS) [1] and the non-conforming KS-FEM [15]. We note that there are some recent elements which we could not include in this survey such as [12, 13]. Moreover, while there are several MFEM with weak symmetry constraints that might also have been worth to consider in our comparison, see e.g. [2, 14, 11], our focus lies on symmetric methods. The reason for including PEERS and KS-FEM is the great popularity of these methods in the engineering community. We also mention that, although out of the scope of this comparison, higher-order PEERS are available which probably would show a more favourable performance than the lowest-order version.

While robustness, locking and computational complexity usually play a pivotal role, singularities in the solution or high regularity may dominate the choice for the method and the mesh-design. The numerical experiments with several Poisson ratios ν close to $1/2$ confirm the theoretical locking-free property of the symmetric MFEM. The theoretical findings of [6], that P_k, $k = 1, 2, 3$, show locking while P_4 is locking free, are empirically verified. For this smooth example the higher-order schemes show faster convergence rates and higher accuracy. However, this

example is not representative from a practical point of view. Experiments for the Cook's membrane and the example with rigid circular inclusion show that singular solutions or curved boundaries can reduce the convergence rates of the methods. For the Cook's membrane problem even the low-order schemes lead to suboptimal convergence rates. This motivates the use of local mesh refinement which is investigated more closely for some L-shaped domain in [9]. The experiments show that graded meshes in contrast to uniform meshes lead to optimal convergence rates. However, the right choice of the grading parameter is not known in practise because it depends on the material parameters. The experiments show that a too small grading parameter results in suboptimal convergence rates while a too large value can lead to errors of different order of magnitude in accuracy. Therefore adaptive mesh refinement strategies for the symmetric MFEM have to be investigated which is postponed to forthcoming work. The experiments of [9] indicate that among the first-order methods P_1, PEERS, KS, AW21, AW15 and S15, the AW15 MFEM shows the best results. Among the second-order methods P_2, AW24 and S27, the AW24 MFEM shows the best results. Among the third-order methods P_3 and AW30, the locking-free AW30 MFEM shows the better results. The comparison of conforming FEM and the MFEM under consideration shows that only the robust version P_4 is competitive and performs best. However, the comparison of the fourth-order scheme with some third-order method clearly shows superiority of the higher-order scheme provided the exact solution is sufficiently smooth. The experiments for the L-shaped domain leads to the conjecture that for $f \equiv 0$ the AW30 and AW24 exhibit some superconvergence phenomenon of order $\mathcal{O}(N^{-2})$. This is in agreement with the conjecture of [10]. These results of the AW30 and AW24 MFEM can compete with those of the one order higher P_4 displacements solution.

References

[1] D. N. Arnold, F. Brezzi, and J. Douglas, *PEERS: A new mixed finite element for plane elasticity*, Jpn. J. Appl. Math. **1** (1984), 347–367.

[2] D. N. Arnold, R. S. Falk, and R. Winther, *Mixed finite element methods for linear elasticity with weakly imposed symmetry*, Math. Comp. **76** (2007), no. 260, 1699–1723.

[3] D. N. Arnold and R. Winther, *Mixed finite elements for elasticity*, Numer. Math. **92** (2002), no. 3, 401–419.

[4] D. N. Arnold and R. Winther, *Nonconforming mixed elements for elasticity*, Math. Models Methods Appl. Sci. **13** (2003), no. 3, 295–307.

[5] F. Brezzi and M. Fortin, *Mixed and hybrid finite element methods*, Springer Series in Computational Mathematics, vol. 15, Springer-Verlag, New York, 1991.

[6] I. Babuška and M. Suri, *Locking effects in the finite element approximation of elasticity problems*, Numer. Math. **62** (1992), no. 4, 439–463.

[7] C. Carstensen, *An adaptive mesh-refining algorithm allowing for an H^1 stable L^2 projection onto Courant finite element spaces*, Constr. Approx. **20** (2004), no. 4, 549–564.

[8] C. Carstensen, G. Dolzmann, S. A. Funken, and D. S. Helm, *Locking-free mixed finite element methods in linear elasticity*, Comput. Methods Appl. Mech. Engrg. **190** (2000), 1701–1781.

[9] C. Carstensen, M. Eigel, and J. Gedicke, *Computational competition of symmetric mixed FEM in linear elasticity*, Comput. Methods Appl. Mech. Engrg. **200** (2011), no. 41-44, 2903–2915.
[10] C. Carstensen, D. Günther, J. Reininghaus, and J. Thiele, *The Arnold-Winther mixed FEM in linear elasticity. Part I: Implementation and numerical verification*, Comput. Methods Appl. Mech. Engrg. **197** (2008), 3014–3023.
[11] B. Cockburn, J. Gopalakrishnan, and J. Guzmán, *A new elasticity element made for enforcing weak stress symmetry*, Math. Comp. **79** (2010), no. 271, 1331–1349.
[12] J. Gopalakrishnan and J. Guzmán, *A second elasticity element using the matrix bubble*, IMA J. Numer. Anal. **32** (2012), no. 1, 352–372.
[13] J. Gopalakrishnan and J. Guzmán, *Symmetric non-conforming mixed finite elements for linear elasticity*, SIAM J. Numer. Anal. **49** (2011), no. 4, 1504–1520.
[14] J. Guzmán, *A unified analysis of several mixed methods for elasticity with weak stress symmetry*, J. Sci. Comput. **44** (2010), no. 2, 156–169.
[15] R. Kouhia and R. Stenberg, *A linear nonconforming finite element method for nearly incompressible elasticity and Stokes flow*, Comput. Methods Appl. Mech. Engrg. **124** (1995), no. 3, 195–212.
[16] A. Pechstein and J. Schöberl, *Tangential-displacement and normal-normal-stress continuous mixed finite elements for elasticity*, Math. Models Methods Appl. Sci. **21** (2011), no. 8, 1761–1782.
[17] R. Stenberg, *A family of mixed finite elements for the elasticity problem*, Numer. Math. **53** (1988), 513–538.

Approximations of incompressible large deformation elastic problems: some unresolved issues!

Ferdinando Auricchio
(joint work with L.Beirao da Veiga, C.Lovadina, A.Reali, R.L.Taylor, P.Wriggers)

1. Introduction

It is well known in the literature that many finite element formulations fail to properly reproduce highly incompressible finite strain solutions, showing unphysical instability hourglass modes [1]. This has been a puzzling point for many researchers who have been devoted many efforts in trying to produce stable and robust numerical schemes also in a finite strain regime. However, up today there is no effective and exhaustive proof that any of the proposed approach is really working, due also to the fact that there is not yet a clear theoretical understanding on the numerical pathologies. This observation is also evident from the numerical point of view, since there is no agreement on which could be effective numerical round-robin tests and on possible benchmark tests to really test and prove the robustness of approximation schemes.

2. Proposed approach

As a consequence, within the framework of incompressible finite elasticity, we focus on some simple two-dimensional examples, reported in Figures 1-2.

In particular, for the first problem we are able to study the stability of the continuum problem, while the second one seems to be a simple numerical problems; we may hope that in the future both problems may become benchmark tests.

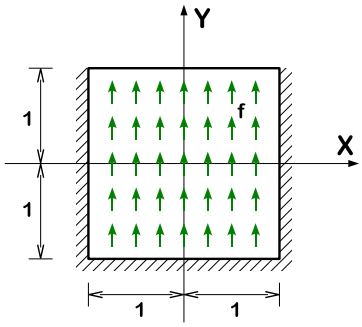

FIGURE 1. Problem 1.

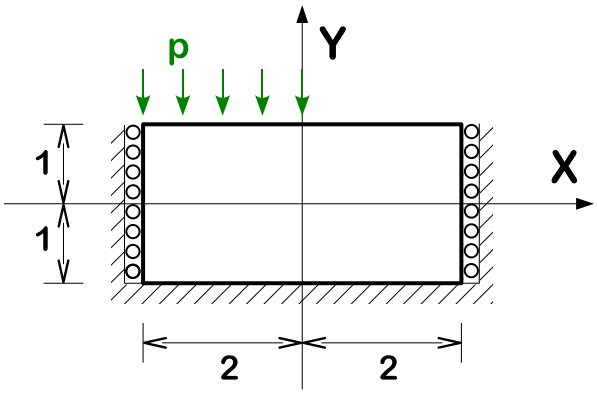

FIGURE 2. Problem 2.

Depending on the specific problem, we theoretically and numerically study the stability of the solutions to the discretized problem, obtained by means of displacement, mixed, mixed-enhanced finite elements, which are well-performing in linear elasticity (some results can be found in [2, 3]).

In particular, we explore the dependency of the numerical results on the specific form of the Θ function enforcing the incompressibily constraint. From a theoretical point the solution of the continuous problem is clearly independent from such a function, while we observe that several reliable approximation schemes show a dependency of the numerical solution on the adopted Θ function.

As an example, in Table 2 we report some numerical results for the case of a quadrilateral element based on quadratic continuous approximation for the displacement and linear discontinuous approximation for the pressure ($Q2 - P1$ element). In particular, we report the maximum load multiplier (Load) and vertical displacement of a point before detecting numerical instability. The results are reported for different meshes and for different Θ functions.

Approx	Θ	Mesh	Load	v
Q2-P1	$(J-1)$	8 x 4	60.3347	0.116456
		16 x 8	60.5748	0.105804
		32 x 16	57.3658	0.098591
		64 x 32	55.2208	0.093658
	$Log(J)$	8 x 4	77.4181	0.161595
		16 x 8	69.2701	0.135808
		32 x 16	64.3658	0.115045
		64 x 32	62.5729	0.109898
	$1-1/J$	8 x 4	88.4547	0.211841
		16 x 8	73.1676	0.157548
		32 x 16	66.7125	0.124232
		64 x 32	63.462	0.111932

TABLE 2. Numerical results for the Q2-P1 approximation for problem 2

From an inspection of the numerical results it is clear that the adopted Θ function plays a significant role and that different instability loads are detected.

3. Conclusions

We conclude drawing some general considerations. In particular, we find out that, in some situations, not only enhanced schemes fail in reproducing the solution stability range, but that similar failures can be also observed when using mixed finite elements generally considered reliable.

References

[1] Reese S., Wriggers P.: A stabilization technique to avoid hourglassing in finite elasticity. *International Journal for Numerical Methods in Engineering* **48**:79–109, 2000.

[2] Auricchio F., Beirao da Veiga L., Lovadina C., Reali A.: A stability study of some mixed finite elements for large deformation elasticity problems. *Computer Methods in Applied Mechanics and Engineering* **194**:1075–1092, 2005.

[3] Auricchio F., Beirao da Veiga L., Lovadina C., Reali A.: The importance of the exact satisfaction of the incompressibility constraint in nonlinear elasticity: mixed FEMs versus NURBS-based approximations, *Computer Methods in Applied Mechanics and Engineering* **99**:314–323, 2010.

Hybrid Discontinuous Galerkin Methods in Solid Mechanics and Fluid Dynamics

Joachim Schöberl
(joint work with Christoph Lehrenfeld)

In this talk we present several aspects of hybrid discontinuous Galerkin methods. The method is explained for the Poission Equation. We look for element-polynomials and facet-polynomials $(u, \lambda) \in P^p(\mathcal{T}) \times P^p(\mathcal{F})$ such that

$$\sum_T \int_T \nabla u \cdot \nabla v + \int_{\partial T} \frac{\partial u}{\partial n}(\mu - v) + \int_{\partial T} \frac{\partial v}{\partial n}(\lambda - u) + (u - \lambda, v - \mu)_{jump} = \int_\Omega fv$$

for all $(v, \mu) \in P^p(\mathcal{T}) \times P^p(\mathcal{F})$. The hybrid DG method shares the advantages of standard DG methods: it allows for upwinding for convection dominated problems, and it enables flexibility for the construciton of approximation spaces. In addition, hybrid DG allows for static condensation, and the problem is reduced to the element interface variables, often called Lagrange parameters. In a recent work [1] we have analyed p-version preconditioners for the resulting system, and proven poly-logarithmic growth in p of the condition number.

In [2, 3] the tangential-displacement normal-normal-stress continuous mixed finite element method (TD-NNS) was presented, and robust anisotropic error estimates have been proven. Here we show that the method can also be formulated as a hybrid - DG method: The element variable u should be chosen with continuous tangential component, the facet variable λ has only normal components.

In [4] a hybrid DG method with normal-continuous, this means $H(\mathrm{div})$-conforming velocity u has been presented. This method produces an exactly divergence free discrete velocity field, and thus is stable in kinetic energy.

References

[1] J. Schöberl and C. Lehrenfeld, *Domain Decomposition Preconditioning for High Order Hybrid Discontinuous Galerkin Methods on Tetrahedral Meshes*, ASC - Report 2012-09, Vienna University of Technology, Institute for Analysis and Scientific Computing

[2] A. Pechstein and J. Schöberl, *Tangential-Displacement and Normal-Normal-Stress Continuous Mixed Finite Elements for Elasticity*, Math. Mod. Meth. Appl Sci., **Vol 21(8)** (2011), 1761–1782.

[3] A. Pechstein and J. Schöberl, *Anisotropic mixed finite elements for elasticity*, Int. J. Numer. Meth. Eng., **Vol 90(2)** (2012), 196–217.

[4] C. Lehrenfeld, *Hybrid Discontinuous Galerkin methods for solving incompressible flow problems*, Master thesis, RWTH Aachen University (2010)

Are High-order and Hybridizable Discontinuous Galerkin methods competitive?

Antonio Huerta
(joint work with Xevi Roca, Aleksandar Angeloski and Jaime Peraire)

The talk covered several issues motivated by a practical engineering wave propagation problem: real-time evaluation of wave agitation in harbors. The first part, presented the application of a reduced order model in the framework of a Helmholtz equation with non-constant coefficients in an unbounded domain. This problem requires large numbers of degrees of freedom (`ndof`) because relatively high frequencies with small (compared with the domain size) geometric features must be considered. The incoming dimensionless wave length and its direction are the two parameters introduced in the reduced order model. Here, the Proper Generalized Decomposition (PGD) [1, 2, 3]. This method imposes a separated representation of the approximation uses the operators associated to the weak form of the problem at hand but not the solution itself as the Proper Orthogonal Decomposition techniques. Consequently, the PGD determines the separated representation without the knowledge a priori of any solution of the problem. This technique is successful in elliptic and parabolic problems, see [4] for an insightful analysis, and with the proper error estimates based on quantities of interest the number of terms can be satisfactorily estimated [5]. PGD is studied here in a wave propagation problem on an unbounded domain. After showing several PGD approaches the issue of *non-optimality* in the convergence of the separable representation is raised. Although an $\mathcal{L}_2$ projection after several PGD steps reduces drastically (in fact, optimally) the rank in the separable representation its cost in the off-line phase is non-negligible.

The second part of the talk addressed two questions, which continuously emanate in advanced computational engineering: are high-order approximations better/worse than low-order ones? and can Discontinuous Galerkin (DG) be more efficient then Continuous Galerkin (CG)?

To compare high versus low order approximations for this wave problem apart from run-time comparisons, which are clearly dependent on implementation and hardware, operation count is proposed. This is done for a direct solver. In particular, for the Hybridizable DG (HDG) see [6, 7, 8, 9, 10], because this is the technique retained for this wave problem. For this, the standard hypotheses for these analyses are employed: large uniform structured mesh (boundary influence is negligible), smooth solution (bounded with bounded derivatives) and the interpolation error is dominant. This allows to estimate the ratio between order-one elements, $n_{\mathtt{e},1}$, and order-p elements, $n_{\mathtt{e},p}$, for a given error tolerance, ε, namely

$$\frac{n_{\mathtt{e},1}}{n_{\mathtt{e},p}} = \frac{\big((p+1)!\big)^{d/p+1}}{\big(2!\big)^{d/2}} \varepsilon^{-d(p-1)/2(p+1)}. \tag{1}$$

The cost of generating the matrices and solving the local (elemental) problems in HDG is also considered. But it is crucial to estimate the operation count for the

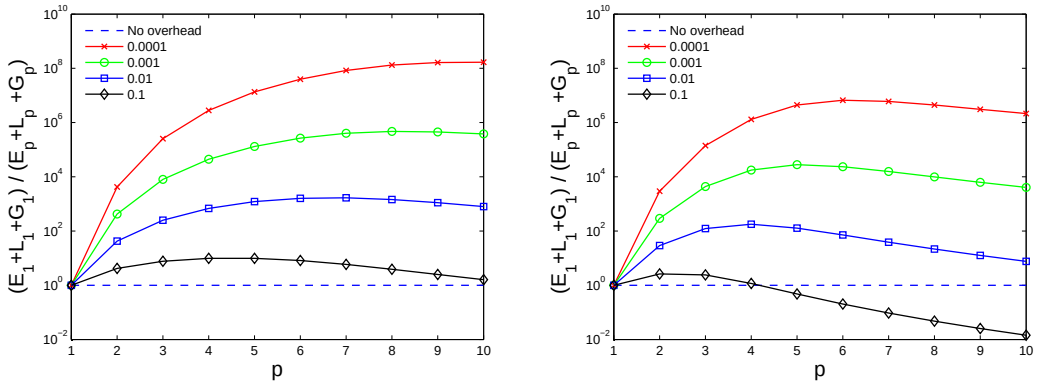

FIGURE 1. Normalized (by order-p elements) cost vs. order p for different error tolerances: tetrahedra (left) and hexahedra (right)

direct solve. For this it is important to note that HDG induces a sparse matrix with uniform pattern and dense blocks (of size the `ndof` in each face). With a duality argument on the faces of the mesh and assuming nested dissection is used to renumber faces the operation count for the global system is

$$G = \left(\frac{d+1}{2}\right)^{(d+1)/2} \left(\frac{d}{p+d}\right)^3 n_{\mathtt{e},p}^{(d+1)/2}\, \mathtt{ndof}_e^3 \qquad \text{for simplexes,}$$

and

$$G = \frac{d^{(d+1)/2}}{(p+1)^3}\, n_{\mathtt{e},p}^{(d+1)/2}\, \mathtt{ndof}_e^3 \qquad \text{for parallelotopes.}$$

Figure 1 shows the total cost (add to the previous expression the cost of generating each local matrix and the cost of the solving the local HDG problems). This is done in a *worse* case scenario (sequential processor). Note that all the elemental computations can be easily parallelized, this is beneficial to high-order approximations. These results show that for a given accuracy, there is an optimal value of $p \geq 1$ and that for *engineering accuracy* (usually two significant digits) high-order always pays-off. On the contrary, in [11] it is stated that it is difficult to improve on linear elements. Two issues support the present conclusions. First, inner degrees of freedom are obviously condensed (also true for CG). Thus, the cost of the global system is only determined by the `ndof` on faces. Second, the $(p+1)!$ factor of the interpolation error is taken into account in (1).

Once high-order is justified, the issue of DG vs. CG is addressed. This is analyzed with a simple operation count for a mesh under the same assumptions as before. In particular, the number of non-zero (`nnz`) terms in the matrix is computed. The results clearly show that for uniform order meshes (same a priori error estimate) the overhead introduced by DG methods is always larger than CG. Table 3 conveys more clearly this conclusion presenting the ratio of the `nnz` for Compact DG (CDG), HDG, and a post-processed HDG (pHDG) solution obtained using the super-convergence property of HDG.

TABLE 3. Ratio of `nnz`, normalized by CG

	triangles			tetrahedra		
p	CDG	HDG	pHDG	CDG	HDG	pHDG
2	3.91	2.93	1.30	8.86	13.14	3.28
5	4.77	1.57	1.09	4.21	3.31	1.69
10	9.08	1.26	1.04	4.88	1.89	1.31

However, it is important to note that an adaptive HDG method would exhibit the best computational efficiency in terms of `ndof` and run-time for this wave propagation problem. The super-convergent post-process of the HDG method is used to construct a simple error estimator. Note that the overhead of such a posteriori error estimate is, in this case, negligible. The error estimator is used to drive an iterative procedure of mesh adaptation aimed at reaching a desired level of error in the zone of interest of the domain. Under these circumstances, p-adaptive high-order HDG is the most efficient technique.

REFERENCES

[1] P. Ladevèze, Nonlinear Computational Structural Mechanics – New Approaches and Non-Incremental Methods of Calculation, Springer-Verlag, 1999.

[2] A. Ammar, B. Mokdad, F. Chinesta, R. Keunings, *A new family of solvers for some classes of multidimensional partial differential equations encountered in kinetic theory modelling of complex fluids*, J. Non-Newton. Fluid Mech. **139**:3 (2006), 153–176.

[3] A. Ammar, B. Mokdad, F. Chinesta, R. Keunings, *A new family of solvers for some classes of multidimensional partial differential equations encountered in kinetic theory modelling of complex fluids. Part II: Transient simulation using space-time separated representations*, J. Non-Newton. Fluid Mech. **144**:2-3 (2007), 98–121.

[4] A. Nouy, *A priori model reduction through Proper Generalized Decomposition for solving time-dependent partial differential equations*, Comput. Methods Appl. Mech. Eng. **199**:23-24 (2010), 1603–1626.

[5] A. Ammar, F. Chinesta, P. Diez and A. Huerta *An error estimator for separated representations of highly multidimensional models*, Comput. Methods Appl. Mech. Eng. **199**:25–28 (2010), 1872–1880.

[6] B. Cockburn, B. Dong, B. and J. Guzmán, *A superconvergent LDG-hybridizable Galerkin method for second-order elliptic problems*, Math. of Comput., **77**:264 (2008), 1887–1916.

[7] B. Cockburn, J. Gopalakrishnan and R. Lazarov *Unified hybridization of discontinuous Galerkin, mixed, and continuous Galerkin methods for second order elliptic problems*, SIAM J. Numer. Anal., **47**:2 (2009), 1319–1365.

[8] N.C. Nguyen, J. Peraire and B. Cockburn, *An implicit high-order hybridizable discontinuous Galerkin method for linear convection-diffusion equations*, J. Comput. Phys., **228**:9 (2009), 3232–3254.

[9] N.C. Nguyen, J. Peraire and B. Cockburn, *A hybridizable discontinuous Galerkin method for Stokes flow*, Comput. Methods Appl. Mech. Eng., **199**:9-12 (2010), 582–597.

[10] N.C. Nguyen, J. Peraire and B. Cockburn, *An implicit high-order hybridizable discontinuous Galerkin method for the incompressible Navier-Stokes equations*, J. Comput. Phys., **230**:4 (2011), 1147–1170.

[11] R. Lohner *Error and work estimates for high-order elements* Int. J. Numer. Meth. Fluids, **67**:12 (2011), 2184–2188.

Isogeometric analysis of solids and structures

Robert L. Taylor

Isogeometric methods have been introduced in an attempt to connect analysis methods more closely to problems defined by CAD systems. The method is described in some detail in the book by Cottrell *et al.*[1]. Output from CAD systems is often in the form of NURBS (non-rational uniform B-splines) which can be refined by degree elevation (p-refinement) and knot insertion (h-refinement). The two together are commonly referred to as 'k-refinement'. Procedures to perform these operations are defined in the book by Piegl and Tiller[2].

Our research is directed to the development of methods to analyze finite deformation behavior. The integration with a CAD system has not been realized in our work and we define our problems manually in terms of control points (nodes) and knot vectors. These are combined to form tensor product surface and solid domains. Subsequent refinement is performed by k-refinement to achieve analysis suitable descriptions. We also have the ability to import regions described by analysis suitable T-splines[3].

To show typical behavior a curved beam subjected to an end shear is considered, Fig. 1(a). This problem has an exact solution that is easily enforced by subjecting x-axis control points to a uniform displacement. The problem is analyzed for the data: $a = 5$, $b = 10$, $E = 10,920$, $\nu = 0.3$ and $u(x, 0) = 0.1$. Using the exact solution the energy error may be computed for different approximations. In Fig. 1(b) we show the error for traditional finite elements where "Qn" denotes a quadrilateral with n nodes. Isogeometric solutions are also shown in which the radial direction is initially a linear NURBS and the circumferential direction a

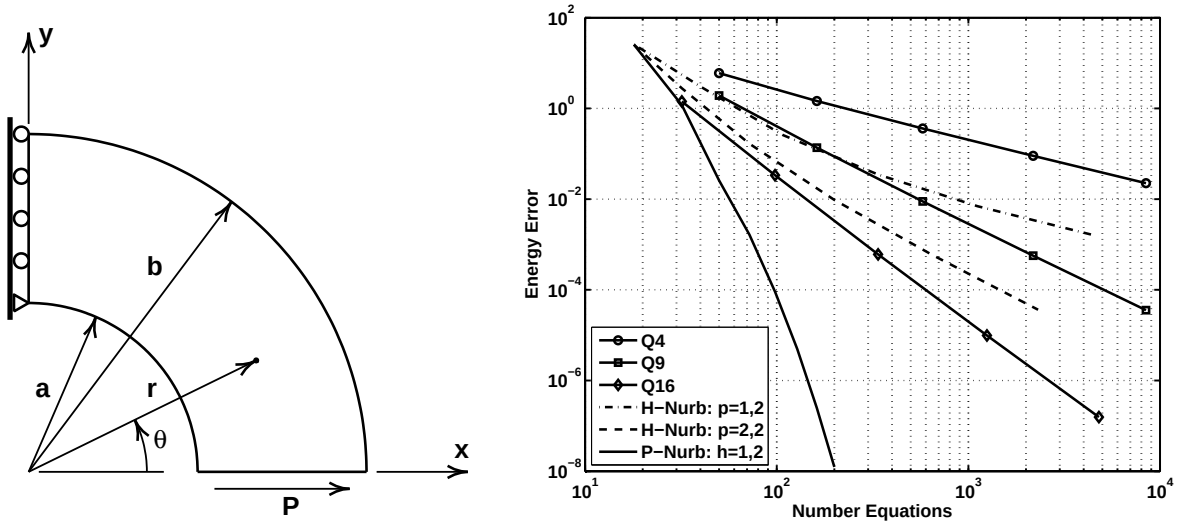

(a) Problem description. (b) Error in energy.

Figure 1. Curved beam subjected to end shear: Problem description and energy errors.

quadratic NURBS. An analysis is shown where only h-refinement is performed and one where the radial direction is elevated to quadratic degree and refined. Finally we show an analysis in which only degree elevation is performed.

A more complex situation arises when finite deformation occurs and the solids are modelled by constitutive models in which near incompressibility occurs. In such situations standard Galerkin solutions employing only displacement approximations do not achieve an optimal solution, especially when low order forms are used. This is also true for NURBS based methods. In engineering applications the use of mixed methods in which displacements are augmented by stress and/or deformation approximations are usually introduced. For solid domains the deformation gradient $\mathbf{F}$ may be split into volumetric and deviatoric parts as

$$\mathbf{F} = \mathbf{F}^v \, \mathbf{F}^d \text{ where } \mathbf{F}^v = J^{1/3} \, \mathbf{I} \text{ and } \mathbf{F}^d = J^{-1/3} \, \mathbf{F}$$

where $J = \det F$. In our mixed form we replace J by $\bar{J}$ and define the mixed deformation gradient and right Cauchy-Green deformation tensor by

$$\bar{\mathbf{F}} = \left(\frac{\bar{J}}{J} \right)^{1/3} \mathbf{F} \text{ and } \bar{\mathbf{C}} = \bar{\mathbf{F}}^T \bar{\mathbf{F}}$$

For a hyperelastic material a variational problem may be defined by

$$\Pi = \int_\Omega \left[W(\bar{\mathbf{C}}) + p \left(J - \bar{J} \right) \right] \, \mathrm{d}\Omega + \Pi_{ext}$$

where $W(\bar{\mathbf{C}})$ denotes a stored energy function and Π_{ext} the boundary and volumetric loading effects. For tensor product NURBS an approximation may be defined in which coordinates and displacements are defined by q degree forms, pressure p by $q-1$ degree forms and $\bar{J}$ by either $q-1$ or discontinuous polynomial forms[4]. This generalizes the approach of Elguedj *et al.*[5] and permits solutions using standard nodal based algorithms. An illustration of the improvement in performance of NURBS based mixed approximations may be observed for a twisted rectangular bar problem. The bar has a square cross section of 1×1 and a length of 5. The material is modeled by a Neohookean material with a small strain bulk modulus of 400942 and a shear modulus of 80.1938. This gives a small strain Poisson ratio of 0.4999. The bar is modeled by quadratic NURBS with k-refinement and twisted to an angle of 90-degrees. The axial stress from a Galerkin displacement method is shown in Fig. 2(a) and that for a mixed solution in Fig. 2(b) using NURBS for displacement and pressure and linear polynomial approximation in each knot interval for $\bar{J}$. The results for the mixed solution compare well with refined finite element solutions. The displacement Galerkin solution produces results with significant errors. Also, of particular note is the robustness of the Newton method used for solution. Very large increments of rotation can be used in the NURBS solutions compared to a standard quadratic finite element solution.

All of our NURBS based solutions are implemented in the general purpose finite element program *FEAP*[6] using user functions. Currently, we are able to analyze problems composed of solids and shells. There are, however, a number of issues that need to be resolved in order to solve realistic engineering problems.

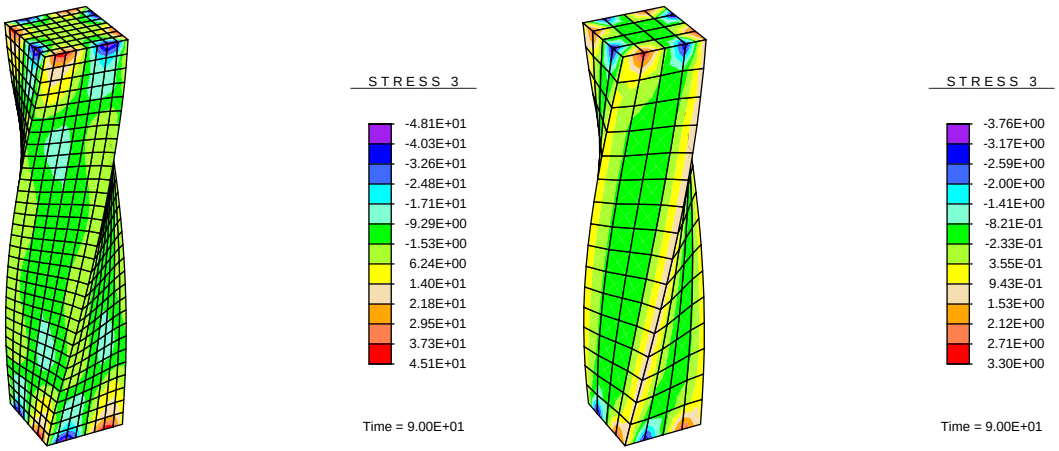

(a) Displacement $\sigma_3 = -48.1$ to -45.1

(b) Mixed $\sigma_3 = -5.75$ to -5.12

FIGURE 2. Twisted bar: Axial stress σ_3 for 90^o twist.

First, is a direct connection to a CAD system in order to generate the models for analysis as well as the features necessary to impose loading and boundary conditions. Since NURBS descriptions are commonly surface based a method to generate the internal knot intervals and control points is needed. For models described by local refinement of NURBS (e.g., T-splines) a more general form to impose constraints is required. For problems in which stresses are computed from models with internal variables such as plastic strain the results are available only at quadrature points. An accurate projection to the control points is required. Currently, this is performed using a local least squares method, however, for high order NURBS this is not stable and improved methods are required.

REFERENCES

[1] J.A. Cottrell and T.J.R. Hughes and Y. Bazilevs, *Isogeometric Analysis: Toward Integration of CAD and FEA*, John Wiley & Sons, New York, (2009).

[2] L. Piegl and W. Tiller, *The NURBS Book (Monographs in Visual Communication)*, 2^{nd} ed., Springer-Verlag, New York, (1997).

[3] M.A. Scott, *T-splines as a Design-Through-Analysis Technology*, The University of Texas at Austin, Austin, Texas, Ph.D dissertation, (2011).

[4] R.L. Taylor, *Isogeometric analysis of nearly incompressible solids*, International Journal for Numerical Methods in Engineering, **87** (2011), 273–288.

[5] T. Elguedj and Y. Bazilevs and V.M. Calo and T.J.R. Hughes, *$\bar{B}$ and $\bar{F}$ projection methods for nearly incompressible linear and non-linear elasticity and plasticity using higher-order NURBS elements*, Computer Methods in Applied Mechanics & Engineering, **197** (2008), 2732–2762.

[6] R.L. Taylor, *FEAP - A Finite Element Analysis Program, User Manual*, University of California, Berkeley, `http://www.ce.berkeley.edu/feap`.

Isogeometric Analysis of Multi-Physics Problems: Formulations, Coupling, and Applications

Yuri Bazilevs
(joint work with Ming-Chen Hsu, Ido Akkerman)

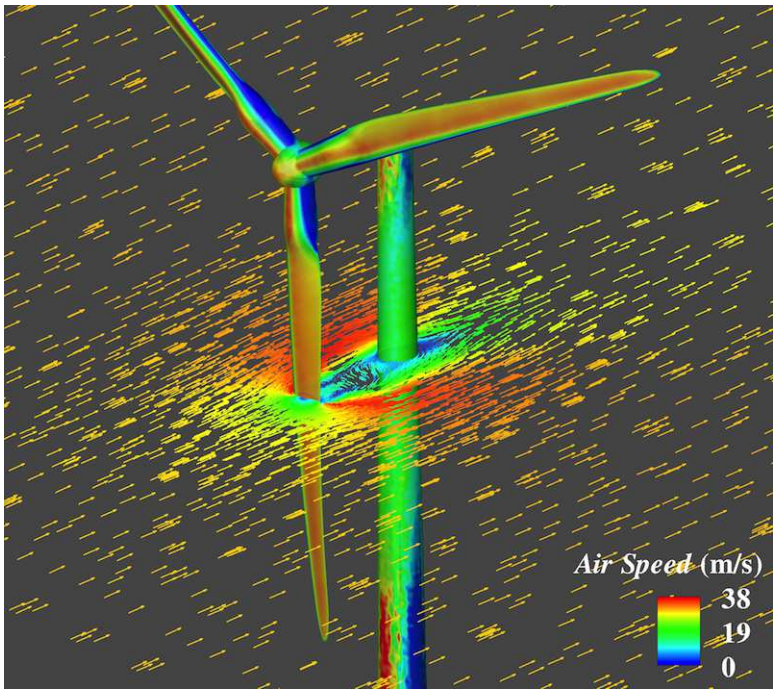

Figure 1. Fluid–structure interaction of a wind turbine in 3D. Example of a simulation, in which it is beneficial to make use of non-matching fluid and structural discretizations. In this case, standard FEM is used for aerodynamics, while isogeometric Kirchhoff–Love shell is employed for the rotor blades. The former significantly simplifies the model and mesh generation process, while the latter provides a very efficient structural discretization.

Isogeometric Analysis (IGA) [1], despite its young age, has significantly matured as a technology for geometry representation and computational analysis. Although NURBS remain the most popular means of geometry modeling for IGA, advances in T-Spline and Subdivison surface representations enabled the solution of computational problems requiring local mesh refinement, which is not easily accomplished with NURBS. Advances in model quality definition and improvement enabled the generation of better parameterized shapes for IGA, thus improving the quality of the computational solution.

Recent efforts to define standardized file formats for data exchange between the geometry modeling and computational analysis software enabled straightforward solution of complicated structural problems that involve large deformation, plasticity and contact, using well-validated commercial FEM software. Furthermore,

IGA is able to naturally handle many applications that otherwise create significant challenges to standard finite element technology.

However, many challenges remain for IGA to be fully accepted as an industrial-grade analysis technology. The ability to create 3D volumetric complex geometry models in an automated manner is one such challenge. Another challenge is to prove that IGA is capable of producing accurate and robust results for complex-geometry multi-physics problems (e.g., fluid-structure interaction), which is one of the major demands of modern computational analysis.

This presentation focused on the coupling strategies, specific to IGA, for multi-physics applications that make use of non-matching descriptions of geometry at the interface between different physical subsystems, as well as different subdomains of a single physical system. These coupling procedures allow greater flexibility in the computational analysis, and, simultaneously, alleviate the difficulties of geometry modeling and construction of interfaces that exactly match geometrically and parametrically (see, e.g., Figure 1).

References

[1] T.J.R. Hughes, J.A. Cottrell, and Y. Bazilevs, *Isogeometric analysis: CAD, finite elements, NURBS, exact geometry and mesh refinemen*, Computer Methods in Applied Mechanics and Engineering **194** (2005), 4135–4195.

Finite Element Methods for a Fourth Order Obstacle Problem

Susanne C. Brenner

(joint work with Christopher B. Davis, Li-yeng Sung, Hongchao Zhang, Yi Zhang)

Let Ω be a bounded convex polygonal domain in $\mathbb{R}^2$. The following optimization problem provides a mathematical model for the bending of a clamped Kirchhoff plate over an obstacle: Find $u \in H_0^2(\Omega)$ such that

$$u = \operatorname*{argmin}_{v \in K} \Big[\frac{1}{2}a(v,v) - (f,v)\Big], \tag{1}$$

where u is the vertical displacement of the middle surface of a thin plate with Ω as the configuration domain, $K = \{v \in H_0^2(\Omega) : v \geq \psi \quad \text{in} \quad \Omega\}$, $\psi \in C^2(\bar{\Omega})$ is the obstacle function, $f \in L_2(\Omega)$ is the load density divided by the flexural rigidity,

$$a(w,v) = \int_\Omega \sum_{i,j=1}^{2} w_{x_i x_j} v_{x_i x_j}\, dx \quad \text{and} \quad (f,v) = \int_\Omega f v\, dx.$$

We assume $\psi < 0$ on $\partial\Omega$.

Since the symmetric bilinear form $a(\cdot,\cdot)$ is bounded and coercive on $H_0^2(\Omega)$, it follows from the standard theory [11] that the obstacle problem (1) has a unique solution characterized by the following variational inequality

$$a(u, v-u) \geq (f, v-u) \qquad \forall\, v \in K. \tag{2}$$

The solution u of (1) belongs to $H^3(\Omega) \cap C^2(\Omega)$, but in general u does not belong to $H^4(\Omega)$ even for smooth data [10, 7]. Thus the complementarity form of (2) only exists in the following weak sense: There exists a nonnegative Borel measure μ supported on the coincidence set $\mathcal{I} = \{x \in \Omega : u(x) = \psi(x)\}$ such that $\Delta^2 u - f$ (in the sense of distributions) is given by the linear functional $\phi \to \int_\Omega \phi \, d\mu$. This is the main difference between the plate obstacle problem and the membrane obstacle problem, where the complementarity form of the second order variational inequality exists in a strong sense because the solution of the membrane obstacle problem belongs to $H^2(\Omega)$ under appropriate assumptions [5]. This difference significantly complicates the numerical analysis of (1)/(2).

Consider a C^1 finite element method where u is approximated by

$$u_h = \operatorname*{argmin}_{v \in K_h} \Big[\frac{1}{2} a(v, v) - (f, v)\Big]. \tag{3}$$

Here

$$K_h = \{v \in V_h : v(p) \geq \psi(p) \; \forall \, p \in \mathcal{V}_h\}, \tag{4}$$

V_h is for example the Hsieh-Clough-Tocher macro finite element space associated with a triangulation of Ω, and $\mathcal{V}_h$ is the set of the vertices of $\mathcal{T}_h$. By a standard argument using the boundedness and coercivity of $a(\cdot, \cdot)$ and the discrete variational inequality for (3), we have

$$|u - u_h|^2_{H^2(\Omega)} \leq C_1 |u - \Pi_h u|^2_{H^2(\Omega)} + C_2 [a(u, \Pi_h u - u_h) - (f, \Pi_h u - u_h)], \tag{5}$$

where $\Pi_h : H^3(\Omega) \longrightarrow V_h$ is a quasi-interpolant such that

$$|u - \Pi_h u|_{H^2(\Omega)} \leq Ch |u|_{H^3(\Omega)}.$$

Hence an optimal $O(h)$ error estimate for $|u - u_h|_{H^2(\Omega)}$ requires an estimate of the form

$$a(u, \Pi_h u - u_h) - (f, \Pi_h u - u_h) \leq Ch^2.$$

However, if we follow the second order approach [9, 6] we will only have a suboptimal estimate. Indeed, if $\mathcal{I}_h$ is the nodal interpolation operator for the P_1 finite element space associated with $\mathcal{T}_h$ (so that $\mathcal{I}_h \psi - \mathcal{I}_h u_h \leq 0$ on Ω), then proceeding as in the second order case will lead to the estimate

$$\begin{aligned}
a(u, \Pi_h u - u_h) - (f, \Pi_h u - u_h) &= \int_\Omega (\Pi_h u - u_h) d\mu \\
&= \int_\Omega [(\Pi_h u - u) + (u - \psi) + (\psi - \mathcal{I}_h \psi) + (\mathcal{I}_h \psi - \mathcal{I}_h u_h) + (\mathcal{I}_h u_h - u_h)] d\mu \\
&\leq \int_\Omega [(\Pi_h u - u) + (\psi - \mathcal{I}_h \psi) + (\mathcal{I}_h u_h - u_h)] d\mu \\
&\leq \mu(\Omega) [\|\Pi_h u - u\|_{L_\infty(\Omega)} + \|\psi - \mathcal{I}_h \psi\|_{L_\infty(\Omega)} + \|\mathcal{I}_h u_h - u_h\|_{L_\infty(\Omega)}] \\
&\leq C[h^2 |u|_{H^3(\Omega)} + h^2 |\psi|_{W^2_\infty(\Omega)} + h |u_h|_{H^2(\Omega)}],
\end{aligned}$$

which is suboptimal.

A general framework for obtaining optimal error estimates for finite element methods for (1)/(2) was introduced in [4]. The finite element approximation is

$$u_h = \operatorname*{argmin}_{v\in K_h} \Big[\frac{1}{2}a_h(v,v) - (f,v)\Big], \tag{6}$$

where the finite element space V_h in the definition of K_h (cf. (4)) can be a C^1 finite element space, a classical nonconforming finite space, or a C^0 Lagrange finite element space, as long as the functions in V_h are continuous at the vertices of $\mathcal{T}_h$. The bilinear form $a_h(\cdot,\cdot)$ is (i) identical with $a(\cdot,\cdot)$ for C^1 finite element methods, (ii) a piecewise version of $a(\cdot,\cdot)$ for classical nonconforming finite element methods, and (iii) a piecewise version of $a(\cdot,\cdot)$ plus symmetrization and stabilization terms for C^0 interior penalty methods. The discrete obstacle problem (6) is equivalent to the variational inequality

$$a_h(u_h, v-u_h) \geq (f, v-u_h) \qquad \forall\, v\in K_h. \tag{7}$$

We were able to show that all these methods have $O(h)$ error in the energy norm, without using the complementarity form of the variational inequality (2). The key idea is to define an intermediate auxiliary obstacle problem

$$\tilde{u}_h = \operatorname*{argmin}_{v\in \tilde{K}_h} \Big[\frac{1}{2}a(v,v) - (f,v)\Big] \tag{8}$$

where

$$\tilde{K}_h = \{v\in H_0^2(\Omega) :\, v(p)\geq \psi(p)\ \forall\, p\in \mathcal{V}_h\}. \tag{9}$$

This problem shares the space $H_0^2(\Omega)$ with the continuous problem (1) and the constraints with the discrete problem (6). Therefore it can be used as a bridge to connect (1) and (6). The convergence analysis based on this new approach involves only the variational inequalities (2) and (7), and the variational inequality

$$a(\tilde{u}_h, v-\tilde{u}_h) \geq (f, v-\tilde{u}_h) \qquad \forall\, v\in \tilde{K}_h$$

for the obstacle problem (8). The complementarity form of these variational inequalities are not needed.

The extension of the results in [4] to nonconvex domains and general Dirichlet boundary conditions have been carried out in [3, 2, 1], where the convergence of u_h to u in $L_\infty(\Omega)$ and convergence of the discrete free boundaries to the continuous free boundaries are also addressed.

This new approach can be applied to the obstacle problem of simply supported plates. It is also relevant for certain optimal control problems with state constraints [8, 12].

References

[1] S.C. Brenner, C.B. Davis and L.-Y. Sung. *A generalized finite element method for the displacement obstacle problem of clamped Kirchhoff plates*, (in preparation), 2012.

[2] S.C. Brenner, L.-Y. Sung, H. Zhang, and Y. Zhang. *A Morley finite element method for the displacement obstacle problem of clamped Kirchhoff plates*, preprint, 2011.

[3] S.C. Brenner, L.-Y. Sung, H. Zhang, and Y. Zhang. *A quadratic C^0 interior penalty method for the displacement obstacle problem of clamped Kirchhoff plates*, preprint, 2011.
[4] S.C. Brenner, L.-Y. Sung, and Y. Zhang. *Finite element methods for the displacement obstacle problem of clamped plates*, Math. Comp., (to appear).
[5] H. R. Brezis and G. Stampacchia. *Sur la régularité de la solution d'inéquations elliptiques*, Bull. Soc. Math. France **96** (1968), 153–180.
[6] F. Brezzi, W. Hager, and P.-A. Raviart. *Error estimates for the finite element solution of variational inequalities*, Numer. Math. **28** (1977), 431–443.
[7] L.A. Caffarelli and A. Friedman. *The obstacle problem for the biharmonic operator*. Ann. Scuola Norm. Sup. Pisa Cl. Sci. (4) **6** (1979), 151–184.
[8] E. Casas. *Control of an elliptic problem with pointwise state control*, SIAM J. Control Optim. **24** (1986), 1309–1318.
[9] R.S. Falk. *Error estimates for the approximation of a class of variational inequalities*, Math. Comp. **28** (1974), 963–971.
[10] J. Frehse. *Zum Differenzierbarkeitsproblem bei Variationsungleichungen höherer Ordnung*, Abh. Math. Sem. Univ. Hamburg **36** (1971), 140–149.
[11] J.-L. Lions and G. Stampacchia. *Variational inequalities*, Comm. Pure Appl. Math. **20** (1967), 493–519.
[12] W. Liu, W. Gong and N. Yan. *A new finite element approximation of a state-constrained optimal control problem*, J. Comp. Math. **27** (2009), 97–114.

Comparison results for first-order FEMs

Mira Schedensack
(joint work with Carsten Carstensen, Daniel Peterseim)

Various first-order finite element methods are known for the Poisson Model Problem (1) and for linear elasticity (2). The recent publications [1] started the comparison between some of these methods for the Poisson Model Problem, which is completed in this presentation and its underlying paper [3].

Given a bounded polygonal Lipschitz domain Ω in the plane and data $f \in L^2(\Omega)$, the Poisson model problem seeks the weak solution $u \in H^1(\Omega)$ of

$$-\Delta u = f \text{ in } \Omega \quad \text{and} \quad u = 0 \text{ on } \partial\Omega. \tag{1}$$

This presentation compares the error of three popular finite element methods (FEM) of Figure 1 for the numerical solution of (1), namely the conforming *Courant* FEM (CFEM) [4], the nonconforming *Crouzeix-Raviart* FEM (CR-NCFEM) [5], and the mixed *Raviart-Thomas* FEM (RT-MFEM) [7] with respective solutions u_{C}, u_{CR}, and $(p_{\mathrm{RT}}, u_{\mathrm{RT}})$ based on a shape-regular triangulation $\mathcal{T}$ of Ω into triangles. The finite element space of CFEM reads $P_1(\Omega) \cap C_0(\Omega)$ for

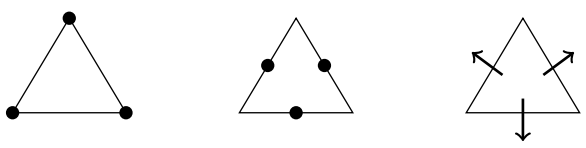

Figure 1. CFEM (left), CR-NCFEM (middle), RT-MFEM (right).

$C_0(\Omega)$ the continuous functions with zero boundary conditions. The finite element

space of Crouzeix-Raviart $\mathrm{CR}^1_0(\mathcal{T})$ consists of all piecewise affines which are continuous at the midpoints of interior edges and vanish at the midpoints of exterior edges. The Raviart-Thomas finite element space for the flux approximation reads $\mathrm{RT}_0(\mathcal{T}) := \{p_{\mathrm{RT}} \in P_1(\mathcal{T},\mathbb{R}^2) \cap H(\mathrm{div},\Omega) \,|\, \forall T \in \mathcal{T}\, \exists\, a_T, b_T, c_T \in \mathbb{R} : p_{\mathrm{RT}}|_T(x) = (a_T, b_T) + c_T x\}$.

The comparison is stated in terms of $A \lesssim B$ which abbreviates the existence of some constant C which only depends on the minimal angle in $\mathcal{T}$, but not on the domain Ω and not on the mesh-size $h_{\mathcal{T}}$, such that $A \leq CB$. The comparison includes data oscillations, namely $\mathrm{osc}(f,\mathcal{T}) := \|h_{\mathcal{T}}(f - \Pi_0 f)\|$ where Π_0 denotes the L^2 orthogonal projection onto the piecewise constants.

The comparison result for CFEM, CR-NCFEM and RT-MFEM states that the errors of CFEM and CR-NCFEM are equivalent up to data oscillations, in the sense that

$$\|\nabla u - \nabla u_{\mathrm{C}}\| \lesssim \|\nabla u - \nabla_{\mathrm{NC}} u_{\mathrm{CR}}\| \lesssim \|\nabla u - \nabla u_{\mathrm{C}}\| + \mathrm{osc}(f,\mathcal{T}).$$

The error of RT-MFEM is superior in the sense that

$$\|\nabla u - \nabla_{\mathrm{NC}} u_{\mathrm{CR}}\| \lesssim \|h_{\mathcal{T}} f\| + \|\nabla u - p_{\mathrm{RT}}\| \lesssim \|\nabla u - \nabla_{\mathrm{NC}} u_{\mathrm{CR}}\| + \mathrm{osc}(f,\mathcal{T}),$$

but the converse is false, i.e.,

$$\|\nabla u - \nabla_{\mathrm{NC}} u_{\mathrm{CR}}\| \not\lesssim \|\nabla u - p_{\mathrm{RT}}\| + \mathrm{osc}(f,\mathcal{T}).$$

The proof of the inequalities is an example of the medius analysis for it combines arguments of an *a priori* with those of an *a posteriori* error analysis. It is emphasised that no regularity assumption is made and the results hold for arbitrary coarse triangulations and not just in an asymptotic regime. The proof of the superiority of RT-MFEM considers a sequence of domains, on which the RT-MFEM has a steeper convergence rate than CR-NCFEM.

The results for the Poisson Model Problem can be generalised for the Navier-Lamé equations from linear elasticity, which seek $u \in H^1_0(\Omega;\mathbb{R}^2)$ with

$$f + 2\mu\Delta u + (\mu+\lambda)\nabla(\mathrm{div}\, u) = 0 \ \text{ in } \Omega. \tag{2}$$

The compared FEMs are the conforming *Courant* FEM (CFEM) [2], the nonconforming *Kouhia-Stenberg* FEM (KS-NCFEM) [6], and the nonconforming *Crouzeix-Raviart* FEM (CR-NCFEM) [2] with respective solutions σ_{C}, σ_{KS} and σ_{CR}. The finite element space of KS-NCFEM reads $\mathrm{KS} := (P_1(\mathcal{T}) \cap C_0(\Omega)) \times \mathrm{CR}^1_0(\mathcal{T})$. The discretisation of CFEM and KS-NCFEM is based on the bilinear form

$$a(u_{\mathrm{KS}}, v_{\mathrm{KS}}) := \int_\Omega \varepsilon_{\mathrm{NC}}(u_{\mathrm{KS}}) : \mathbb{C}\varepsilon_{\mathrm{NC}}(v_{\mathrm{KS}})\, dx,$$

while the discretisation of CR-NCFEM involves the bilinear form

$$a(u_{\mathrm{CR}}, v_{\mathrm{CR}}) := \int_\Omega \big(\mu\, D_{\mathrm{NC}} u_{\mathrm{CR}} : D_{\mathrm{NC}} v_{\mathrm{CR}} + (\mu+\lambda)\ \mathrm{div}_{\mathrm{NC}}\, u_{\mathrm{CR}}\, \mathrm{div}_{\mathrm{NC}}\, v_{\mathrm{CR}}\big) dx.$$

The comparison result for linear elasticity involves the Lamé modulus λ, which effects the locking and the $\lesssim$ notation means, that, in addition, the underlying

constants do not depend on the Lamé modulus λ. Then

$$\|\sigma - \sigma_{\mathrm{C}}\| \lesssim \lambda \, \|\sigma - \sigma_{\mathrm{KS}}\| \lesssim \lambda \, \big(\|\sigma - \sigma_{\mathrm{C}}\| + \operatorname{osc}(f, \mathcal{T})\big)$$

and

$$\|\sigma - \sigma_{\mathrm{KS}}\| + \operatorname{osc}(f, \mathcal{T}) \approx \|\sigma - \sigma_{\mathrm{CR}}\| + \operatorname{osc}(f, \mathcal{T}).$$

References

[1] D. Braess, *An a posteriori error estimate and a comparison theorem for the nonconforming P_1 elemen*, Calcolo **46** (2009), 149–155.

[2] S.C. Brenner, L.R. Scott, *The mathematical theory of finite element methods*, Texts in Applied Mathematics **15** (2008).

[3] C. Carstensen, D. Peterseim, M. Schedensack, *Comparison Results of Three First-order Finite Element Methods for the Poisson Model Problem*, Preprint **#831** (2011).

[4] R. Courant, *On a method for the solution of boundary-value problems*, in: Theodore von Kármán Anniversary Volume (1941), 189–194.

[5] M. Crouzeix, P.A. Raviart, *Conforming and nonconforming finite element methods for solving the stationary Stokes equations. I*, Rev. Française Automat. Informat. Recherche Opérationnelle Sér. Rouge **7** (1973), 33–75.

[6] R. Kouhia, R. Stenberg, *A linear nonconforming finite element method for nearly incompressible elasticity and Stokes flow*, Comput. Methods Appl. Mech. Engrg. **124** (1995), 195–212.

[7] P.A. Raviart, J.M. Thomas *A mixed finite element method for 2nd order elliptic problems*, in: Mathematical aspects of finite element methods (Proc. Conf., Consiglio Naz. delle Ricerche (C.N.R.), Rome, 1975) (1977), 292–315.

Quasi optimal adaptive pseudostress approximation of the Stokes equations

Dietmar Gallistl

(joint work with Carsten Carstensen, Mira Schedensack)

The pseudostress-velocity formulation [3, 5] of the stationary Stokes equations

$$-\Delta u + \nabla p = f \quad \text{and} \quad \operatorname{div} u = 0 \quad \text{in } \Omega \tag{1}$$

with Dirichlet boundary conditions along the polygonal boundary $\partial\Omega$ allows the stresses-like variables σ in Raviart-Thomas mixed finite element spaces [2] $\mathrm{RT}_k(\mathcal{T})$ with respect to a regular triangulation $\mathcal{T}$, and hence allows for higher flexibility in arbitrary polynomial degrees.

The weak form of problem (1) is formally equivalent and reads: Given $f \in L^2(\Omega;\mathbb{R}^2)$ and $g \in H^1(\Omega;\mathbb{R}^2) \cap H^1(\mathcal{E}(\partial\Omega);\mathbb{R}^2)$ with $\int_{\partial\Omega} g \cdot \nu \, ds = 0$ seek $\sigma \in H(\operatorname{div}, \Omega; \mathbb{R}^{2\times 2})/\mathbb{R}$ and $u \in L^2(\Omega;\mathbb{R}^2)$ such that

$$\begin{aligned} \int_\Omega \operatorname{dev} \sigma : \tau \, dx + \int_\Omega u \cdot \operatorname{div} \tau \, dx &= \int_{\partial\Omega} g \cdot \tau \, \nu \, ds, \\ \int_\Omega v \cdot \operatorname{div} \sigma \, dx &= -\int_\Omega f \cdot v \, dx \end{aligned} \tag{2}$$

for all $(\tau, v) \in H(\mathrm{div}, \Omega; \mathbb{R}^{2\times 2})/\mathbb{R} \times L^2(\Omega; \mathbb{R}^2)$, where the deviatoric part of the tensor σ reads $\mathrm{dev}\,\sigma := \sigma - 1/2\ \mathrm{tr}(\sigma) I_{2\times 2}$. The discrete formulation of (2) seeks $\sigma_{\mathrm{PS}} \in \mathrm{PS}(\mathcal{T}) := \mathrm{RT}_k(\mathcal{T}) \cap H(\mathrm{div}, \Omega; \mathbb{R}^{2\times 2})/\mathbb{R}$ and $u_{\mathrm{PS}} \in P_0(\mathcal{T}_\ell; \mathbb{R}^2)$ such that

$$\int_\Omega \mathrm{dev}\,\sigma_{\mathrm{PS}} : \tau_{\mathrm{PS}}\, dx + \int_\Omega \mathrm{div}\,\tau_{\mathrm{PS}} \cdot u_{\mathrm{PS}}\, dx = \int_{\partial\Omega} g \cdot \tau_{\mathrm{PS}} \nu\, ds$$
$$\int_\Omega \mathrm{div}\,\sigma_{\mathrm{PS}} \cdot v_{\mathrm{PS}}\, dx = -\int_\Omega f \cdot v_{\mathrm{PS}}\, dx$$

for all $(\tau_{\mathrm{PS}}, v_{\mathrm{PS}}) \in \mathrm{PS}(\mathcal{T}) \times P_k(\mathcal{T}; \mathbb{R}^2)$.

The reliability and efficiency up to data oscillations of the explicit residual-based error estimator η_ℓ have been established in [5]. The contributions on each triangle T with edges $E \in \mathcal{E}(T)$ and tangents τ_E and jumps $[\cdot]_E$ read

$$\eta^2(T) := \mathrm{osc}^2(f, T) + |T|\, \|\mathrm{curl}(\mathrm{dev}\,\sigma_{\mathrm{PS}})\|^2_{L^2(T)} + |T|^{1/2} \sum_{E\in\mathcal{E}(T)} \|[\mathrm{dev}\,\sigma_{\mathrm{PS}}]_E \tau_E\|^2_{L^2(E)}.$$

This gives rise to run the following adaptive algorithm APSFEM with the steps Solve, Estimate, Mark, Refine, in each loop iteration.

Input: Initial triangulation $\mathcal{T}_0$, bulk parameter $0 < \theta < \theta_0 \ll 1$
Loop: For $\ell = 0, 1, 2, \ldots$
Solve. Compute (u_ℓ, σ_ℓ) with respect to the triangulation $\mathcal{T}_\ell$
Estimate. Compute the piecewise contributions of η_ℓ
Mark. Mark minimal subset $\mathcal{M}_\ell \subset \mathcal{T}_\ell$ such that

$$\theta\eta_\ell^2 \le \eta_\ell^2(\mathcal{M}_\ell) := \sum_{T\in\mathcal{M}_\ell} \eta_\ell^2(T).$$

Refine. Refine $\mathcal{M}_\ell$ in $\mathcal{T}_\ell$ with newest vertex bisection, generate $\mathcal{T}_{\ell+1}$
Output: Sequences $(\mathcal{T}_\ell)_\ell$ and $(u_\ell, \sigma_\ell)_\ell$

The definition of quasi-optimal convergence is based on the concept of approximation classes. For $s > 0$, let

$$\mathcal{A}_s := \big\{(\sigma, f, g) \in H(\mathrm{div}, \Omega; \mathbb{R}^{2\times 2})/\mathbb{R} \times L^2(\Omega; \mathbb{R}^2) \times \big(H^1(\Omega; \mathbb{R}^2) \cap H^1(\mathcal{E}(\partial\Omega); \mathbb{R}^2)\big) \,\big|\, |(\sigma, f, g)|_{\mathcal{A}_s} < \infty\big\}$$

with $|(\sigma, f, g)|_{\mathcal{A}_s} :=$

$$\sup_{N\in\mathbb{N}} N^s \inf_{|\mathcal{T}|-|\mathcal{T}_0|\le N} \Big(\|\mathrm{dev}(\sigma - \sigma_{\mathcal{T}})\|^2_{L^2(\Omega)} + \mathrm{osc}^2(f, \mathcal{T}) + \mathrm{osc}^2\big(\frac{\partial g}{\partial s}, \mathcal{E}(\partial\Omega)\big)\Big)^{1/2}.$$

In the infimum, $\mathcal{T}$ runs through all admissible triangulations (with respective discrete solutions $\sigma_{\mathcal{T}}$) that are refined from $\mathcal{T}_0$ by newest vertex bisection of [1, 7] and that satisfy $|\mathcal{T}| - |\mathcal{T}_0| \le N$. The main result relies on a novel observation from ongoing work of Carstensen, Kim, and Park on the equivalence with nonconforming schemes in the spirit of [6] and is therefore restricted to the lowest-order Raviart-Thomas finite element functions. The main theorem states quasi-optimal convergence in the following sense. For any sufficienty small bulk parameter $0 < \theta < \theta_0$

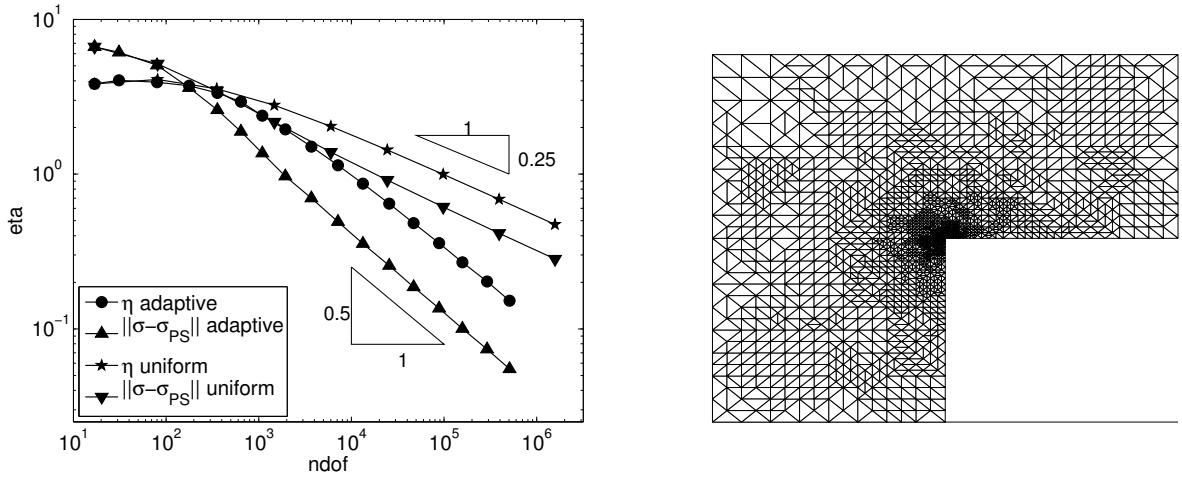

FIGURE 1. Convergence history for uniform and adaptive mesh-refinement in the L-shaped domain example and mesh generated by APSFEM.

and $(\sigma, f, g) \in \mathcal{A}_s$, APSFEM generates sequences of triangulations $(\mathcal{T}_\ell)_\ell$ and discrete solutions $(u_\ell, \sigma_\ell)_\ell$ of optimal rate of convergence in the sense that

$$(|\mathcal{T}_\ell| - |\mathcal{T}_0|)^s \Big(\|\mathrm{dev}(\sigma - \sigma_\ell)\|^2_{L^2(\Omega)} + \mathrm{osc}^2(f, \mathcal{T}_\ell) + \mathrm{osc}^2(\partial g/\partial s, \mathcal{E}_\ell(\partial\Omega)) \Big)^{1/2} \leq C_{\mathrm{opt}} \, |(\sigma, f, g)|_{\mathcal{A}_s} \, .$$

The main ingredients of the proof are the quasi-orthogonality, which leads to a contraction of some linear combination of error, estimator, and data oscillations, and the discrete reliability. Those are established for the lowest-order case.

REFERENCES

[1] P. Binev, W. Dahmen, and R. DeVore, *Adaptive finite element methods with convergence rates*, Numer. Math. **97** (2004), 219–268.

[2] S.C. Brenner and L.R. Scott, *The Mathematical Theory of Finite Element Methods*, Texts in Applied Mathematics, **15** (2008), 3rd edition, New York, Berlin, Heidelberg.

[3] Z. Cai, C. Tong, P.S. Vassilevski, and C. Wang, *Mixed finite element methods for incompressible flow: Stationary Stokes equations*, Numer. Methods Part. Diff. Eqs. **26** (2010), 957–978.

[4] C. Carstensen, D. Gallistl, and M. Schedensack, *Quasi optimal adaptive pseudostress approximation of the Stokes equations*, In preparation (2012).

[5] C. Carstensen, D. Kim, and E.J. Park, *A Priori and A Posteriori Pseudostress-Velocity Mixed Finite Element Error Analysis for the Stokes Problem*, SIAM J. Numer. Anal. **49** (2011), 2501–2523.

[6] L.D. Marini, *An inexpensive method for the evaluation of the solution of the lowest order Raviart-Thomas mixed method*, SIAM J. Numer. Anal. **22** (1985), 493–496.

[7] R. Stevenson, *The completion of locally refined simplicial partitions created by bisection*, Mathematics of Computation **77** (2008), 227–241.

Model reduction in nonlinear biomechanics

Stefanie Reese
(joint work with Annika Radermacher)

The constantly rising requirements of accuracy and complexity of simulations in various fields, especially in biomechanical applications, together with the nonlinearity of those systems lead to numerical models with an increasing number of degrees-of-freedom (dof). Biomechanical simulations, such as surgery training programs or online supports should be performed in minimal computational time (possibly in real time) and provide results with a high level of accuracy. Therefore model reduction is needed to allow for the required real time simulation. There exist a variety of different approaches to reduce a problem in the literature. In the medical field, one often uses spring mass (e.g. [8]) or tensor mass systems (e.g. [4]) for training simulations. In other research fields like turbulence modeling, fluid dynamics, image processing or signal analysis many different model reduction methods exist. Based on [1] two classes of model reduction methods are identified: the singular value decomposition (SVD)-based methods and the Krylov-based methods. The methods which we will discuss here are SVD-based reduction methods. These methods project the equation system on a subspace of smaller dimension $\mathbf{\Phi}$. There exist a lot of different possibilities to choose this subspace. For instance, the modal basis reduction (MOD) method (e.g. [10]) developed in the field of dynamical structural analysis chooses the modal eigenforms as subspace. In the load-dependent Ritz (RITZ) method (e.g. [11]) these eigenvectors are approximated by the so-called Ritz vectors. The promising proper orthogonal decomposition (POD) method (e.g. [9, 3, 2]) builds up the subspace by using snapshots from a precomputation. All concepts mentioned above were developed and are widely used for solving linear problems. There exist a few strategies to expand these methods to nonlinear mechanical systems (e.g. [6, 7]). Especially in biomechanical applications Niroomandi et al. [12] and Dogan and Serdar [5] use proper orthogonal decomposition based methods to reduce their systems.

Reduction. The discrete form of the general equations of nonlinear solid mechanics

$$\mathbf{G}(\mathbf{U}) = \mathbf{R}(\mathbf{U}) - \mathbf{P} = \mathbf{0} \tag{1}$$

is based on the momentum equation. $\mathbf{R}$ is the residual force vector, $\mathbf{P}$ the external load vector and $\mathbf{U}$ the global vector of nodal displacements. The dimension of this equation is n, the number of dofs. To reduce eq. (1) the SVD-based methods use the approximation $\mathbf{U} \approx \mathbf{\Phi}\mathbf{U}_{red}$ for the displacement vector. The reduced vector of unknowns $\mathbf{U}_{red}$ has a dimension of $m \times 1$ with $m \ll n$. Inserting this approximation [13] into the linearization of eq. (1) leads to the reduced equation

$$\mathbf{\Phi}^T\mathbf{G}(\mathbf{\Phi}\mathbf{U}_{red,i}) + \mathbf{\Phi}^T\mathbf{K}_T(\mathbf{\Phi}\mathbf{U}_{red,i})\mathbf{\Phi}\Delta\mathbf{U}_{red,i+1} = \mathbf{0}. \tag{2}$$

In the latter relation i represent the Newton iteration step. Note that the $m \times n$ dimensional subspace matrix $\mathbf{\Phi}$ is held constant during one load step. There are

different possibilities to choose the subspace matrix. By using the POD method the subspace matrix is built up from a certain data set, the so-called snapshots. To collect the snapshots the full system has to be computed beforehand in a precomputation. The solution vectors are saved in the snapshot matrix $\mathbf{D} = [\mathbf{U}(t_1), \mathbf{U}(t_2), ..., \mathbf{U}(t_l)]$. The first m eigenvectors of the correlation matrix $\mathbf{R} = 1/l\ \mathbf{D}^T\mathbf{D}$ are used to fill the subspace matrix $\mathbf{\Phi}$. The computation of eq. (2) is here denoted as the reduced computation.

Numerical examples. To compare the three model reduction methods (MOD, RITZ, POD) a cube under compression with large deformation with different material laws (hyperelastic, viscoelastic and elastoplastic) is investigated. The model reduction methods are implemented into the finite element solver FEAP developed by Taylor [14]. Figure 1 shows the results for the elastoplastic cube. It is obvious

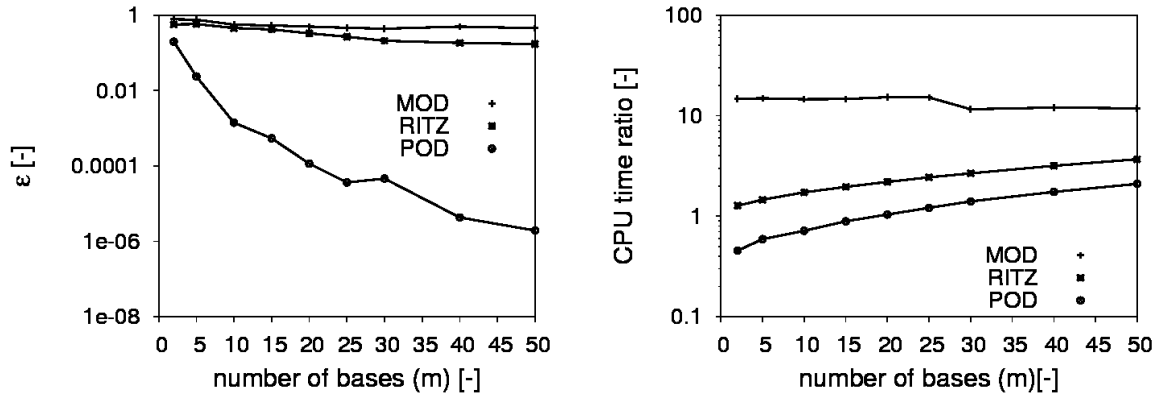

FIGURE 1. Error and CPU time ratio of the three methods.

that the POD method leads to the smallest error in the displacement averaged over time. Additionally, the POD method reaches the largest reduction of the CPU time ratio. Furthermore we have studied different POD parameters such as the time increments, the total time of the precomputation and the number of bases. The best approximation is reached by using the same time increments and the same total time values in the precomputation and in the reduced computation. A suitable number of bases can be found by a study of the eigenvalues of the correlation matrix. Figure 2 shows the reduction of a realistic biomechanical model of a simplified inferior turbinate. The results shows, that a reduction to about 0.1% of the original number of dofs leads to a satisfactory good approximation of displacements and stresses while simultaneously reducing the computational time enormously. In spite of this very large reduction in CPU time, the desired real time requirement is currently not reached. To reduce the CPU time further, we intend to modify the assembly of the reduced matrix and investigate other solver strategies (e.g. BFGS). Also other extended reduction approaches based on POD shall be investigated.

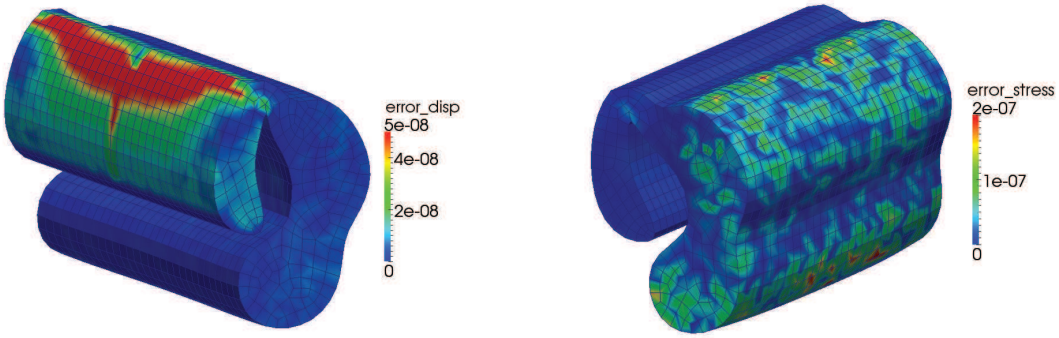

FIGURE 2. Displacement and stress error of the reduction of a turbinate.

REFERENCES

[1] Antoulas, A.C.; Sorensen, D.C.; Approximation of large-scale dynamical systems: An overview, *International Journal of Applied Mathmatics and Computer Science* **11**(5):1093-1121, 2001.

[2] Breuer, K.S.; Sirovich, L.; The use of the Karhunen-Loeve procedure for the calculation of linear eigenfunctions, *Journal of Computational Physics* **96**(2):277-296, 1991.

[3] Chatterjee, A.; An introduction to the proper orthogonal decomposition, *Current science* **78**(7):808-817, 2000.

[4] Cotin, S.; Delingette, H.; Ayache, N.; A hybrid elastic model for real-time cutting, deformations, and force feedback for surgery training and simulation, *The Visual Computer* **16**(8):437-452, 2000.

[5] Dogan, F.; Serdar Celebi, M.; Real-time deformation simulation of non-linear viscoelastic soft tissues, *Simulation* **87**(3):179-187, 2011.

[6] Kapania, R.K.; Byun, C.; Reduction methods based on eigenvectors and Ritz vectors for nonlinear transient analysis, *Computational Mechanics* **11**:65-82, 1993.

[7] Kerfriden, P.; Gosselet, P.; Adhikari, S.; Bordas, S.; Passieux, J.-C.;POD-based model order reduction for the simulation of strong nonlinear evolutions in structures: Application to damage propagation, *IOP Conference Series: Materials Science and Engineering* **10**, 2010.

[8] Lloyd, B.A.; Szekely, G.; Harders, M.; Identification of spring parameters for deformable object simulation, *IEEE Transactions on Visalization and Computer Graphics* **13**(5):1081-1094, 2007.

[9] Lumley, J.L.; Holmes, P.; Berkooz, G.; *Turbulence, coherent structures. Dynamical systems and symmetry*, Cambridge University Press, 1996.

[10] Meyer, M.; Matthies, H.G.; Efficient model reduction in non-linear dynamics using the Karhunen-Loeve expansion and dual-weighted-residual methods, *Computational Mechanics* **31**:179-191, 2003.

[11] Mourelatos, Z.; An efficient crankshaft dynamic analysis using substructuring with Ritz vectors, *Journal of Sound and Vibration* **238**(3):495-527, 2000.

[12] Niroomandi, S.; Alfaro, I.; Cueto, E.; Chinesta, F.; Real-time deformable models of non-linear tissues by model reduction techniques, *Comput. Methods Prog. Biomed.* **91**(3):223-231, 2008.

[13] Radermacher, A.; Reese, S.; Model Reduction for Complex Continua – At the Example of Modeling Soft Tissue in the Nasal Area, *in: Advances in Extended & Multifield Theories for Continua, Ed.: B. Markert; Lecture Notes in Applied and Computational Mechanics* **59**:197–217, 2011.

[14] Taylor, R.L.; Department of Civil and Environmental Engineering, University of California at Berkeley, USA, www.ce.berkeley.edu/projects/feap.

PGD approximations in Multiscale Structural Mechanics: basic features and verification

Pierre Ladevèze

Computational Mechanics carries on supplying numerous science and engineering problems which remain inaccessible to standard FE codes. Not all these problems are exotic, and many are indeed practical problems. A significant number of these engineering problems are related to today's growing interest in physics-based material models described on a scale smaller than that of the macroscopic structure, with applications such as the design of new materials, structural design and manufacturing. In addition to these large-scale, time-dependent and highly nonlinear problems, one can mention numerous problems involving multiple parameters and uncertainties (e.g. bolted assemblies), cyclic viscoplastic problems with many cycles, and real-time simulations of complex thermomechanical systems.

The main approach we are developing in order to solve these very-large-scale nonlinear problems (which cannot be addressed by multiscale calculation strategies alone) is the Proper Generalized Decomposition (PGD). This is an extension of POD, which we introduced in 1986 under the name "Radial Time-Space Approximation". The main idea consists in calculating shape functions and the solution itself simultaneously using an iterative procedure. A priori, these shape functions are arbitrary and must only verify a variable separation assumption.

The talk will first present the basic features of PGD and the mechanical explanation of its considerable advantages in terms of computation time and storage requirements, and also its limits. New verification tools will also be introduced. A last PGD technique will be detailled for time-dependent nonlinear multiscale problems thanks to the LATIN method , and illustrations based on engineering problems will be shown.

References

[1] P. Ladevèze, J.C. Passieux, D. Néron, *The LATIN multiscale computational method and the Proper Generalized Decomposition*, Computer Methods in Applied Mechanics & Engineering **199** (2010), 1287–1296.

[2] P. Ladevèze, *Nonlinear Computational Structural Mechanics - New Approaches and Non)Incremental Methods of Calculation*, Springer Verlag (1999).

[3] F. Chinesta, P. Ladevèze, E. Cueto, *Short review on model order reduction based on the Proper Generalized Decomposition*, Archives of Computational Methods in Engineering **18** (2011), 395–404.

[4] P. Ladevèze, L. Chamoin, *On the verification of model reduction methods based on the Proper Generalized Decomposition*, Computer Methods in Applied Mechanics & Engineering **200** (2011), 2034–2047.

PGD Based Model Reduction: A Route Towards Simulation-Based Control and Augmented Reality

Adrien Leygue
(joint work with Francisco Chinesta)

In simulation-based engineering models should sometimes be solved very fast, in some cases in real time, for many different parameters value on light computing platforms. Classical simulation techniques often fail to fulfill the above constraints. Despite constant impressive advances in numerical analysis, discretization techniques, computer science and high performance computing, many thermo-mechanical problems remain today intractable using classical simulation approaches. This can stem either from the sheer complexity of the problem or from time constraints on the solution method. As advanced numerical simulations strive to be on the limit of what modern computers allow, they often can generate results at a maximum pace that is totally incompatible with the requirements of e.g. virtual reality or real time applications. Additionally the increase in available computing power is often balanced by a corresponding increase in the complexity and/or size of the model to be solved. Among the many cases where these limitations occur we distinguish the following cases:

(1) Optimization, control and inverse problems require the computation of a large number of solutions for many different values of the identified/optimized parameters. The number of solutions to compute increases further when derivatives of the function to optimize with respect to the parameters have to be evaluated. In the case of large problems this large number of direct problems constitute the dominant computing cost. Such costs make the use of advanced optimization algorithms (genetic algorithms, simulated annealing), or simply the computation of high dimensional gradients prohibitive. An alternative of course lies in the use of approximate surrogate models. Such models however need to be identified which is a non-trivial task as the "true model" is often large and nonlinear.
(2) For real-time and virtual reality applications based on a complex model, the simulation has to be fast enough to incorporate in real time external inputs. Surrogate models are therefore a common alternative, with the drawbacks discussed before. Should one wish to pre-compute the true model for "all" possible input scenarios, modern mesh-based techniques would face at least two major obstacles:
    - It would take ages to a priori simulate all scenarios.
    - The mere storage of the outputs of these scenarios would be unfeasible.

An appealing alternative consists in considering off-line solutions of parametric models, in which all the sources of variability - loads, boundary conditions, material parameters, geometrical parameters, etc. - are considered as extra-coordinates. Thus, by solving only once the resulting multidimensional model one has access

to the solution of the model for any value of the parameters considered as extra-coordinates. This off-line solution can be used on-line for real time post-processing, optimization, inverse analysis, analysis of sensibilities, stochastic analysis. Since most of the computation is performed in the offline phase light computing platforms such as smartphones are powerful enough. On-line adaptation within the framework of dynamic data-driven application systems - DDDAS - is also possible. The price to pay is the solution of parametric models defined in high dimensional spaces that could involve hundreds of coordinates. The use of the Proper Generalized Decomposition, allows the computation of such solutions while alleviating the associated pitfalls often referred to as "the curse of dimensionality" and maintaining very low computational and memory costs. This off-line-on-line Proper Generalized Decomposition Based Dynamic Data-Driven Application Systems could constitute a new paradigm in computational sciences.

Ammar et al. introduced the PGD [1] in the framework of computational rheology for solving models originating from the kinetic theory description of viscoelastic fluids. An overview of the PGD applications in this field can be found in [2]. At the core of the PGD, lies the separated representation of the unknown field as a finite sum of functional products involving functions defined on lower dimensionality spaces. For example a scalar field $u(x, y, z, t, \alpha, \beta)$ defined on a space of dimension 6 can be approximated in the following way:

$$u(x, y, z, t, \alpha, \beta) \approx \sum_{i=1}^{N} X_i(x) \cdot Y_i(y) \cdot Z_i(z) \cdot T_i(t) \cdot A_i(\alpha) \cdot B_i(\beta) \ , \tag{1}$$

where x,y,z and t are the usual space-time dimensions and α and β might be some model parameters that are introduced as extra-coordinates. The specific partition of the problem variables in the above functional product depends on the problem being solved. A similar partition of space and time variables has been proposed in the early 80s by P. Ladeveze in the framework of the LATIN Method [3]. The PGD incrementally computes the different terms of the finite sum, making use of an appropriate linearization strategy to compute the different factors of the functional product. Using this approach, high dimensionality problems are never solved and as soon as the solution exhibits some degree of regularity, the number N of terms in the finite sum is limited (from a few tens to some hundreds) hence the low computational and memory costs. The two following features of the method particularly interest us:

- The separation of variables depicted above can be applied to the space coordinates in order to break down the complexity of the problem. Many relevant engineering problems are formulated on degenerate domains for which one can separate at least one space coordinate from the others. This is the case for example in plate or shell domains where one can separate the out-of-plane coordinate from the in-plane coordinates. This features allows the solution of the full 3D problem (e.g. thermal, mechanical) at a numerical cost scaling like 2D without resorting to a priori assumption on the unknown field like in classical plate theories [4].

- The method allows the introduction of many extra-coordinates to the problem. Such coordinates are not restricted to the classical space-time variables but can be material, process or design parameters of the simulated system. These two features are clearly of interest for problems needing a fast solution. The key point for real time and optimization applications is that the PGD solution needs to be computed once in an offline step, possibly on a powerful computing platform. During the online step (i.e. the real time application), one only needs to particularize the different variables depending on the scenario and evaluate the solution or its derivative, which is computationally very cheap [5, 6].

This talk reports recent advances in the use of the Proper Generalized Decomposition applied to structural mechanics, optimization, control and inverse problems, virtual prototyping and virtual reality applications.

References

[1] A. Ammar, B. Mokdad, F. Chinesta, R. Keunings, *A new family of solvers for some classes of multidimensional partial differential equations encountered in kinetic theory modeling of complex fluids*, Journal of Non-Newtonian Fluid Mechanics **139** (2006), 153–176.

[2] F. Chinesta, A. Ammar,A. Leygue, R. Keunings, *An overview of the proper generalized decomposition with applications in computational rheology*, Journal of Non-Newtonian Fluid Mechanics **166** (2011), 578–592.

[3] P. Ladeveze, Nonlinear computational structural mechanics, Springer, NY, 1999.

[4] B. Bognet, F. Bordeu, F. Chinesta, A. Leygue, A. Poitou, *Advanced simulation of models defined in plate geometries: 3D solutions with 2D computational complexity*, Computer Methods In Applied Mechanics And Engineering **201-204** (2012), 1–12.

[5] Ch. Ghnatios, F. Chinesta, E. Cueto, A. Leygue, P. Breitkopf, P. Villon, *Methodological approach to efficient modeling and optimization of thermal processes taking place in a die: Application to pultrusion*, Composites Part A **42** (2011), 1169–1178.

[6] Ch. Ghnatios, F. Masson, A. Huerta, E. Cueto, A. Leygue, F. Chinesta, *Proper Generalized Decomposition based dynamic data-driven control of thermal processes*, Computer Methods in Applied Mechanics and Engineering **213-216** (2012), 29–4.

Mixed FEM of Higher-Order for Variational Inequalities

Andreas Schröder

1. Introdution and notation

In this note, we present a posteriori estimates for mixed finite element methods of higher-order for frictional contact problems in linear elasticity as well as elastoplasticity. The mixed method is based on a saddle point formulation, where the constraints are captured by Lagrange multipliers. The latter are discretized by piecewise polynomial and discontinuous functions with constraints which are only ensured on a finite set of points. This results in a certain non-conformity of the discretization.

We use the following notation: Let $\Omega \subset \mathbb{R}^k$, $k \in \{2, 3\}$, be a domain with sufficiently smooth boundary $\Gamma := \partial\Omega$. Moreover, let $\Gamma_D \subset \Gamma$ be closed with

positive measure and let $\Gamma_C \subset \Gamma \backslash \Gamma_D$ with $\overline{\Gamma}_C \subsetneq \Gamma \backslash \Gamma_D$ (without corners in Γ_C). We set $H^1_D(\Omega) := \{v \in H^1(\Omega) \mid \gamma(v) = 0 \text{ on } \Gamma_D\}$ with the trace operator γ and $V := H^1_D(\Omega; \mathbb{R}^k)$. Let $(\cdot,\cdot)_0$, $(\cdot,\cdot)_{0,\Gamma'}$ denote the usual L^2-scalar products on Ω and $\Gamma' \subset \Gamma$. Note, that the linear and bounded mapping $\gamma_C : H^1_D(\Omega) \to H^{1/2}(\Gamma_C)$ with $\gamma_C(v) := \gamma(v)_{|\Gamma_C}$ is surjective and continuous due to the assumptions on Γ_C, cf. [3, p.88]. For a function v, we define the positive part by $(v)_+ := \max\{v, 0\}$ and the cutoff functions $(\cdot)_\zeta$ by $(v)_\zeta := v$ if $|v| \leq \zeta$ and $(v)_\zeta := \zeta v/|v|$ otherwise. Here, ζ is a non-negative function and $|\cdot|$ the euclidian norm. We set $H^{1/2}_+(\Gamma_C) := \{v \in H^{1/2}(\Gamma_C) \mid v \geq 0\}$ and $\Lambda_t := \{\mu \in L^2(\Gamma_C; \mathbb{R}^{k-1}) \mid |\mu| \leq \zeta(s, \tilde{s})\}$, where $\zeta(s, \tilde{s})$ is defined as $s/\tilde{s}$ on $\operatorname{supp} \tilde{s}$ and 0 on $\Gamma_C \backslash \operatorname{supp} \tilde{s}$ for $s \in L^2(\Gamma_C)$, $s \geq 0$ and $\tilde{s} \in \{1, s\}$. Furthermore, we define the dual cone $\Lambda_n := (H^{1/2}_+(\Gamma_C))' := \{\mu \in \tilde{H}^{-1/2}(\Gamma_C) \mid \forall w \in H^{1/2}_+(\Gamma_C) : \langle \mu, w \rangle \geq 0\}$ and set $\Gamma_N := \Gamma \backslash (\Gamma_D \cup \overline{\Gamma}_C)$. For a displacement field $v \in V$ the linearized symmetric strain tensor is defined as $\varepsilon(v) = \frac{1}{2}(\nabla u + \nabla u^\top)$. Let the elasticity tensor $\mathbb{C}$ with $\mathbb{C}_{ijkl} \in L^\infty(\Omega)$ satisfy the standard symmetry condition $\mathbb{C}_{ijkl} = \mathbb{C}_{jilk} = \mathbb{C}_{klij}$ and be uniformly elliptic. We define the stress tensor $\sigma(v) := \mathbb{C}\varepsilon(v)$ in the case of linear elasticity and $\sigma(v, \mathfrak{q}) := \mathbb{C}(\varepsilon(v) - \mathfrak{q})$ in the case of elastoplasticity, where $\mathfrak{q} \in \mathfrak{Q} := \{\mathfrak{q} \in L^2(\Omega; \mathbb{R}^{k \times k}_{\text{sym}}) \mid \operatorname{tr}(\mathfrak{q}) = 0\}$ is the plastic strain. Furthermore, we set $\Lambda_d := \{\mathfrak{q} \in \mathfrak{Q} \mid |\mathfrak{q}| \leq 1\}$. The vector-valued function n describes the outer unit normal vector with respect to Γ_C and the $k \times (k-1)$-matrix-valued function t contains the tangential vectors. Finally, we define $\gamma_n(v) := \gamma_C(v_i) n_i$, $\gamma_t(v)_j := \gamma_C(v_i) t_{ij}$ and $\gamma_N(v)_i := \gamma(v_i)_{|\Gamma_N}$.

2. Variational inequalities and their mixed discretizations

The variational inequality for Signorini's problem with Tresca friction is to find $u \in K := \{v \in V \mid g - \gamma_n(v) \geq 0\}$, such that

$$(1)\quad (\sigma(u), \varepsilon(v-u))_0 + (s, |\gamma_t(v)| - |\gamma_t(u)|)_{0,\Gamma_C} \geq (f, v-u)_0 + (f_N, \gamma_N(v-u))_{0,\Gamma_N}$$

is fulfilled for all $v \in K$. Here, $f \in L^2(\Omega)$, $f_N \in L^2(\Gamma_N)$ and $g \in H^{1/2}(\Gamma_C)$. It is well-known that (1) has a unique solution and is equivalent to the mixed formulation: Find $(u, \lambda_n, \lambda_t) \in V \times \Lambda_n \times \Lambda_t$ such that

$$(2)\quad \begin{aligned} &(\sigma(u), \varepsilon(v))_0 = (f, v)_0 + (f_N, \gamma_N(v))_{0,\Gamma_N} - \langle \lambda_0, \gamma_n(v) \rangle - (\lambda_t, \tilde{s}\gamma_t(v))_{0,\Gamma_C}, \\ &\langle \mu_n - \lambda_n, \gamma_n(u) - g \rangle + (\mu_t - \lambda_t, \tilde{s}\gamma_t(u))_{0,\Gamma_C} \leq 0 \end{aligned}$$

for all $(v, \mu_n, \mu_t) \in V \times \Lambda_n \times \Lambda_t$, cf. [3]. The existence of a unique solution of (2) is guaranteed, since Λ_t is bounded and $\alpha \|\mu_n\|_{-1/2,\Gamma_C} \leq \sup_{v \in V,\, \|v\|_1 = 1} \langle \mu_n, \gamma_n(v) \rangle$ holds for a constant $\alpha > 0$ and all $\mu_n \in \tilde{H}^{-1/2}(\Gamma_C)$, cf. [3, 7]. A higher-order finite element discretization based on quadrangles or hexahedrons is given as follows: Let $\mathcal{T}$ be a finite element mesh of Ω with mesh size h and let $\mathcal{E}$ be a mesh of Γ_C with size H. Furthermore, let $\Psi_T : [-1,1]^k \to T \in \mathcal{T}$ and $\Phi_T : [-1,1]^{k-1} \to T \in \mathcal{T}$ be bijective and sufficiently smooth transformations and let $p, q \in \mathbb{N}$. Using the polynomial (Serendipity) tensor product space $Q_{k,p}$ of order p on the reference element $[-1,1]^k$, we substitute V by $V_{hp} := \{v \in V \mid \forall T \in \mathcal{T} : v_{|T} \circ \Psi_T \in (Q_{k,p})^k\}$ and define $M_{Hq} := \{\mu \in L^2(\Gamma_C) \mid \forall E \in \mathcal{E} : \mu_{|E} \circ \Phi_E \in Q_{k-1,q}\}$. To substitute

Λ_n and Λ_t, we enforce the constraints on a finite set of points. For this purpose, let $\mathcal{M} \subset [-1,1]$ be this finite set and define

$$\Lambda_{n,Hq} := \{\mu_{n,Hq} \in M_{Hq} \mid \forall E \in \mathcal{E} : \forall x \in \mathcal{M}^{k-1} : \ \mu_{n,Hq}(\Phi_E(x)) \geq 0\},$$
$$\Lambda_{t,Hq} := \{\mu_{t,Hq} \in (M_{Hq})^{k-1} \mid \forall E \in \mathcal{E}, \forall x \in \mathcal{M}^{k-1} : \ |\mu_{t,Hq}(\Phi_E(x))| \leq (\zeta(s,\tilde{s}))(\Phi_E(x))\}.$$

Note that the definition of $\Lambda_{n,Hq}$ and $\Lambda_{t,Hq}$ using discrete points leads to the non-conformity $\Lambda_{n,Hq} \not\subset \Lambda_n$ and $\Lambda_{t,Hq} \not\subset \Lambda_t$. In order to ensure the stability of the discretization scheme, we have to verify a discrete inf-sup condition with a constant independent of the mesh sizes h and H as well as the polynomial degrees p and q. This is done for quasi-uniform meshes in [4, 7], where $hq^2(Hp)^{-1}$ is assumed to be sufficiently small. Some convergence results of the scheme for similar problems are given in [6, 8] where Gauss quadrature points are chosen to define the set $\mathcal{M}$. To estimate the discretization error given by the discrete solution $(u_{hp}, \lambda_{n,Hq}, \lambda_{t,Hq}) \in V_{hp} \times \Lambda_{n,Hq} \times \Lambda_{t,Hq}$, we consider the residual $\mathrm{Res} \in V'$ defined by $\langle \mathrm{Res}, v\rangle := (f,v)_0 + (f_N, \gamma_N(v))_{0,\Gamma_N} - (\lambda_{n,Hq}, \gamma_n(v))_{0,\Gamma_C} - (\lambda_{t,Hq}, \gamma_t(v))_{0,\Gamma_C} - (\sigma(u_{hp}), \varepsilon(v))_0$ and assume the inf-sup condition

$$\hat{\kappa}(\|\mu_n\|_{-1/2,\Gamma_C} + \|\mu_t\|_{-1/2,\Gamma_C}) \leq \sup_{v \in V, \|v\|_1 = 1} \langle \mu_n, \gamma_n(v)\rangle + (\mu_t, \tilde{s}\gamma_t(v))_{0,\Gamma_C} \tag{3}$$

for a constant $\hat{\kappa} > 0$ and all $(\mu_n, \mu_t) \in \tilde{H}^{-1/2}(\Gamma_C) \times L^2(\Gamma_C; \mathbb{R}^{k-1})$. In the case $\tilde{s} = 1$, condition (3) directly results from the surjectivity of γ_n and γ_t. With

$$\begin{aligned}\eta := {} & \|\,\mathrm{Res}\,\|_{V'}^2 + \|\lambda_{n,Hq} - (\lambda_{n,Hq})_+\|_{-1/2,\Gamma_C}^2 + \|\lambda_{t,Hq} - (\lambda_{t,Hq})_{\zeta(s,\tilde{s})}\|_{0,\Gamma_C}^2 \\ & + \|(\gamma_n(u_{hp}) - g)_+\|_{1/2,\Gamma_C}^2 + |(\lambda_{n,Hq}, (\gamma_n(u_{hp}) - g)_+)_{0,\Gamma_C}| \\ & + |\langle (\lambda_{n,Hq})_+, g - \gamma_n(u_{hp})\rangle| + |(s, |\gamma_t(u_{hp})|)_{0,\Gamma_C} - ((\lambda_{t,Hq})_{\zeta(s,\tilde{s})}, \tilde{s}\gamma_t(u_{hp}))_{0,\Gamma_C}|,\end{aligned}$$

there holds the a posteriori error estimation

$$E_{hpHq} := \|u - u_{hp}\|_1^2 + \|\lambda_n - \lambda_{n,Hq}\|_{-1/2,\Gamma_C}^2 + \|\lambda_t - \lambda_{t,Hq}\|_{-1/2,\Gamma_C}^2 \lesssim \eta \tag{4}$$

The proof can be found in [5].

In quasi-static elastoplasticity, one pseudo time-step of the primal problem with linear kinematic hardening is given by the variational inequality: Find $(v, \mathfrak{p}) \in K \times \mathfrak{Q}$ such that

$$\begin{aligned}(\sigma(u,\mathfrak{p}), \varepsilon(v-u))_0 + (s, |\gamma_t(v)| - |\gamma_t(u)|)_{0,\Gamma_C} + (\mathbb{H}\mathfrak{p} - \sigma(u,\mathfrak{p}), \mathfrak{q} - \mathfrak{p})_0 \\ + (\sigma_y, |\mathfrak{q}| - |\mathfrak{p}|)_0 \geq (f, v-u)_0 + (f_N, \gamma_N(v-u))_{0,\Gamma_N}\end{aligned} \tag{5}$$

holds for all $(v, \mathfrak{q}) \in K \times \mathfrak{Q}$, cf. [1]. Here, $\mathbb{H}$ denotes the symmetric and positive definite hardening tensor and $\sigma_y > 0$ the yield stress. The variational inequality (5) is equivalent to find $(u, \mathfrak{p}, \lambda_n, \lambda_t, \lambda_d) \in V \times \mathfrak{Q} \times \Lambda_n \times \Lambda_t \times \Lambda_d$ such that

$$\begin{aligned}(\sigma(u,\mathfrak{p}), \varepsilon(v))_0 + (\mathbb{H}\mathfrak{p} - \sigma(u,\mathfrak{p}), \mathfrak{q})_0 = {} & (f,v)_0 + (f_N, \gamma_N(v))_{0,\Gamma_N} - \langle \lambda_n, \gamma_n(v)\rangle \\ & - (\lambda_t, \tilde{s}\gamma_t(v))_{0,\Gamma_C} - (\lambda_d, \sigma_y\mathfrak{q})_0, \\ \langle \mu_n - \lambda_n, \gamma_n(u) - g\rangle + (\mu_t - \lambda_t, \tilde{s}\gamma_t(u))_{0,\Gamma_C} + (\mu_d - \lambda_d, \sigma_y\mathfrak{p})_0 \leq 0 & \end{aligned}$$

for all $(v, \mathfrak{q}, \mu_n, \mu_t, \mu_d) \in V \times \mathfrak{Q} \times \Lambda_n \times \Lambda_t \times \Lambda_d$. A higher-order finite element discretization is given by $\mathfrak{Q}_{hp} := \{\mathfrak{q} \in \mathfrak{Q} \mid \forall T \in \mathcal{T} : \mathfrak{q}_{ij|T} \circ \Psi_T \in Q_{k,p-1}\}$ and

$$\Lambda_{d,hp} := \{\mu_{d,hp} \in \mathfrak{Q}_{hp} \mid \forall T \in \mathcal{T} : \forall x \in \mathcal{D} : |\mu_{d,hp|T}(\Psi_T(x))| \leq 1\},$$

where $\mathcal{D} \subset [-1,1]^k$ is a finite set and $\mathfrak{p}_{hp} \in \mathfrak{Q}_{hp}$ and $\lambda_{d,hp} \in \Lambda_{d,hp}$ are discrete solutions. Extending (3) by the contributions related to the Lagrange multiplier of elastoplasticity and replacing $\sigma(u_{hp})$ by $\sigma(u_{hp}, \mathfrak{p}_{hp})$ in the definition of Res, we obtain the following estimate with similar arguments as in the frictional case,

$$\begin{aligned}(6)\quad & E_{hpHq} + \|\lambda_d - \lambda_{d,hp}\|_0^2 \lesssim \eta + \|\lambda_{d,hp} - (\lambda_{d,hp})_1\|_0^2 \\ & + |(\sigma_y, |\mathfrak{p}_{hp}| - (\lambda_{d,hp})_1 : \mathfrak{p}_{hp})_0| + \|\operatorname{dev}(\sigma(u_{hp}, \mathfrak{p}_{hp}) - \mathbb{H}\mathfrak{p}_{hp}) - \sigma_y \lambda_{d,hp}\|_{0,\Omega}^2.\end{aligned}$$

In both error estimates (4) and (6), $\|\operatorname{Res}\|_{V'}$ can be estimated by well-known techniques of a posteriori error estimation for variational equations. The remainder terms capture errors with respect to geometrical and complementary conditions and constraints given by friction and elastoplasticity as well as errors resulting from the non-conformity of the Lagrange multipliers.

References

[1] W. Han, B. Reddy, *On the finite element method for mixed variational inequalities arising in elastoplasticity*, SIAM J. Numer. Anal., **32** (1995), 1778–1807.

[2] J. Haslinger, I. Hlavacek, *Approximation of the Signorini problem with friction by a mixed finite element method*, J. Math. Anal. Appl., **86** (1982), 99–122.

[3] N. Kikuchi, J.T. Oden, *Contact problems in elasticity: A study of variational inequalities and finite element methods.*, SIAM Studies in Applied Mathematics, **8** (1988).

[4] A. Schröder, *Mixed finite element methods of higher-order for model contact problems*, SINUM J. Numer. Anal., **49** (2011), 2323-2339.

[5] A. Schröder, *A posteriori error estimates of higher-order finite elements for frictional contact problems*, Computer Methods in Applied Mechanics and Engineering, accepted (2012).

[6] A. Schröder, *Mixed FEM for a frictional contact problem*, PAMM, **11** (2011), 7-10.

[7] A. Schröder, H. Blum, A. Rademacher, H. Kleemann, *Mixed FEM of higher order for contact Problems with friction*, Journal Numerical Analysis & Modeling, **8** (2011), 302-323.

[8] A. Schröder, H. Kleemann, Heiko, H. Blum, Heribert, *Mixed finite element methods for two-body contact problems*, HU Berlin, Department of Mathematics, Preprint 11-02, (2011).

Goal-oriented error estimation in Computational Mechanics

Ludovic Chamoin

Numerical simulations are nowadays a common tool in mechanical engineering and design, as they enable to predict the behavior of complex structures submitted to a given environment. Nevertheless, in order to represent the real world accurately, this tool requires a permanent control of the various mathematical and numerical models it involves. This scientific concern, known as model Verification and Validation (V&V), is a component of simulations which is fundamental for robustness and reliability aspects. However, in many cases, numerical simulations do not aim at predicting the whole solution of the physical phenomenon under study, but

only some specific aspects, i.e. local features (maximal displacement, stress intensity factors, etc...) referred as quantities of interest and primarily used for design purposes. It is therefore sound to control only parameters which are influent for these outputs of interest, leading to a goal-oriented and simplified V&V procedure.

In this talk, we present some of our recent works that aim at building simulation models which are optimized with respect to a given quantity of interest. We particularly focus on works dealing with "classical" model verification [1, 2, 3], i.e. assessing discretization errors and leading to discretizations (finite element mesh for instance) and numerical techniques which are dedicated to the computation of such quantities. We first show that guaranteed and accurate local error bounds can be obtained for a large class of mechanical problems, such as (visco-)elasticity [4, 5], fracture mechanics [6], visco-dynamics [7], or plasticity [8], using the concept of Constitutive Relation Error [2] as well as adjoint-based procedures [9]. The obtained strict bounding of the error on a given quantity of interest I reads:

$$|I_{ex} - I_h - I_{hh}| \leq E_{CRE} \times \tilde{E}_{CRE}$$

where I_{ex} is the exact unknown value of I, I_h is the approximate finite element value of I, I_{hh} is a computable correcting term, and E_{CRE} (resp. $\tilde{E}_{CRE}$) is the constitutive relation error of the reference (resp. adjoint) problem.

In that framework, we focus on the construction of an admissible stress field which is required to get guaranteed bounds [10, 11]. We also introduce a bounding procedure that avoids the use of the Cauchy-Schwarz inequality and leads to more accurate bounds. This procedure is based on relations among discretization errors defined over homothetic domains (mathematical view of Saint-Venant's principle).

In a second part, we present non-intrusive techniques [12, 7] that optimize the quality of error bounds and enable to implement the proposed goal-oriented error estimation tools into commercial softwares. These techniques consist of an enrichment of the adjoint solution by means of so-called *handbook functions* [13], that correspond here to (generalized) Green's functions computed in a (semi-)infinite domain. The adjoint displacement field is then searched under the form:

$$\tilde{\mathbf{u}} = \tilde{\mathbf{u}}^{hand}\Phi + \tilde{\mathbf{u}}^{res}$$

where $\tilde{\mathbf{u}}^{hand}$ is the handbook function associated with the quantity of interest under study; Φ is a weighting function, with bounded support, so that the enrichment is introduced locally; $\tilde{\mathbf{u}}^{res}$ is a residual term that enables to verify boundary conditions of the adjoint problem. Performing such an enrichment leads to an accurate solution of the adjoint problem without mesh refinement; it also enables to deal with pointwise quantities of interest in space and time.

Capabilities of the proposed *a posteriori* goal-oriented error estimation method are illustrated on 2D and 3D numerical experiments.

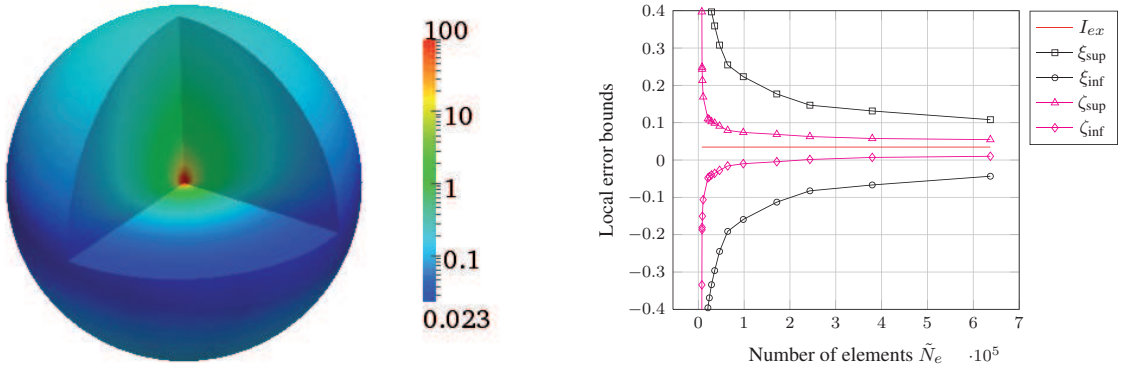

FIGURE 1. Example of 3D Green's function (left), and comparison between classical and optimal bounds with respect to the discretization of the adjoint problem (right).

REFERENCES

[1] E. Stein (ed), *Error-controlled Adaptive Finite Elements in Solid Mechanics*, J. Wiley (2003).

[2] P. Ladevèze, J.P. Pelle, *Mastering Calculations in Linear and Nonlinear Mechanics*, Springer NY (2004).

[3] S. Prudhomme, J.T. Oden, *On goal-oriented error estimation for elliptic problems: application to the control of pointwise errors*, Computer Methods in Applied Mechanics & Engineering **176** (1999), 313–331.

[4] L. Chamoin, P. Ladevèze, *Bounds on history-dependent of independent local quantities in viscoelasticity problems solved by approximate methods*, International Journal for Numerical Methods in Engineering **71**(12) (2007), 1387–1411.

[5] P. Ladevèze, L. Chamoin, *Calculation of strict error bounds for finite element approximations of non-linear pointwise quantities of interest*, International Journal for Numerical Methods in Engineering **84** (2010), 1638–1664.

[6] J. Panetier, P. Ladevèze, L. Chamoin, *Strict and effective bounds in goal-oriented error estimation applied to fracture mechanics problems solved with XFEM*, International Journal for Numerical Methods in Engineering **81**(6) (2010), 671–700.

[7] J. Waeytens, L. Chamoin, P. Ladevèze, *Guaranteed error bounds on pointwise quantities of interest for transient viscodynamics problems*, Computational Mechanics (2011), online.

[8] P. Ladevèze, *Strict upper error bounds for calculated outputs of interest in computational structural mechanics*, Computational Mechanics **42**(2) (2008), 271–286.

[9] R. Becker, R. Rannacher, *An optimal control approach to shape a posteriori error estimation in finite element methods*, A. Isereles (Ed.), Acta Numerica **10**, Cambridge University Press (2001), 1–120.

[10] P. Ladevèze, L. Chamoin, E. Florentin, *A new non-intrusive technique for the construction of admissible stress fields in model verification*, Computer Methods in Applied Mechanics & Engineering **199**(9-12) (2010), 766–777.

[11] F. Pled, L. Chamoin, P. Ladevèze, *On the techniques for constructing admissible stress fields in model verification: performances on engineering examples*, International Journal for Numerical Methods in Engineering **88**(5) (2011), 2032–2047.

[12] L. Chamoin, P. Ladevèze, *A non-intrusive method for the calculation of strict and efficient bounds of calculated outputs of interest in linear viscoelasticity problems*, Computer Methods in Applied Mechanics & Engineering **197**(9-12) (2008), 994–1014.

[13] T. Strouboulis, I. Babuška, K. Copps, *The design and analysis of the Generalized Finite Element Method*, Computer Methods in Applied Mechanics & Engineering **181** (2000), 43–69.

Numerical Upscaling and Preconditioning of flows in highly heterogeneous porous media

Raytcho D. Lazarov

(joint work with Yalchin Efendiev, Juan Galvis, Joerg Willems)

The generalized Stokes equations (called also Brinkman equations),

$$-\mu\Delta \boldsymbol{u} + \nabla p + \mu\kappa^{-1}\boldsymbol{u} = \boldsymbol{f},\ \nabla\cdot\boldsymbol{u} = 0 \ \text{ in } \Omega, \tag{1}$$

where μ is the viscosity and κ is the permeability, are used for modeling flows in highly porous media. Examples of such media are industrial open foams, filters, and insulation materials, shown on Figure 1. For high values of κ these equations recover flows at Darcy's regime. Motivated by industrial applications of such materials we have derived, studied, and tested a numerical upscaling procedure, of the class of multiscale FEM, e.g. [4], for highly porous media with complicated internal structure of the permeability κ that covers both limits, Brinkman and Darcy. These are modeled by (1) whith a contrast, ratio $\eta = \max_x \kappa(x)/\min_x \kappa(x)$, in the range $10^4 - 10^8$.

Figure 1. Various highly porous media on a micro-scale level

There are two different applications of the proposed method: (1) numerical upscaling of Brinkman equations on coarse-grid that incorporates fine-grid features, and (2) an alternating Schwarz iteration that uses the coarse-grid approximation in the overlapping domain decomposition setting. The presented numerical examples demonstrate the performance of both the subgrid approximation and the iterative procedure.

First, we derive two-scale finite element approximation of Brinkman equations. The method uses two main ingredients: (1) discontinuous Galerkin finite element method for Stokes equations, proposed and studied by J. Wang and X. Ye [7] and (2) subgrid approximation developed by T. Arbogast in [1] for Darcy's equations. The main idea is scetched below.

We set up the finite element partition of the domain by introducing a coarse grid $\mathcal{T}_H$ and further refine the coarse grid to obtain a fine grid $\mathcal{T}_h$. The construction of the finite elements spaces on this composite grid is done in the following manner (see, e.g. [6, 8]): on the mesh $\mathcal{T}_H$ we introduce the finite element spaces $\mathcal{V}_H$ of

vector functions that belong to the class of BDM1 (see, [7]) and for $\mathscr{W}_H$ we choose the space of piece-wise constant functions with mean value zero over Ω. Further, on the mesh $\mathcal{T}_h$ we introduce the spaces $\mathscr{V}_H$ piece-wise polynomial functions of the class BDM1, which have zero normal component on each coarse-mesh interface and $\mathscr{W}_H$, piece-wise constant functions with mean zero on each coarse-mesh element. Then the composite approximation spaces are $\mathscr{V}_H \oplus \mathscr{V}_h$ and $\mathscr{W}_H \oplus \mathscr{W}_h$ for the velocity u and the pressure p. These spaces have the following fundamental properties: (1) $\nabla \cdot \mathscr{V}_h = \mathscr{W}_h$, (2) $\nabla \cdot \mathscr{V}_H = \mathscr{W}_H$, and (3) $\mathscr{W}_H \perp \mathscr{W}_h$ in the L^2-inner product.

Then one can set up a Galerkin method for solving (1) using the composite spaces introduced above. This decomposition yields the following weak form: find $\boldsymbol{u}_H + \boldsymbol{u}_h \in \mathscr{W}_h \oplus \mathscr{W}_H$, and $p_H + p_h \in \mathscr{V}_h \oplus \mathscr{V}_H$ such that

$$a(\boldsymbol{u}_H + \boldsymbol{u}_h, \boldsymbol{v}_H + \boldsymbol{v}_h) + (\nabla \cdot (\boldsymbol{v}_H + \boldsymbol{v}_h), p_H + p_h) = (\boldsymbol{f}, \boldsymbol{v}_H + \boldsymbol{v}_h),$$
$$(\nabla \cdot (\boldsymbol{u}_H + \boldsymbol{u}_h), q_H + q_h) = 0,$$

for all $\boldsymbol{v}_H + \boldsymbol{v}_h \in \mathscr{W}_h \oplus \mathscr{W}_H$ and $q_H + q_h \in \mathscr{V}_h \oplus \mathscr{V}_H$. Here the bilinear form $a(\cdot, \cdot)$ is an approximation of the discontinuous Galerkin finite element method applied to $H(div)$-conforming spaces with stabilization of the discontinuity of the tangential component of the gradient of $\boldsymbol{u}$, (cf. [7, 8]).

Due to the properties of the spaces $\mathscr{V}_H$, $\mathscr{V}_h$, $\mathscr{W}_H$ and $\mathscr{W}_h$ we show that the solution process of this system could be made in two separate stages: for a given $\boldsymbol{u}_H$ we find the fine grid response $(\boldsymbol{u}_h(\boldsymbol{u}_H), p_h(\boldsymbol{u}_H))$, computed in parallel over all coarse finite elements by solving

$$a(\boldsymbol{u}_h(\boldsymbol{u}_H), \boldsymbol{v}_h) + (\nabla \cdot \boldsymbol{v}_h, p_h(\boldsymbol{u}_H)) + (\nabla \cdot \boldsymbol{u}_h(\boldsymbol{u}_H), q_h) = -a(\boldsymbol{u}_H, \boldsymbol{v}_h)$$

for all $\boldsymbol{v}_h \in \mathscr{V}_h$ and $q_h \in \mathscr{W}_h$. Similarly we define the fine-grid responses $(\overline{\delta}_{\boldsymbol{u}}, \overline{\delta}_p)$ of the data $\boldsymbol{f}$ by solving

$$a(\overline{\delta}_{\boldsymbol{u}}, \boldsymbol{v}_h) + (\nabla \cdot \boldsymbol{v}_h, \overline{\delta}_p) + (\nabla \cdot \overline{\delta}_{\boldsymbol{u}}, q_h) = (\boldsymbol{f}, \boldsymbol{v}_h), \ \forall \boldsymbol{v}_h \in \mathscr{V}_h, \ \forall q_h \in \mathscr{W}_h.$$

Then the upscaled equation is defined only on $(\mathscr{V}_H, \mathscr{W}_H)$ and involves solving the problem for $(\boldsymbol{u}_H, p_H)$

$$a(\boldsymbol{u}_H + \boldsymbol{u}_h(\boldsymbol{u}_H), \boldsymbol{v}_H + \boldsymbol{v}_h(\boldsymbol{v}_H)) + (\nabla \cdot \boldsymbol{v}_H, p_H) + (\nabla \cdot \boldsymbol{u}_H, q_H) = (\boldsymbol{f}, \boldsymbol{v}_H) - a(\overline{\delta}_{\boldsymbol{u}}, \boldsymbol{v}_H),$$

for all $\boldsymbol{v}_H \in \mathscr{V}_H$ and $q_H \in \mathscr{W}_H$. This has a natural description and implementation in term of the nodal basis functions in $\mathscr{V}_H$.

On Figure 2 we show the results of this procedure applied to Brinkman equation in vuggy media on sequence of coarse meshes. It is clear that along the coarse-grid faces we have much larger error. It is reduces by refining the mesh, but the error remains in the range 8-10% for the velocity measured in L^2-norm (for more details see, [6, 8]). In order to improve the results we can perform similar solves on a staggered grid, which will will result in improving the accuracy across the coarse-grid interfaces. Such approach are described in [6] and the results of numerical computations for a 2-D section of the SPE10 benchmark are shown on Figure 3.

In the second part of the talk we present an iterative method for solving the system of algebraic equations obtained on a global fine grid. Due to the small mesh-size and high contrast, the overlapping domain decomposition method (like

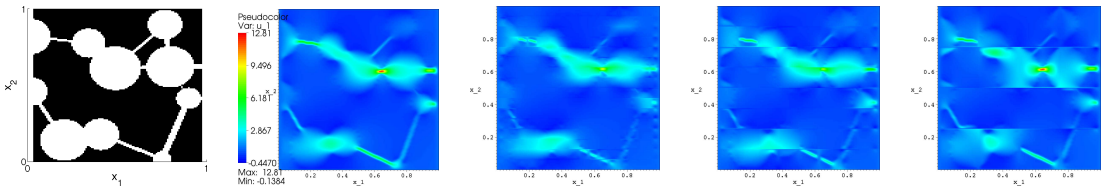

FIGURE 2. Vuggy porous media (shown on the left figure) with low permeability (dark region) and high permeability (the white region); On the four figures we show the reference solution for the horizontal velocity obtained on 128×128 grid and approximate solutions obtained on coarse grids with 16×16, 8×8, and 4×4 finite elements

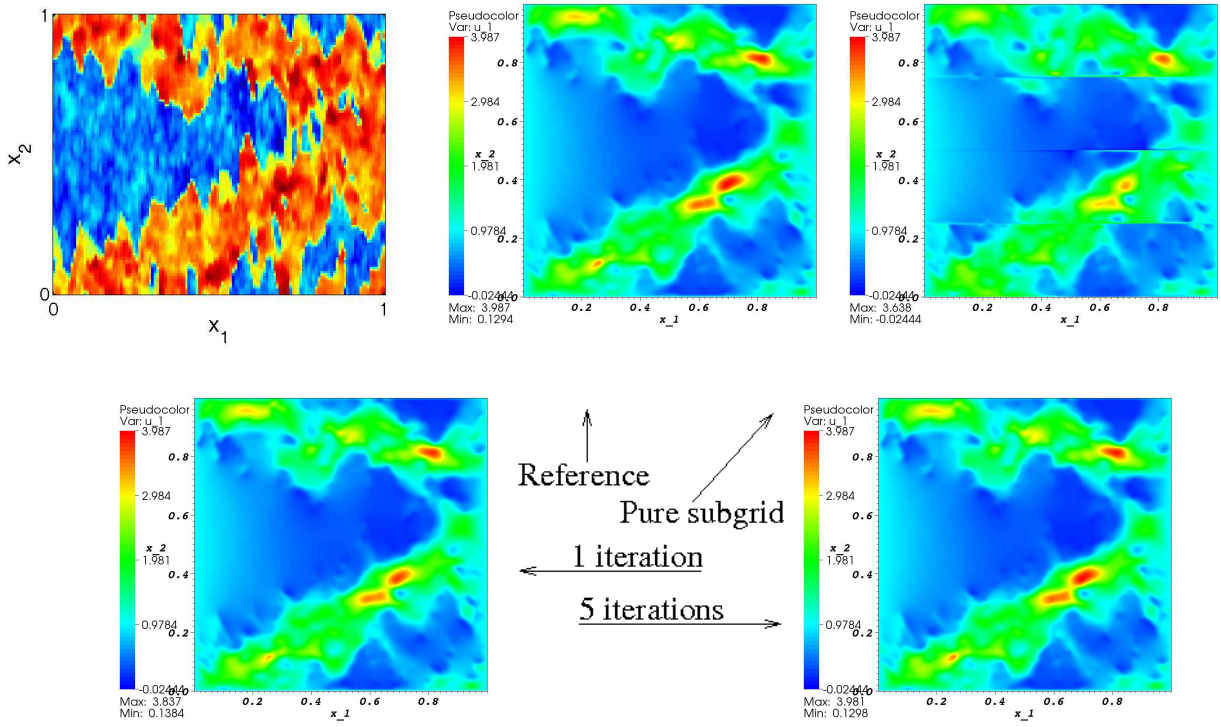

FIGURE 3. Numerical results for media of permeability field distribution shown on the top left picture; Top middle picture is a computed reference solution on a fine mesh and top right picture is the upscaled solution obtained on 4×4 coarse mesh; the bottom two figures show the solution after one iteration and five iterations

those used in the computations shown on Figure 3) are very slow and might not converge at all for very high contrast in Brinkman equation. Therefore, special care should be taken in the case of highly heterogeneous media with high contrast. In [5] such a method, based on overlapping domain decomposition technique, has

been devised and justified for second order elliptic problems. In [2, 3] we were able to extend this theory to abstract symmetric positive definite bilinear forms.

The construction of a robust with respect to the contrast method relies on an augmented coarse space defined on a partition of Ω into a number of overlapping subdomains with size H. The standard coarse grid finite element space is augmented with functions that are solutions of certain local eigenvalue problems (for details see, e.g. [2, 3, 5]). This "spectral" coarse space $\mathscr{V}_H^{sp}$ leads to a new decomposition of a function form the global finite element space into a sum of local functions and a function from this coarse space. A remarkable property of this decomposition is that the sum of the "energy" of the components is bounded by the energy of the function with a constant independent of the contrast. This results in an overlapping domain decomposition preconditioner that produces condition number that is independent of the contrast η. An example illustrating its perfomence for a partucular permability distribution is shown on Table 4. Using stream function in 2-D we have reduced the mixed finite element method for Darcy equations and discontinuous Galerkin method Brinkman equations to fit into this apstract setting and have used it for computing flows in high contrast materials. Examples of such computations are shown in our papers [2, 3].

	$\mathscr{V}_H$			$\mathscr{V}_H^{sp}$		
η	iter.	dim $\mathscr{V}_H$	cond.	iter.	dim $\mathscr{V}_H{}^{sp}$	cond.
$1e2$	27	49	2.1e1	21	49	10.8
$1e4$	70	49	2.2e3	22	60	10.9
$1e6$	113	49	1.2e5	22	60	11.0

TABLE 4. Comparison of the condition numbers and the dimensions of the coarse spaces $\mathscr{V}_H$ used in the standard DD method and our space $\mathscr{V}_H^{sp}$ for a model second order elliptic problem with highly heterogeneous permability with contrast η.

REFERENCES

[1] T. Arbogast, *Analysis of a two-scale, locally conservative subgrid upscaling for elliptic problems*, SIAM J. Numer. Anal., **42(2)** (2004), 576–598.

[2] Y. Efendiev, J. Galvis, R. Lazarov, J. Willems, *Robust DD preconditioners for abstract symmetric positive definite bilinear forms*, **46** (2012) 1175-1199, DOI: 10.1051/m2an/2011073.

[3] Y. Efendiev, J. Galvis, R. Lazarov, J. Willems, *Robust solvers for SPD operators and weighted Poincare inequalities*, Lect. Notes in Computer Science, (2011), 41–50.

[4] Y. Efendiev and T. Hou, *Multiscale finite element methods. Theory and applications*, Springer, 2009.

[5] J. Galvis, and Y. Efendiev, *Domain decomposition preconditioners for multiscale flows in high contrast media*, Multiscale Model. Simul. **8** (2010), 1461–1483.

[6] O. Iliev, R.D. Lazarov, and J. Willems, *Variational multiscale finite element method for flows in highly porous media*, SIAM Multiscale Model. Simul., **9 (4)** (2011), 1350–1372.

[7] J. Wang and X. Ye, *New finite element methods in computational fluid dynamics by H(div) elements*, SIAM J. Numer. Anal., **45(3)** (2007), 1269–1286.

[8] J. Willems, *Numerical Upscaling for Multiscale Flow Problems*, PhD thesis, University of Kaiserslautern, 2009.

Finite Element Discretization of Multiscale Elliptic Problems

Daniel Peterseim
(joint work with Axel Målqvist)

Background. The numerical solution of second order elliptic problems with strongly heterogeneous and highly varying (non-periodic) diffusion coefficient is a challenging part within the simulation of modern composite materials. The coefficient may represent different materials or material phases and, hence, heterogeneities and oscillations of the coefficient typically appear on several non-separated scales. Similar difficulties arise in geophysical applications such as ground water flow, oil recovery modeling, or CO_2 sequestration.

The abstract mathematical setup of this note is as follows. Given some bounded polygonal Lipschitz domain Ω in 2 or 3 space dimensions, some uniformly elliptic diffusion matrix $A \in L^\infty\left(\Omega, \mathbb{R}^{d\times d}_{\mathrm{sym}}\right)$, and some force $f \in L^2(\Omega)$, we seek $u \in V := H^1_0(\Omega)$ such that

$$a(u,v) := \int_\Omega \langle A\nabla u, \nabla v\rangle \,\mathrm{d}x = \int_\Omega fv \,\mathrm{d}x =: F(v) \quad \text{for all } v \in V.$$

If A varies rapidly on microscopic scales, classical polynomial based finite element methods are unable to capture neither the microscopic nor the macroscopic behavior of the solution unless the meshwidth is chosen fine enough (i.e., smaller than the smallest scale in the coefficient). To overcome this lack of performance, many methods that are based on general (non-polynomial) ansatz functions have been developed, amongst others [5, 4, 2, 1]. In these methods, the problem is split into coarse and (possibly several) fine scales. The fine scale effect on the coarse scale is either computed numerically or modeled analytically. The resulting modified coarse problem can then be solved numerically and its solution contains crucial information from the fine scales. Although many of these approaches show promising results in practice, their convergence analysis typically relies on strong assumptions such as periodicity and scale separation. Those assumptions, which essentially justify homogenization, appear unrealistic in the applications under consideration.

A New Variational Multiscale Method [8]**.** Without any additional assumptions on the coefficient, we construct for any (possibly coarse) shape regular mesh $\mathcal{T}_H$ of size H an upscaled variational problem with solution u_H^{ms} such that the estimate $\|u - u_H^{\mathrm{ms}}\|_{H^1(\Omega)} \leq C_f H$ holds with a constant C_f that depends on f and the contrast of A but *not* on its variations. The upscaled problem is related to a Galerkin method with respect to a modified coarse space. This coarse space is spanned by one modified nodal basis function per vertex in $\mathcal{T}_H$ and their computation involves only local solves on patches of coarse elements.

We shall briefly summarize our construction. Let V_H denote the space of continuous $\mathcal{T}_H$-piecewise affine finite element functions that matches the homogeneous Dirichlet boundary condition. The key tool in our construction is linear surjective (quasi-)interpolation operator $\mathfrak{I}_{\mathcal{T}} : V \to V_H$ from [3, Section 6]. Its kernel $V^{\mathrm{f}} := \{v \in V \mid \mathfrak{I}_{\mathcal{T}} v = 0\}$ represents the microscopic features of V that are not captured by V_H. Since V^{f} is a closed subspace, we have the decomposition

$$V = V_H^{\mathrm{ms}} \oplus V^{\mathrm{f}},$$

where V_H^{ms} denotes the orthogonal complement of V^{f} in V for the scalar product a. The space V_H^{ms} is coarse in the sense that $\dim V_H^{\mathrm{ms}} = \dim V_H$. Given the classical nodal basis (tent) function $\lambda_x \in V_H$ for some x in the set of vertices $\mathcal{N}_H$ of $\mathcal{T}_H$, let $\phi_x \in V^{\mathrm{f}}$ solve the corrector problem

$$a(\phi_x, w) = a(\lambda_x, w) \quad \text{for all } w \in V^{\mathrm{f}}. \tag{1}$$

We then have $V_H^{\mathrm{ms}} = \operatorname{span}\{\lambda_x - \phi_x \mid x \in \mathcal{N}_H\}$. Needless to say that the corrections ϕ_x have theoretical purpose only because they are solution of some infinite dimensional problem and because they have global support in general. However, [8] shows that both issues can be handled efficiently. The correction ϕ_x decays exponentially fast (with respect to the number of layers of coarse elements) away from x and that a simple truncation leads to localized basis functions with good approximation properties. This decay is due to the fact that ϕ_x solves a variational problem in the kernel of the interpolation operator where functions are constraint to have vanishing averages in nodal patches. Moreover, this result is stable with respect to perturbations arising from the discretization of the local problems.

Denote nodal patches of k-th order about $x \in \mathcal{N}_H$ by ω_x^k. Given some finescale finite element space $V_h \supset V_H$ that captures microscopic scales sufficiently well, define discrete and localized finescale spaces $V_h^{\mathrm{f}}(\omega_{x,k}) := \{v \in V^{\mathrm{f}} \cap V_h \mid v|_{\Omega \setminus \omega_{x,k}} = 0\}$, $x \in \mathcal{N}_H$. Then the solutions $\phi_{x,k}^h \in V_h^{\mathrm{f}}(\omega_{x,k})$ of

$$a(\phi_{x,k}^h, w) = a(\lambda_x, w) \quad \text{for all } w \in V_h^{\mathrm{f}}(\omega_{x,k}), \tag{2}$$

are discrete approximations of ϕ_x from (1) with local support. Note that these corrector problems are completely decoupled and can be computed in parallel without any communication.

The proposed (variational) multiscale finite element method then seeks an approximation $u_{H,k}^{\mathrm{ms},h}$ of u in the coarse multiscale space

$$V_{H,k}^{\mathrm{ms},h} = \operatorname{span}\{\lambda_x - \phi_{x,k}^h \mid x \in \mathcal{N}_H\} \subset V. \tag{3.a}$$

The approximation $u_{H,k}^{\mathrm{ms},h}$ satisfies the upscaled system of equations

$$a(u_{H,k}^{\mathrm{ms},h}, v) = F(v) \quad \text{for all } v \in V_{H,k}^{\mathrm{ms},h}. \tag{3.b}$$

This method is a new variant of the variational multiscale methods introduced in [6]. Note that $\dim V_{H,k}^{\mathrm{ms},h} = |\mathcal{N}_H| = \dim V_H$, i.e., the number of degrees of freedom of the proposed method (3) is the same as for the classical finite element method

related to the space V_H. The basis functions of the multiscale method have local support. The overlap is proportional to the parameter k.

Review of A Priori Error Analysis. The error analysis in [8] shows that the error $u - u_{H,k}^{\mathrm{ms},h}$ for $k \approx \log \frac{1}{H}$ satisfies the following a priori estimate:

$$\|A^{1/2}\nabla(u - u_{H,k}^{\mathrm{ms},h})\| \leq C_f H + \inf_{v_h \in V_h} \|A^{1/2}\nabla(u - v_h)\|; \tag{4}$$

H being the mesh size of the underlying coarse finite element mesh, h being the fine mesh size for the local (parallel) computations. The desired accuracy TOL, e.g., $TOL \approx 0.01$ is achieved by choosing $H \approx TOL$ independent of any scales in the problem and by ensuring that the local problems are solved sufficiently accurate. For example, if $A \in W^{1,\infty}$ (bounded with bounded weak derivative) and ε is the smallest present scale, i.e., $\|\nabla A\|_{L^\infty(\Omega)} \lesssim \varepsilon^{-1}$, the second term in the right-hand side of (4) may be replaced by the worst case bound $Ch\varepsilon^{-1}$ for a first-order ansatz space V_h (see [9]). In this case, $C_f(H + \frac{h}{\varepsilon})$ bounds the error of our multiscale approximation (3).

The proof in [8] does not rely on regularity of the solution and gives a very explicit expression for the rate of convergence. The analysis confirms previous numerical results in [6, 7] and gives the (variational) multiscale method the solid theoretical foundation that has previously been missing. We further stress that our result is not asymptotic but holds for arbitrary coarse mesh parameter H.

The author is supported by the DFG Research Center Matheon Berlin.

References

[1] I. Babuška and R. Lipton. The penetration function and its application to microscale problems. *Multiscale Model. Simul.*, 9(1):373–406, 2011.

[2] F. Brezzi, L. Franca, T. Hughes, and A. Russo. $b = \int g$. *Comput. Methods Appl. Mech. Engrg.*, 145:329–339, 1997.

[3] C. Carstensen and R. Verfürth. Edge residuals dominate a posteriori error estimates for low order finite element methods. *SIAM J. Numer. Anal.*, 36(5):1571–1587 (electronic), 1999.

[4] T. Y. Hou and X.-H. Wu. A multiscale finite element method for elliptic problems in composite materials and porous media. *J. Comput. Phys.*, 134(1):169–189, 1997.

[5] T. J. R. Hughes, G. R. Feijóo, L. Mazzei, and J.-B. Quincy. The variational multiscale method—a paradigm for computational mechanics. *Comput. Methods Appl. Mech. Engrg.*, 166(1-2):3–24, 1998.

[6] M. G. Larson and A. Målqvist. Adaptive variational multiscale methods based on a posteriori error estimation: energy norm estimates for elliptic problems. *Comput. Methods Appl. Mech. Engrg.*, 196(21-24):2313–2324, 2007.

[7] A. Målqvist. Multiscale methods for elliptic problems. *Multiscale Model. Simul.*, 9:1064–1086, 2011.

[8] A. Målqvist and D. Peterseim Localization of Elliptic Multiscale Problems. *Matheon Preprint*, 807, arXiv:1110.0692v2, 2011.

[9] D. Peterseim and S. A. Sauter. Error estimates for finite element discretizations of elliptic problems with oscillatory coefficients. *DFG Research Center Matheon Berlin, Preprint Series*, 756, 2011.

On the treatment of interfaces in coupled problems (with a special focus on fluid-structure interaction)

Wolfgang A. Wall
(joint work with M.W Gee, A. Gerstenberger, T. Klöppel, A. Popp, S. Shahmiri)

The numerical simulation of coupled problems, in particular of fluid-structure interaction (FSI) phenomena, has long been a field of intensive research because of many applications in civil, mechanical, aerospace and biomechanical engineering. Of particular interest is the interaction of incompressible fluid flow with flexible structures. Crucial issues for such surface coupled problems are the treatment of the interface and the way the overall coupled problem is solved. Over the past decades, a manifold of solution schemes ranging from weakly coupled partitioned over strongly coupled partitioned to monolithic algorithms have been developed. Our focus here is on advanced approaches for the treatment of the interfaces that also favorably interplay with the different coupled solution schemes.

In order to establish the coupling between the fields, usually the no-slip condition at the interface Γ is applied, i.e.

$$\frac{\partial \mathbf{d}_\Gamma^{\mathrm{S}}}{\partial t} = \mathbf{u}_\Gamma^{\mathrm{F}} \quad \text{in} \quad \Gamma \times (0,T). \tag{1}$$

The superscript $\cdot^{\mathrm{S}}$ denotes quantities in the structure field, whereas $\cdot^{\mathrm{F}}$ refers to the fluid field. Additionally to condition (1), the interface tractions $\mathbf{h}_\Gamma^{\mathrm{S}}$ and $\mathbf{h}_\Gamma^{\mathrm{F}}$ of structure and fluid, respectively, have to match, yielding

$$\mathbf{h}_\Gamma^{\mathrm{S}} = -\mathbf{h}_\Gamma^{\mathrm{F}} \quad \text{in} \quad \Gamma \times (0,T). \tag{2}$$

Note that *a priori* the interface tractions is to be introduced to the system as unknown quantity.

Most FSI coupling schemes are based on the assumption of a conforming interface discretization, for which enforcing the coupling conditions is rather straightforward. However, this assumption will hold only in very rare cases. Different resolution requirements in the domains or simply a complex interface geometry make the creation of matching meshes cumbersome or even impossible.

A possible remedy for moving grid FSI (with an arbitrary Lagrangean-Eulerian (ALE) formulation for the fluid field) has been proposed in [1], where the dual mortar method is integrated into the FSI framework. This is done in a similar way as it was previously done in the context of structure meshtying and finite deformation contact [2]. In this approach, the method of weighted residuals is applied to (1), which introduces a Lagrange multiplier field. Characteristic for the method is the interpolation of this multiplier with so-called dual shape functions. Due to the particular interpolation, one of the two resulting mortar matrices is a diagonal matrix.

For Dirichlet-Neumann partitioned approaches this diagonality can be used for a numerically cheap transfer of interface degrees of freedom from structure to fluid field and of forces from fluid to structure. Focussing on monolithic coupling schemes, the dual mortar method allows for an efficient and robust elimination of

the additional Lagrange multiplier degrees of freedom from the coupled linear system by static condensation. Numerically, this condensation, which is only possible because of the particular interpolation of the multiplier, is very import for the applicability of state-of-the-art iterative solvers, as for standard mortar methods, the choice of applicable solvers is limited by the saddle-point-like structure of the system matrix.

The condensed system has the same block structure as its counterpart for the conforming case. Thus, two recently developed, very efficient coupled solvers presented in [3] can be used without any further modification. The first approach is based on a standard block Gauss-Seidel approach, where approximate inverses of the individual field blocks are based on a algebraic multigrid hierarchy tailored for the type of the underlying physical problem. The second is based on a monolithic coarsening scheme for the coupled system that makes use of prolongation and restriction projections constructed for the individual fields. The resulting method, therefore, involves coupling of the fields on coarse approximations to the problem yielding significantly enhanced performance.

Generally, moving grid algorithm with an ALE formulation suffer from an inability to realize very large rotations of the interface due to extreme mesh distortion around the interface of the fluid grid. An extension of the algorithm presented in [1] has been developed, which allows for a sliding motion of the fluid grid on the FSI surface. The algorithm uses the fact that, since conforming interfaces are no longer required, fluid grid and structure displacements can be decoupled, while the no-slip condition is still fulfilled.

In case of extreme deformations and rotations and in particular for multiple structures embedded within a fluid domain or cases where the domain topology changes, even sliding of the fluid grid on the FSI interface is not sufficient to avoid extreme mesh distortion. Therefore, an FSI approach based on the extended finite element method (XFM) has been developed [4]. In this fixed grid FSI approach, a Lagrangean structure is coupled with an extended fixed Eulerian background fluid field. Due to this setup, the no-slip condition (1) has to be enforced on an embedded interface, which requires tailored formulations as derived in [5]. This fixed grid FSI method provides enough flexibility to even allow for the treatment of topology changes in the fluid domain, which is for example the case with contacting structures within a fluid domain [6]. For the contact algorithm again a dual mortar method has been employed.

This XFEM based coupling approach can also be used to couple an extended Eulerian background fluid field with a second embedded fluid field [7]. The second fluid domain allows to resolve the boundary layers around a rigid obstacle in the flow. Moreover, the approach is not restricted to the Eulerian description of the embedded fluid. Thus, if the second field is formulated in an ALE framework it allows to resolve the boundary layer for the flow around a flexible and moving structure.

References

[1] T. Klöppel, A. Popp, U. Küttler, W.A. Wall, *Fluid-structure interaction for non-conforming interfaces based on a dual mortar formulation*, Computer Methods in Applied Mechanics and Engineering **200** (2011), 3111-3126.

[2] A. Popp, M. Gitterle, M.W. Gee, W.A. Wall, *A dual mortar approach for 3D finite deformation contact with consistent linearization*, International Journal for Numerical Methods in Engineering **83** (2010), 1428-1465

[3] M.W. Gee, U. Küttler, W.A. Wall, *Truly Monolithic Algebraic Multigrid for Fluid-Structure Interaction*, International Journal for Numerical Methods in Engineering **85** (2010), 987-1016

[4] A. Gerstenberger, W.A. Wall, *An extended finite element method / Lagrange multiplier based approach for fluid-structure interactions*, Computer Methods in Applied Mechanics and Engineering **197** (2008), 1699-1714

[5] A. Gerstenberger, W.A. Wall, *An embedded Dirichlet formulation for 3D continua*, International Journal for Numerical Methods in Engineering **82** (2010), 537-563

[6] U.M. Mayer, A. Popp, A. Gerstenberger, W.A. Wall, *3D fluid-structure-contact interaction based on a combined XFEM FSI and dual mortar contact approach*, Computational Mechanics **46** (2010), 53-67

[7] S. Shahmiri, A. Gerstenberger, W.A. Wall, *An XFEM based embedding mesh technique for incompressible viscous flows*, International Journal for Numerical Methods in Fluids **65** (2010), 166-190

Multiscale Modelling of Fracture

Stefan Loehnert

(joint work with Dana Mueller-Hoeppe, Corinna Prange, Matthias Holl)

In brittle materials microcracks in the vicinity of the crack front of a macrocrack can have a significant influence on the propagation of the macrocrack. Thus, it is important to accurately resolve the microstructural behaviour in such critical domains. It is difficult to account for these microstructural effects within a macroscopic part accurately in a single scale numerical analysis. Thus, error controlled adaptive multiscale strategies for the accurate prediction of microcrack / macrocrack interaction and propagation are required.

In contrast to multiscale techniques based on the RVE concept, the multiscale projection method has the advantage to directly capture microstructural effects including localization in detail and mesh independent. Shielding and amplification effects can be taken into account accurately. Due to the definition of a decoupled fine scale problem, multiple fine scale simulations of different regions of the macroscopic domain can be calculated independently and in parallel. This leads to a significant speedup of the method.

When cracks propagate the fine scale domains are automatically updated and move with the zone of interest around the propagating crack front. Cracks are modelled by means of the extended finite element method (XFEM) in 2D and 3D. Even though the XFEM is capable of producing accurate results for coarse meshes,

error controlled strategies are required to make sure that the numerical solution for arbitrary crack shapes and arbitrary boundary conditions leads to small errors without an unnecessary increase of numerical effort.

Recently the multiscale projection method was extended with error controlled mesh refinement strategies based on the simple Zienkiewicz Zhu error estimator. The stress smoothing technique is modified to account for the physical stress discontinuities due to cracks. The XFEM is applied also for the stress smoothing process. This error controlled strategy leads to a further significant reduction of numerical effort especially for three dimensional simulations. Different error estimation techniques like goal oriented estimators are possible.

In combination with the discretization error controlled strategy, recently also the model error is investigated and controlled. A fine scale model is only required where microcracks can develop and / or have a significant influence on the propagation behaviour of a macrocrack front. Since microcracks develop in domains of high stresses and stress gradients, the stress gradient is used to estimate where a fine scale model is required.

The accurate and error controlled prediction of 3D crack propagation remains a challenge.

Since the XFEM can be used for arbitrary discontinuities, it is also applied to heterogeneous media like metal foams. Recently in a joint work with the University of Split and the University of Maribor the effects of soft filler material on the energy absorption behavior of metal foams was investigated. Here one of the main challenges is the robust calculation of level set values for the definition of the foam geometry by means of a computer tomography scan to guarantee that the geometry of the foam with filler and without filler material is the same.

In a similar way the XFEM can be used to calculate other types of heterogeneities like polycristalline materials and their effective behavior during forming processes. Currently these processes are simulated using standard finite elements. However, for the simulation of fracture processes during forming the XFEM is an ideal tool. The simulation of multiphysical behavior in that context is still an open task.

References

[1] S. Loehnert, T. Belytschko, *A Multiscale Projection Method for Macro/Microcrack Simulations.*, Int. J. Numer. Meth. Engng. **71** (2007), 1466 – 1482.

[2] S. Loehnert, T. Belytschko, *Crack shielding and amplification due to multiple microcracks interacting with a macrocrack.*, International Journal of Fracture **145** (2007), 1 – 8.

[3] T. Belytschko, S. Loehnert, J.H. Song, *Multiscale Aggregating Discontinuities: A Method for Circumventing Loss of Material Stability.*, Int. J. Numer. Meth. Engng. **73** (2008), 869 – 894.

[4] S. Loehnert, D.S. Mueller-Hoeppe, *Multiscale Methods for Fracturing Solids.*, GACM Report (2008), 30 – 34.

[5] S. Loehnert, D.S. Mueller-Hoeppe, P. Wriggers, *3D corrected XFEM approach and extension to finite deformation theory.*, Int. J. Numer. Meth. Engng. **86** (2010): 431 – 452.
[6] S. Loehnert, L. Krstulovic-Opara, M. Vesenjak, D.S. Mueller-Hoeppe, *Homogenization principle based multi-scale modeling of cellular structures.*, Journal of the Serbian Society for Computational Mechanics **4** (2010): 97 – 109.
[7] C. Hoppe, S. Loehnert, P. Wriggers, *Error estimation for crack simulations using the XFEM.*, submitted to Int. J. Numer. Meth. Engng. (2011)
[8] M. Holl, S. Loehnert, P. Wriggers, *An adaptive multiscale method for crack propagation and crack coalescence.*, submitted to Int. J. Numer. Meth. Engng. (2011)

Enforcing interface flux continuity in enhanced XFEM: stability analysis

Pedro Díez
(joint work with Sergio Zlotnik and Régis Cottereau)

XFEM is found to be an efficient approach for solving multiphase problems. The model problem reads as follows, find u taking values in $\Omega_1 \cup \Omega_2$ such that

$$\nabla\cdot(-\nu_1\nabla u) = f \qquad \text{in } \Omega_1 \tag{1a}$$

$$\nabla\cdot(-\nu_2\nabla u) = f \qquad \text{in } \Omega_2 \tag{1b}$$

$$-\nu\nabla u\cdot\mathbf{n} = g_N \qquad \text{on } \Gamma_N \tag{1c}$$

$$u = u_D \qquad \text{on } \Gamma_D \tag{1d}$$

$$\nu_1\nabla u|_{\Omega_1}\cdot\mathbf{n} = \nu_2\nabla u|_{\Omega_2}\cdot\mathbf{n} \qquad \text{on } \Gamma := \partial\Omega_1 \cap \partial\Omega_2 \tag{1e}$$

The level set representation of the phase domains allows having a grid independent of the location of the interface [2]. In order to introduce the necessary gradient discontinuities inside the elements crossed by the interface, XFEM uses the partition of the unity idea to enrich the discretization. In this context, a sensible choice for the enrichment is using a ridge function R defined as

$$R = \sum_{i=1}^{n_H} N_i|\phi_i| - \left|\sum_{i=1}^{n_H} N_i\phi_i\right|,$$

being N_i the shape functions and ϕ_i the nodal values of the level set, for $i = 1,\dots,n_H$, see [1, 3]. Thus, the XFEM approximation reads

$$u_X = \sum_{i=1}^{n_H} N_i u_i + \sum_{j\in\mathcal{N}_a} RN_j a_j,$$

where the coefficients u_i for $i = 1,\dots,n_H$ are the standard Finite Element nodal unknowns and a_j, $j \in \mathcal{N}_a$, stand for the enriched nodal coefficients.

XFEM provides a much better approximation of the multiphase solution, improving the quality the global quantity (energy like) that the variational form of the problem seeks minimizing. Nevertheless, when applied to diffusion problems in a multiphase setup with high diffusivity contrast, the XFEM strategy suffers from an inaccurate representation of the local fluxes in the vicinity of the interface. The XFEM enrichment improves the global quality of the solution but it is not

properly enforcing any local feature to the fluxes. Thus, the resulting numerical fluxes in the vicinity of the interface are not realistic, in particular when the parametric contrast between the two phases is important. An additional restriction to the XFEM formulation is introduced, aiming at properly reproducing the features of the local fluxes in the transition zone. This restriction is implemented through Lagrange multipliers. The resulting enlarged variational problem reads find the XFEM approximation $u_X \in V_X$ and the (discrete) Lagrange multiplier $\lambda_H \in \tilde{V}_H$ such that

$$a(u_X, w) + b(\lambda_H, w) = \ell(w) \qquad \forall w \in V_{X,0} \tag{2a}$$

$$b(\mu, u_X) = 0 \qquad \forall \mu \in \tilde{V}_H \tag{2b}$$

being $a(\cdot,\cdot)$ the standard bilinear form representing the weak form of problem (1) and

$$b(\mu, u) := \int_\Gamma (\nu_1 \nabla u|_{\Omega_1} - \nu_2 \nabla u|_{\Omega_2}) \cdot \mathbf{n}\, \mu \, d\Gamma. \tag{3}$$

Note that (2b) is the weak form of (1e) and it is the restriction aiming at improving the quality of the flux continuity and, consequently, the quality of the fluxes in the vicinity of the interface. Several examples are presented and the solutions obtained from (2) show a spectacular improvement of the quality of the fluxes with respect to the standard XFEM.

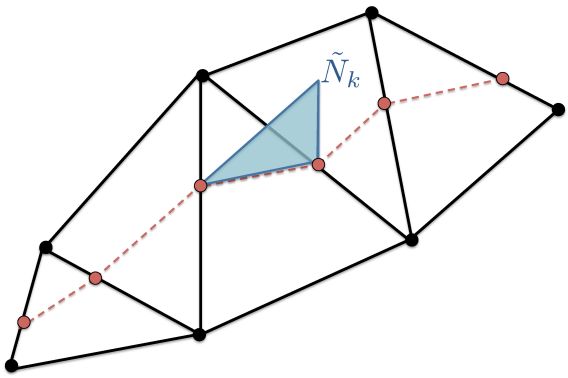

FIGURE 1. Illustration of the semi-hat functions of the Lagrange multipliers space, $\tilde{N}_k$.

The problem of choosing the proper Lagrange multiplier space introduces a classical dilemma: if $\tilde{V}_H$ is too *small* the restriction is not properly enforced and if it is too *large* the resulting method may be unstable. After some numerical tests, the option selected corresponds to the semi hat functions along the interface, as illustrated in figure 1. In this case, the dimension of $\tilde{V}_H$ is twice the number of elements crossed by the interface.

The mathematical proof of the stability of the numerical scheme requires checking if the LBB condition (also known as inf-sup condition) is fulfilled for the elected spaces and bilinear restriction. We propose a novel approach to prove this proposition by introducing an equivalent form of the theorem and two auxiliary lemmas.

Recall that the well-known LBB compatibility condition, is sufficient to guarantee the stability of the formulation. In other words, the formulation is stable if it exists $k > 0$ such that

$$\inf_{\mu \in \tilde{V}_H} \sup_{w \in V_X} \frac{b(\mu, w)}{||\mu||\,||w||} \geq k \tag{4}$$

The LBB condition is equivalent to the following
Proposition: $\exists \alpha > 0$ such that $\forall \mu \in \tilde{V}_H$, $\exists v \in V_X$ verifying

$$[\![\nu \nabla v \cdot \mathbf{n}]\!] = \mu \tag{5a}$$

$$\|v\|_{V_X} \leq \alpha \|\mu\|_{\tilde{V}_H} \tag{5b}$$

The equivalence is straightforwardly shown by considering that

$$b(\mu, w) = \int_\Gamma \mu^2 d\Gamma = ||\mu|| \text{ and } \frac{b(\mu, v)}{||\mu||\,||v||} = \frac{||\mu||}{||v||}$$

Thus, since $||v|| \leq \alpha ||\mu||$, taking $k = 1/\alpha$ the LBB condition follows.

The latter proposition is reduced to proof the two following lemmas.

Lemma 1 (local version of the proposition, restricted to one element): Let Ω^k be one linear triangular element crossed by the interface Γ. The restriction of Γ to Ω^k is denoted Γ^k. The nodes of Ω^k are denoted P_1, P_2 and P_3, choosing the order such that P_1 and P_2 are on the same side of the interface. As classically done in XFEM, we assume that $\exists \epsilon > 0$ such that $|\Gamma^k| > \epsilon$. The restrictions of the functional spaces V_X and $\tilde{V}_H$ to Ω^k and Γ^k are denoted V_X^k and $\tilde{V}_H^k$, with respective norms $\|v\|^2_{V_X^k} = \int_{\Omega^k} v^2 d\Omega$ and $\|\mu\|^2_{\tilde{V}_H^k} = \int_{\Gamma^k} \mu^2 d\Gamma$. The standard FE shape function corresponding to the node P_1 is denoted N_1, and the ridge function R.

Then, $\exists \alpha > 0$ such that $\forall \mu \in \tilde{V}_H^k$, $\exists v \in \text{span}\{N_1, RN_1\} \subset V_X^k$ (i.e. describing v with the d.o.f. corresponding to P_1 only) verifying

$$[\![\nu \nabla v \cdot \mathbf{n}]\!] = \mu \tag{6a}$$

$$\|v\|_{V_X^k} \leq \alpha \|\mu\|_{\tilde{V}_H^k} \tag{6b}$$

Lemma 2 (controlled propagation of the norm along the interface elements strip): Let Ω^k and Ω^{k+1} be two contiguous elements crossed by the interface. Let us denote P_1 and P_3 the common nodes to Ω^k and Ω^{k+1}, being P_2 the third node in Ω^k. P_1 is selected such that it is on the same side of the interface as P_2. The third node in Ω^{k+1} is denoted as P_4. Then, $\exists \beta > 0$ such that,

for any v defined by the d.o.f. of Ω^k, $v \in \text{span}\{N_i, RN_i\}$, $i = 1, 2, 3$ it holds that $\|v\|_{V_X^{k+1}} \leq \beta \|v\|_{V_X^k}$.

References

[1] Moës N, Cloirec M, Cartaud P, Remacle JF. A computational approach to handle complex microstructure geometries. *Comp. Meth. Appl. Mech. Engrg.* 2003; **192**(28-30):3163–3177,

[2] Sethian JA. *Level Set Methods and Fast Marching Methods: Evolving Interfaces in Computational Geometry, Fluid Mechanics, Computer Vision, and Materials Science*. Cambridge University Press: Cambridge, U.K., 1999.

[3] Zlotnik S, Díez P. Hierarchical X-FEM for n-phase flow (n>2). *Comp. Meth. Appl. Mech. Engrg.* 2009; **198**(30-32):2329–2338,

Isoparametric C^0 Interior Penalty Methods for Plate Bending Problems on Smooth Domains

Li-yeng Sung

(joint work with Susanne C. Brenner and Michael Neilan)

Let Ω be a bounded smooth domain in $\mathbb{R}^2$ such that $\partial\Omega$ is the union of the disjoint closed curves Γ_C, Γ_S and Γ_F. The bending problem of a thin Kirchhoff plate [7] is to find $u \in V$ such that

$$\int_\Omega \{(\Delta w)(\Delta v) - (1-\nu)[w,v]\}\,dx = \int_\Omega f v\,dx \qquad \forall\, v \in V, \tag{1}$$

where $V = \{v \in H^2(\Omega) : v = 0 \text{ on } \Gamma_C \cup \Gamma_S \text{ and } \partial v/\partial n = 0 \text{ on } \Gamma_C\}$, $\nu \in (0, \frac{1}{2})$ is the Poisson ratio, and

$$[w,v] = \Big(\frac{\partial^2 w}{\partial x_1^2}\Big)\Big(\frac{\partial^2 v}{\partial x_2^2}\Big) + \Big(\frac{\partial^2 w}{\partial x_2^2}\Big)\Big(\frac{\partial^2 v}{\partial x_1^2}\Big) - 2\Big(\frac{\partial^2 w}{\partial x_1 \partial x_2}\Big)\Big(\frac{\partial^2 v}{\partial x_1 \partial x_2}\Big)$$

is the Monge-Ampère bilinear form.

Here u is the vertical displacement of the middle surface of the plate, $f \in L_2(\Omega)$ is the vertical load density divided by the flexural rigidity of the plate, and Γ_C (resp. Γ_S and Γ_F) is the clamped (resp. simply supported and free) part of $\partial\Omega$. We assume $|\Gamma_C| + |\Gamma_S| > 0$ so that (1) is well-posed.

In order to obtain high order convergence, the computational domain of a finite element method for (1) must approximate Ω to a high order. For second order problems this can be accomplished by the isoparametric approach [6, 9, 4]. But the construction of C^1 finite element methods on non-polygonal domains is much more complicated [14, 15, 12, 10, 11, 13].

We have shown in [3] that by combining isoparametric finite element spaces for second order problems with the C^0 interior penalty methodology [8, 5, 2], it is possible to solve the plate bending problem (1) efficiently. In this approach the discrete problem is obtained by the following procedure.

We construct a curvilinear polygon Ω_h whose corners belong to $\partial\Omega$ such that Ω_h is the union of the triangles in a quasi-uniform triangulation $\mathcal{T}_h$. We assume that Ω_h is a good approximation of Ω so that $\partial\Omega_h$ is the union of the disjoint closed subsets $\Gamma_{C,h}$, $\Gamma_{S,h}$ and $\Gamma_{F,h}$ that approximate Γ_C, Γ_S and Γ_F respectively. Each of the triangles in $\mathcal{T}_h$ can have at most one curved edge and only those triangles with more than one vertex on $\partial\Omega$ can have a curved edge. We assume that each triangle

$T \in \mathcal{T}_h$ is the diffeomorphic image of the reference triangle $\hat{T}$ under a polynomial map $F_T : \hat{T} \longrightarrow T$ of degree less than or equal to k ($k \geq 2$).

Let $\tilde{V}_h \subset H^1(\Omega_h)$ be the isoparametric P_k Lagrange finite element space associated with $\mathcal{T}_h$. We assume that all the nodes associated with $\tilde{V}_h$ belong to $\bar{\Omega}$ and the boundary nodes of $\tilde{V}_h$ also belong to $\partial\Omega$. Under the assumption that

$$f \in W_p^{k-1}(\Omega) \quad \text{where} \quad \begin{cases} p > 2 & \text{if } k = 2 \\ p = 2 & \text{if } k > 2 \end{cases}, \tag{2}$$

we can then define the nodal interpolant $f_h\,(\in \tilde{V}_h)$ of f.

The discrete problem for (1) is to find $u_h \in V_h$ such that

$$a_h(u_h, v) = \int_{\Omega_h} f_h v \, dx \qquad \forall\, v \in V_h, \tag{3}$$

where $V_h = \{v \in \tilde{V}_h : v = 0 \text{ on } \Gamma_{C,h} \cup \Gamma_{S,h}\}$,

$$\begin{aligned} a_h(w, v) = \sum_{T \in \mathcal{T}_h} \int_T \Big((\Delta w)(\Delta v) - (1-\nu)[w, v] \Big) dx \\ - \sum_{e \in \mathcal{E}_h^I \cup \mathcal{E}_h^C} \int_e \Big(\{\!\{ M_e(w) \}\!\} [\![\partial v / \partial n_e]\!] + \{\!\{ M_e(v) \}\!\} [\![\partial w / \partial n_e]\!] \Big) ds \\ + \sum_{e \in \mathcal{E}_h^I \cup \mathcal{E}_h^C} \frac{\sigma}{|e|} \int_e [\![\partial w / \partial n_e]\!] [\![\partial v / \partial n_e]\!] \, ds, \end{aligned}$$

$\mathcal{E}_h^I$ is the set of the interior edges of $\mathcal{T}_h$, $\mathcal{E}_h^C$ is the set of the edges of $\mathcal{T}_h$ along $\Gamma_{C,h}$,

$$\{\!\{ M_e(v) \}\!\} = \{\!\{ -\Delta v + (1-\nu)(\nabla^2 v) t_e \cdot t_e \}\!\}$$

is the average of the bending moment across the edge e, $[\![\partial v / \partial n_e]\!]$ is the jump of the normal derivative across the edge e, $|e|$ is the length of e, and $\sigma > 0$ is a penalty parameter.

Let the mesh-dependent energy norm $\| \cdot \|_h$ be defined by

$$\begin{aligned} \|v\|_h^2 = \sum_{T \in \mathcal{T}_h} \Big(\nu \|\Delta v\|_{L_2(T)}^2 + (1-\nu) |v|_{H^2(T)}^2 \Big) \\ + \sum_{e \in \mathcal{E}_h^I \cup \mathcal{E}_h^C} \frac{|e|}{\sigma} \|\{\!\{ M_e(v) \}\!\}\|_{L_2(e)}^2 + \sum_{e \in \mathcal{E}_h^I \cup \mathcal{E}_h^C} \frac{\sigma}{|e|} \|[\![\partial v / \partial n_e]\!]\|_{L_2(e)}^2. \end{aligned}$$

The bilinear form $a_h(\cdot, \cdot)$ is bounded with respect to $\| \cdot \|_h$, and for a sufficiently large σ, it is also coercive. Therefore we have a standard abstract error estimate [6, 4] for the solution u_h of (3):

$$\|u - u_h\|_h \leq C \Big[\inf_{v \in V_h} \|u - v\|_h + \sup_{w \in V_h \setminus \{0\}} \frac{a_h(u - u_h, w)}{\|w\|_h} \Big]. \tag{4}$$

Under the regularity assumption (2), the magnitude of the first term on the right-hand side of (4) is easily shown to be $O(h^{k-1})$ by the interpolation error estimates developed in [1]. Thus the main difficulty for traditional approaches

to fourth order problems on curved domains, namely the constructions of good interpolants, disappears in the C^0 interior penalty approach.

The second term on the right-hand side of (4), which measures the consistency error, can also be handled in a standard fashion. It follows that

$$\|u - u_h\|_h \leq Ch^{k-1}, \tag{5}$$

which is optimal. If the free boundary is absent, we can also prove an L_2 error estimate

$$\|u - u_h\|_{L_2(\Omega_h)} \leq Ch^{k+\min(3,k)-2} \tag{6}$$

under the assumption that $f \in W^{k+\min(3,k)-2}$. The estimate (6) is optimal for $k \geq 3$.

Details for (5) and (6) can be found in [3], where subparametric C^0 interior penalty methods are also discussed.

References

[1] C. Bernardi, *Optimal finite-element interpolation on curved domains*, SIAM J. Numer. Anal. **26** (1989), 1212–1240.

[2] S.C. Brenner, C^0 *Interior Penalty Methods*, In J.Blowey and M. Jensen, editors, *Frontiers in Numerical Analysis-Durham 2010*, volume 85 of *Lecture Notes in Computational Science and Engineers*, pages 79–147. Springer-Verlag, Berlin-Heidelberg, 2012.

[3] S.C. Brenner, M. Neilan, and L.-Y. Sung, *Isoparametric C^0 interior penalty methods for plate bending problems on smooth domains*, Calcolo (to appear), 2012.

[4] S.C. Brenner and L.R. Scott, *The Mathematical Theory of Finite Element Methods* (*Third Edition*). Springer-Verlag, New York, 2008.

[5] S.C. Brenner and L.-Y. Sung, *C^0 interior penalty methods for fourth order elliptic boundary value problems on polygonal domains*, J. Sci. Comput. **22/23** (2005), 83–118.

[6] P.G. Ciarlet, *The Finite Element Method for Elliptic Problems*. North-Holland, Amsterdam, 1978.

[7] G. Duvaut and J.L. Lions, *Inequalities in Mechanics and Physics*. Springer-Verlag, Berlin, 1976.

[8] G. Engel, K. Garikipati, T.J.R. Hughes, M.G. Larson, L. Mazzei, and R.L. Taylor, *Continuous/discontinuous finite element approximations of fourth order elliptic problems in structural and continuum mechanics with applications to thin beams and plates, and strain gradient elasticity*, Comput. Methods Appl. Mech. Engrg. **191** (2002), 3669–3750.

[9] M. Lenoir, *Optimal isoparametric finite elements and error estimates for domains involving curved boundaries*, SIAM J. Numer. Anal. **23** (1986), 562–580.

[10] L. Mansfield, *Approximation of the boundary in the finite element solution of fourth order problems*, SIAM J. Numer. Anal. **15** (1978), 568–579.

[11] L. Mansfield, *A Clough-Tocher type element useful for fourth order problems over nonpolygonal domains*, Math. Comp. **32** (1978), 135–142.

[12] L.R. Scott, *A survey of displacement methods for the plate bending problem*, In *Formulations and computational algorithms in finite element analysis* (*U.S.-Germany Sympos., Mass. Inst. Tech., Cambridge, Mass., 1976*), pages 855–876. M.I.T. Press, Cambridge, Mass., 1977.

[13] A. Ženíšek, *Curved triangular finite C^m-elements*, Apl. Mat. **23** (1978), 346–377.

[14] M. Zlámal, *Curved elements in the finite element method. I*, SIAM J. Numer. Anal. **10** (1973), 229–240.

[15] M. Zlámal, *Curved elements in the finite element method. II*, SIAM J. Numer. Anal. **11** (1974), 347–362.

Optimal Mesh Refinement Strategies

Hella Rabus
(joint work with Carsten Carstensen)

1. Marking strategies in adaptive mesh refinement

In general adaptive finite element algorithms consist of successive loops of the steps

$$\text{Solve} \longrightarrow \text{Estimate} \longrightarrow \text{Mark} \longrightarrow \text{Refine}.$$

The choice of the error estimator η_ℓ and the particular marking strategy play an elementary role in the analysis of the convergence of discrete solutions. In particular the generated sequence of meshes $(\mathcal{T}_\ell)_\ell$ needs to resolve oscillations of the right-hand side f sufficiently. Oscillations of $f \in L^2(\Omega)$ on a $\mathcal{T}_\ell$ are defined via

$$\operatorname{osc}_\ell^2 := \operatorname{osc}^2(f, \mathcal{T}_\ell) := \sum_{T \in \mathcal{T}_\ell} \operatorname{osc}^2(f, T) \text{ with } \operatorname{osc}(f, \omega) \quad := |\omega|^{1/2} \, \|f - f_\omega\|_{L^2(\omega)},$$

where f_ω is the integral mean of f on the subset $\omega \subseteq \Omega$.

One possible strategy is to reduce oscillations a priori (cf. [8, for conform FEM] and [7, for mixed FEM]). Before running the Afem algorithm itself, an initial mesh $\hat{\mathcal{T}}_0$ is generated (e.g., by Approx [3]), which satisfies $\operatorname{osc}(f, \hat{\mathcal{T}}_0) \leq \text{Tol}$ for a given $\text{Tol} > 0$.

When oscillations are simultaneously reduced within the Afem-loop, one basically distinguishes between separate and collective marking strategies. Collective marking relies on error estimators, which dominate oscillations and therefore oscillation are simultaneously reduced.

Separate marking means that oscillations are treated separately, they are not necessarily dominated by the specific error estimator. One strategy is to introduce an inner loop for oscillations reduction [11], which may cause additional computational effort. Another separate marking strategy is to switch between cases depending on whether oscillations are small compared to the error estimator. Two possibilities, which result in quasi-optimal convergent algorithms, have been presented recently for the Raviart-Thomas finite element method and the Poisson model problem, cf. [1, BM-Amfem] and [6, Amfem]. Whereas BM-Amfem applies a standard Dörfler marking in both cases, Amfem makes use of the Approx algorithm if oscillations are large. The Amfem-loop reads as follows.

After having solved the problem on $\mathcal{T}_\ell$, with right-hand side $f \in L^2(\Omega)$ and $\eta_\ell(E)$, and osc_ℓ are computed in step estimate. Then, the algorithm switches between **Case (a)** if $\operatorname{osc}_\ell^2 \leq \kappa \eta_\ell^2$ and **Case (b)** otherwise as follows

Case (A): Mark: Compute $\mathcal{M}_\ell$ s.t. $\theta \eta_\ell^2 \leq \eta_\ell^2(\mathcal{M}_\ell)$.
Refine: $\mathcal{T}_{\ell+1} = \text{Refine}(\mathcal{T}_\ell, \mathcal{M}_\ell, \text{NVB})$.

Case (B): Mark: Run Approx [3] to generate optimal refinement $\mathcal{T}$ of $\mathcal{T}_0$ with $\operatorname{osc}^2(\mathcal{T}, f) \leq \text{Tol}^2 = \rho_B \operatorname{osc}^2(\mathcal{T}_\ell, f)$, for $\rho_B < 1$.
Refine: Compute $\mathcal{T}_{\ell+1} = \mathcal{T}_\ell \oplus \mathcal{T}$.

One difficulty arises in the analysis of quasi-optimal convergence, when in step REFINE the overlay $\mathcal{T}_{\ell+1} = \mathcal{T}_\ell \oplus \mathcal{T}$ of $\mathcal{T}_\ell$ and $\mathcal{T}$ has to be computed. Numerical experiments verify that for AMFEM a proper choice of ρ_B leads to a significant reduction of number of loops where Case (B) applies, while the Dörfler marking for oscillations in BM-AMFEM allows less flexibility.

2. The pure displacement problem in linear elasticity

The Navier Lamé equations read in terms of the pure Dirichlet problem in linear elasticity as $-\mu\Delta u - (\lambda+\mu)\nabla \operatorname{div} u = f$ in Ω and $u = 0$ on $\partial\Omega$. For the symmetric gradient $\operatorname{sym} \mathrm{D}\, u = (\mathrm{D}\, u + \mathrm{D}\, u^T)/2$, and Lamé parameters λ and μ this formulation is known to be equivalent to

$$-\operatorname{div}(\mathbb{C} \operatorname{sym} \mathrm{D}\, u) = f \text{ in } \Omega$$

with $\mathbb{C}A = 2\mu A + \lambda \operatorname{tr}(A)\, \mathbb{1}$ for all $A \in \mathbb{R}^{2\times 2}$. Let $V_\ell := V(\mathcal{T}_\ell) := \mathrm{CR}^1_0(\mathcal{T}_\ell) \times \mathrm{CR}^1_0(\mathcal{T}_\ell)$ be the nonconforming space of piecewise affine Crouzeix-Raviart functions in two dimensions with homogeneous Dirichlet boundary conditions. The discrete problem reads: Seek discrete displacements $u_\ell \in V_\ell$ such that

$$a_{NC(\ell)}(u_\ell, v_\ell) = F(v_\ell) \text{ for all } v_\ell \in V_\ell, \tag{1}$$

with $a_{NC(\ell)}(u_\ell, v_\ell) := \int_\Omega \mathrm{D}_\ell\, u_\ell : \mathbb{C}\, \mathrm{D}_\ell\, v_\ell \,\mathrm{dx}$ for $u_\ell, v_\ell \in V_\ell$.

ACRFEM

Input: Initial coarse triangulation $\mathcal{T}_0$, $0 < \theta < \theta_0 \le 1$.

Loop: For $\ell = 0, 1, \ldots$

- **Solve** problem (1) on $\mathcal{T}_\ell$.
- **Estimate** $\eta_\ell^2 := \sum_{T\in\mathcal{T}_\ell} \eta_\ell^2(T)$ with
$$\eta_\ell^2(T) := |T|\, \|f\|^2_{L^2(T)} + |T|^{1/2} \sum_{E\in\mathcal{E}(T)} \|[\partial u_\ell/\partial s]_E\|^2_{L^2(E)}\,.$$
- **Mark** a minimal subset $\mathcal{M}_\ell \subseteq \mathcal{T}_\ell$ of triangles with
$$\theta\eta_\ell^2 \le \eta_\ell^2(\mathcal{M}_\ell) := \sum_{T\in\mathcal{M}_\ell} \eta_\ell^2(T).$$
- **Refine** $\mathcal{M}_\ell$ in $\mathcal{T}_\ell$ with NVB and generate $\mathcal{T}_{\ell+1}$.

(Update ℓ)

Output: Sequence of triangulations $(\mathcal{T}_\ell)$ and discrete solutions (u_ℓ).

With respect to some approximation class $\mathcal{A}_s := \{(u,f) \mid |(u,f)|_{\mathcal{A}_s} < \infty\}$, for $s > 0$ the adaptive algorithm ACRFEM is of quasi-optimal convergence [5] in the sense that for any $0 < \theta < \theta_0 \le 1$ with θ_0 independent of λ ACRFEM generates sequences $(\mathcal{T}_\ell)_\ell$, $(u_\ell)_\ell$ of quasi-optimal rates of convergence in the sense that

$$|\mathcal{T}_\ell| - |\mathcal{T}_0| \le C_{\mathrm{opt}} \left(|\!|\!| u - u_\ell |\!|\!|^2_{NC(\ell)} + \|h_\ell f\|^2_{L^2(\Omega)} \right)^{-1/(2s)}.$$

As the analysis proves robustness in λ as $\lambda \to \infty$, ACRFEM provides an algorithm of quasi-optimal convergence for the Stokes problem, cf. [2, 9, 4]. Furthermore numerical experiments verify this robustness, cf. the subsequent figure for a comparison of the convergence behaviour for the pure displacement problem in linear elasticity on the L-shaped domain. For conform FEM locking is observed, while the convergence rates of the nonconforming CR FEM are robust in λ.

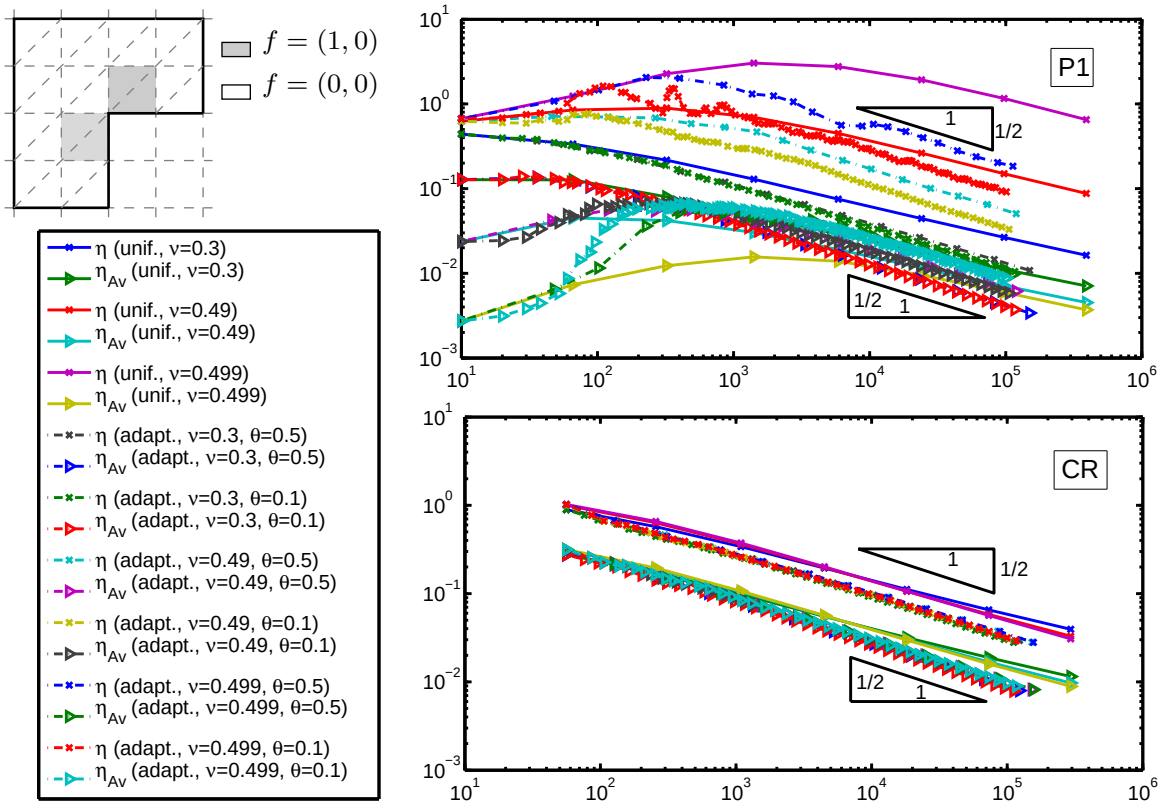

References

[1] R. Becker and S. Mao. *An optimally convergent adaptive mixed finite element method.* Numer. Math., 111:35–54, 2008.

[2] R. Becker and S. Mao. *Adaptive nonconforming finite elements for the Stokes equations.* SIAM J. Numer. Anal., 49(3):970–991, 2011.

[3] P. Binev, W. Dahmen, and R. de Vore. *Adaptive finite element methods with convergence rates.* Numer. Math., 97:219–268, 2004.

[4] C. Carstensen, D. Peterseim, and H. Rabus. *The adaptive nonconforming FEM for the pure Displacement problem in linear elasticity is optimal and robust.* Numer. Math., submitted.

[5] C. Carstensen and H. Rabus. *The adaptive nonconforming fem for the pure displacement problem in linear elasticity is optimal and robust.* SIAM J. Numer. Anal., 2012. accepted.

[6] C. Carstensen and H. Rabus. *An optimal adaptive mixed finite element method.* Math. Comp., 80(274):649–667, 2011.

[7] L. Chen, M. Holst, and J. Xu. *Convergence and optimality of adaptive mixed finite element methods.* Math. Comp., 78(265):35–53, 2009.

[8] W. Dörfler. *A convergent adaptive algorithm for Poisson's equation.* SIAM J. Numer. Anal., 33(3):1106–1124, 1996.

[9] J. Hu and J. Xu. *Convergence of adaptive conforming and nonconforming finite element methods for the perturbed Stokes equation.* Research Report, 2007. School of Mathematical Sciences and Institute of Mathematics, Peking University, available at www.math.pku.edu.cn:8000/var/preprint/7297.pdf.

[10] H. Rabus. *A natural adaptive nonconforming FEM of quasi-optimal complexity.* Comput. Methods Appl. Math., 10(3):315–325, 2010.

[11] R. Stevenson. *The completion of locally refined simplicial partitions created by bisection.* Math. Comp., 77(261):227–241, 2008.

Error estimation in a non-overlapping domain decomposition framework

Christian Rey
(joint work with P. Gosselet, A. Parret-Fréaud)

For the last decades, three trends have grown and reinforced each other: the fast growth of hardware computational capacities, the requirement of finer and larger finite element models for industrial simulations and the development of efficient computational strategies amongst which non-overlapping domain decomposition (DD) methods [1, 3, 4] are very popular since they have proved to be scalable in many applications. One main fallout lies on the verification of the discretized models in order to warranty the quality of numerical simulations (global or goal-oriented error estimators). Among the different classes of global error estimators, the one based on the evaluation of the constitutive relation error $e_{cr(\Omega)}(\hat{u},\hat{\sigma})$ [5], offers a simple and efficient way to obtain a guaranteed upper bound of the discretization error,

$$|||u-\hat{u}||| \leq e_{cr(\Omega)}\left(\hat{u},\hat{\sigma}\right)$$

where, $|||.|||$ is the standard energy norm and $(\hat{u},\hat{\sigma})$ is a pair of admissible fields (typically a displacement-stress pair in elasticity). In a standard FE context, the FE solution $\hat{u}$ being admissible, the key point then reduces to the construction of an admissible stress field $\hat{\sigma}$. Classical methods are the dual approach [8], the element equilibrium technique [6] which have been improved by the use of the concept of partition of unity which lead to [7] and the *flux-free* technique [10].

In this talk, we present some of our recent works [2] that aim at building error estimators based on the constitutive relation error in a non-overlapping domain decomposition framework. Let us consider a non-overlapping domain decomposition of $\bar{\Omega}=\cup_s\bar{\Omega}^{(s)}$ in N_{sd} subdomains. We focus on the construction of a fully parallel global error estimator by the use of a global error estimator, as a black box, on each subdomains $\Omega^{(s)}$. It is based on the construction of a pair of admissible interface fields (u_b,λ_b) that satisfy (i) a continuity condition for u_b and (ii) for λ_b both a flux condition (balance condition) and the Fredholm's alternative that ensures, on each subdomain, the well-posedness of Neumann problems. Note that the last condition involves the solution to a coarse problem. Let us denote $u_D=\left\{u_D^{(s)}\right\}_s$ (resp. $u_N=\left\{u_N^{(s)}\right\}_s$) the collection of FE solutions on each subdomain associated to u_b-Dirichlet (resp. λ_b-Neumann) boundary type condition at the interface, we then can prove :

$$|||u-u_D||| \leq e_{cr}^{ddm}(u_D,\hat{\sigma}\left(u_N\right)) = \left(\sum_s\left(e_{cr(\Omega^{(s)})}\left(u_D^{(s)},\hat{\sigma}(u_N^{(s)})\right)\right)^2\right)^{1/2}$$

which defines a first simple and fully parallel DD-error estimator. Connection with both primal (BDD) and dual (FETI) iterative domain decomposition solver can be derived. The estimator yields a guaranteed upper bound on the discretization error whatever the state (converged or not) of the associated iterative solver. It

has been numerically observed that our DD-error estimator enables to recover the same efficiency factor as the standard sequential one. Figure (1) illustrates, on a small crack opening problem already used in [10], the convergence of the DD-error estimator as well as its local contribution (element level) along FETI iterations.

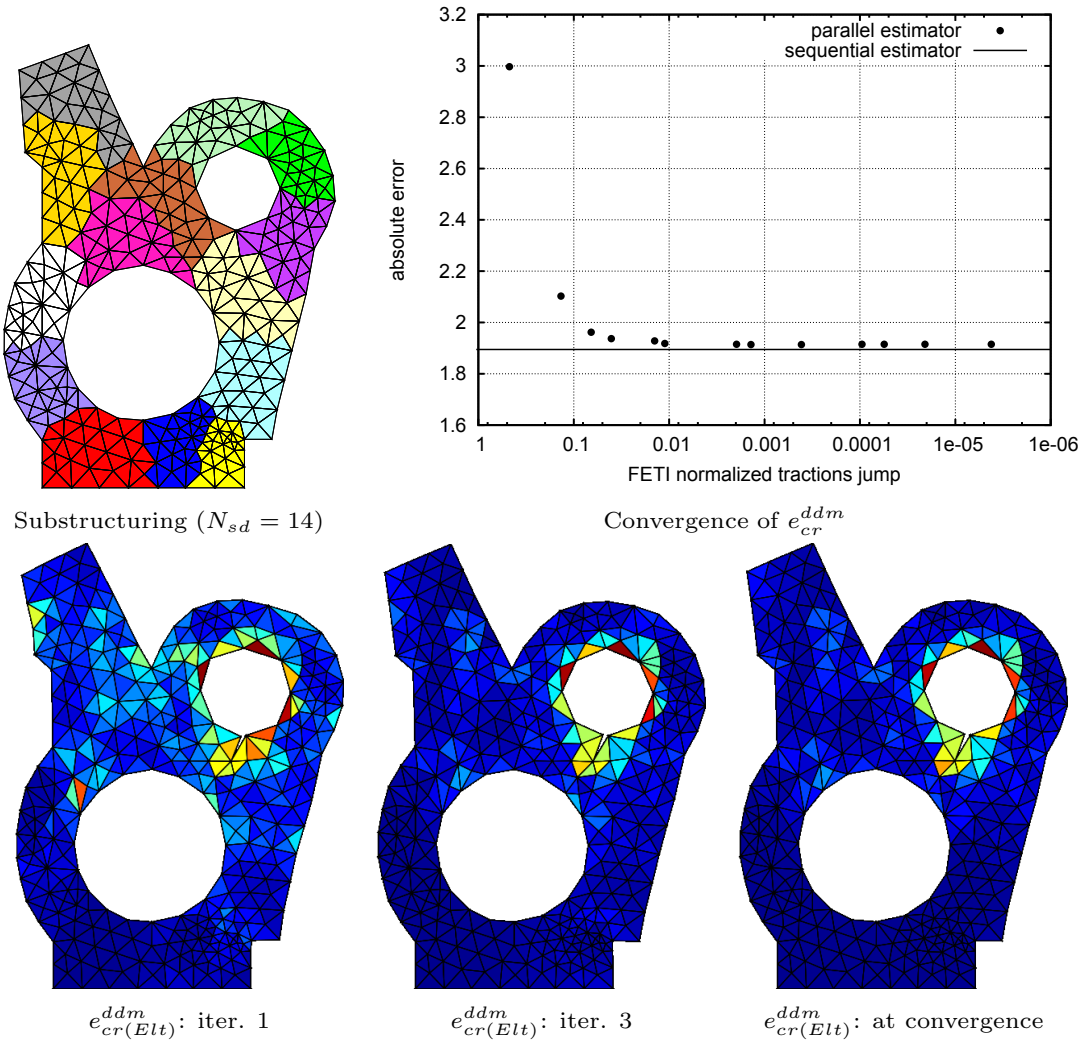

FIGURE 1. Crack opening problem: Convergence of e_{cr}^{ddm} vs. interface residual and elementary contributions to $e_{cr(Elt)}^{ddm}$

The fast convergence numerically observed of both indicators, strongly suggests to improve the previous upper bounds so that to separate contributions coming from both the discretization error and the algebraic error related to the used of the DD-iterative solver. Using results from [9], we eventually prove the following upper bound,

$$|||u - u_N||| \leq |[u_N]|_b + e_{cr}^{ddm}\left(u_N, \hat{\sigma}\left(u_N\right)\right)$$

where $|.|_b$ is the norm associated to the FETI preconditioner and $[u_N]$ is the jump of u_N at the interface. This last inequality clearly enable us to separate the algebraic error related to the FETI solver and discretization error $e_{cr}^{ddm}\left(u_N, \hat{\sigma}\left(u_N\right)\right)$. This

enables to stop FETI iterations as soon as the norm of the FETI preconditioned residual is small enough compared to the discretization error.

Works in progress are related to (i) goal-oriented error estimator (ii) nonlinear problems.

References

[1] P. Gosselet, C. Rey *Non-overlapping domain decomposition methods in structural mechanics*, Arch. Comput. Meth. Engng. **13** (2006), 515–572.

[2] A. Parret-Fréaud, C. Rey, P. Gosselet, F. Feyel *Fast estimation of discretization error for FE problems solved by domain decomposition*, Comput. Methods Appl. Mech. Engrg. **199** (2010), 3315–3323.

[3] C. Farhat, F. X. Roux, *Implicit Parallel Processing in Structural Mechanics*, Computational Mechanics Advances, **2**, (1994), 1–124.

[4] P. Le Tallec, *Domain-decomposition methods in computational mechanics*, Computational Mechanics Advances, **1**, (1994), 121–220.

[5] P. Ladevèze *Comparaison de modèles de milieux continus*, Thèse de doctorat, Université Pierre et Marie Curie, Paris, France, (1975).

[6] P. Ladevèze, D. Leguillon, *Error estimate procedure in the finite element method and application*, SIAM J. Numer. Anal. **20** (1983) 485–509.

[7] P. Ladevèze, L. Chamoin, E. Florentin, *A new non-intrusive technique for the construction of admissible stress fields in model verification*, Comput. Methods Appl. Mech. Eng. **199** (2010) 766–777.

[8] P. Beckers, E. Dufeu, *3-d error estimation and mesh adaptation using improved r.e.p. method*, Stud. Appl. Mech. **47** (1998) 413–426.

[9] M. Vohralik, *A posteriori error estimates for lowest-order mixed finite element discretization of convection-diffusion-reaction equations*, SIAM J. Numer. Anal. **45** (2007), 1570–1599.

[10] N. Parés, P. Díez, A. Huerta, *Subdomain-based flux-free a posteriori error estimators*, Comp. Methods Appl. Mech. Eng. **195** (2006) 297–323.

Automation of Finite Element Method

Jože Korelc

The automated generation of computational models has been explored by researchers from the fields of mathematics, computer science and computational mechanics, resulting in a variety of approaches (e.g. object-oriented, domain specific languages [2] and hybrid symbolic-numeric methods [1]) and available software tools (e.g. symbolic and algebraic systems, automatic differentiation tools, problem solving environments and numerical libraries).

The obvious solution to use general computer algebra tools like Mathematica or Maple directly to derive complex nonlinear finite elements has proved to be extremely difficult and results in uncontrollable expression swell, redundant operations and inefficient codes. Additionally, the nonlinear problems require highly specific solution procedures and, as usual in science, the high uniqueness of a specific formulation renders the whole concept of automation questionable. The above have stipulated an intensive scientific research into the problem of automation in recent years. Automation can address all steps of a finite element solution procedure from the strong form of a boundary-value problem to the visualization

of results (FEniCS [2] is a recent examples of the approach), or it can be applied only to the automation of selected (usually deterministic) steps in a whole procedure. In the first case we can speak of automation of numerical solution of physical or mathematical problem and in the second case about automation of scientific research to optimal computational approach to the solution of physical or mathematical problem.

The paper presents a hybrid symbolic-numeric approach to automation of derivation of nonlinear finite-elements [1]. The hybrid symbolic-numeric approach employs general-purpose automatic code generator AceGen [1] to derive and code characteristic finite element quantities (e.g. residual vector and stiffness matrix) at the level of individual finite element and a general-purpose finite element environment AceFEM [1] to solve the global problem. The automatic code generation approach presented combines a symbolic system Mathematica, an automatic differentiation technique with the simultaneous expression optimization and an automatic generation of program code in a selected compiled language.

The true advantages of automation become apparent only if the description of the problem, the notation and the mathematical apparatus used are changed as well. It is demonstrated in the paper that this can be achieved using the automatic differentiation technique. The purpose of the automatic differentiation (AD) technique is to compute the derivative of function f, as defined by the algorithm, with respect to variables $\mathbf{a}$. Let define the corresponding *computational derivative* with the following formalism $\nabla f := \frac{\hat{\delta} f(\mathbf{a})}{\hat{\delta}\mathbf{a}}$. The operator $\hat{\delta} f(\mathbf{a})/\hat{\delta}\mathbf{a}$ has a dual purpose, to indicate the mathematical operation of differentiation as well as to indicate the AD algorithm used to obtain the required quantity. However, as powerful as automatic differentiation technique is, the results of the automatic differentiation procedure might not automatically correspond to the specific mathematical formalism used to describe the problem. The essential feature of the proposed approach is that it extends the classical formulation of automatic differentiation technique by additional operators defining exceptions in automatic differentiation procedure. Let $\mathbf{b}$ be a set of mutually independent intermediate variables that are part of evaluation of function f, $\mathbf{G}$ a set of arbitrary functions of $\mathbf{a}$ such that $\mathbf{b} := \mathbf{G}(\mathbf{a})$, and $\mathbf{M}$ an arbitrary matrix. The following formalism,

$$\nabla f_A := \left. \frac{\hat{\delta} f(\mathbf{a}, \mathbf{b}(\mathbf{a}))}{\hat{\delta}\mathbf{a}} \right|_{\frac{D\mathbf{b}}{D\mathbf{a}}=\mathbf{M}} \tag{1}$$

indicates that during the AD procedure, the total derivatives (indicated by $D\mathbf{b}/D\mathbf{a}$) of intermediate variables $\mathbf{b}$ with respect to independent variables $\mathbf{a}$ are set to be equal to matrix $\mathbf{M}$, and the actual way how the variables $\mathbf{b}$ are evaluated in the algorithm is neglected for the evaluation of derivatives of $\mathbf{b}$.

Finite-strain elastoplasticity is a typical application area where the use of the presented apparatus can greatly simplify the derivation of the governing equations of the problem and the derivation of consistent tangent matrix. The elasto-plastic problem is defined by a hyperelastic strain energy density function W, a yield

condition f and a set of algebraic constraints $\mathbf{Q}_g(\mathbf{h}_g) = \mathbf{0}$ to be fulfilled at Gauss point g when the material point is in plastic state. Vector of local, Gauss point unknowns $\mathbf{h}_g$ is composed of an appropriate measure of plastic strains, hardening variables and consistency parameter, while $\mathbf{Q}_g$ are composed of the corresponding set of discretized evolution equations that describe the evolution of plastic strains and hardening variables and the consistency condition $f = 0$.

As presented in [1], the automatic differentiation based form of contribution of the internal forces $\mathbf{R_e}$ to the weak form of equilibrium equations is for the 1^{st} Piola-Kirchhof stress tensor $\mathbf{P}$ and the deformation gradient $\mathbf{F}$ given by

(2)
$$\mathbf{R}_e = \int_{\Omega_e} \frac{\partial W}{\partial \mathbf{F}} \frac{\partial \mathbf{F}}{\partial \mathbf{p_e}}\, dV = \int_{\Omega_e} \left.\frac{\hat{\delta} W}{\hat{\delta} \mathbf{p_e}}\right|_{\frac{D\mathbf{h_g}}{D\mathbf{F}}=\mathbf{0}} dV \approx \sum_{g=1}^{n_g} w_g \left.\frac{\hat{\delta} W}{\hat{\delta} \mathbf{p_e}}\right|_{\frac{D\mathbf{h_g}}{D\mathbf{F}}=\mathbf{0}} = \sum_{g=1}^{n_g} w_g \mathbf{R}_g$$

where $\mathbf{p_e}$ is a vector of generalized displacements of e-th element. The automatic differentiation based evaluation of Gauss point contribution to consistent tangent is then obtained from (2) as follows

(3)
$$\mathbf{K}_g = \frac{\partial \mathbf{R}_g}{\partial \mathbf{p_e}} + \frac{\partial \mathbf{R_g}}{\partial \mathbf{h_g}} \frac{\partial \mathbf{h_g}}{\partial \mathbf{p_e}} = \left.\frac{\hat{\delta} \mathbf{R_g}}{\hat{\delta} \mathbf{p_e}}\right|_{\frac{D\mathbf{h_g}}{D\mathbf{p_e}} = -(\frac{\hat{\delta}\mathbf{Q_g}}{\hat{\delta}\mathbf{h_g}})^{-1} \frac{\hat{\delta}\mathbf{Q_g}}{\hat{\delta}\mathbf{p_e}}}.$$

An essential part of the formulation of finite-strain plasticity problems is time integration of evolution equations. Evolution equations of the form $\dot{\mathbf{B}} = \mathbf{A}(\mathbf{t})\mathbf{B}$, $\mathbf{B}(\mathbf{t_0}) = \mathbf{B_0}$ with $\mathbf{A}$ and $\mathbf{B}$ as second order tensors can be integrated by first-order, implicit integration scheme based on the exponential map as follows,

(4)
$$\mathbf{B_{n+1}} = \exp((\mathbf{t_{n+1}} - \mathbf{t_n})\mathbf{A_{n+1}})\mathbf{B_n}.$$

The main beneficial feature of the exponential map integrators is that they preserve exactly the plastic incompressibility condition as well as symmetry of tangent matrix and objectivity of the resulting finite element, while the drawback is numerically expansive and often ill-conditioned evaluation of matrix exponential. As shown in [3], for the evaluation of the matrix exponential of a 3×3 matrix $\mathbf{A}$, a scalar generating function $G(\mathbf{A})$ can be constructed in terms of the eigenvalues λ_i of $\mathbf{A}$,

(5)
$$G(\mathbf{A}) = e^{\lambda_1} + e^{\lambda_2} + e^{\lambda_3},$$

such that the derivative of G with respect to $\mathbf{A}^{\mathrm{T}}$ gives the exponential of $\mathbf{A}$. While the closed form expressions for eigenvalues of 3×3 matrix are known to be ill-conditioned around multiple eigenvalues, the scalar generating function G is smooth and well defined on the whole domain. With a numerically stable definition of the generating function G, automatic differentiation can be applied to obtain matrix exponential and its first derivative directly

(6)
$$\exp \mathbf{A} := \frac{\hat{\delta} G}{\hat{\delta} \mathbf{A}^{\mathrm{T}}}, \qquad D \exp \mathbf{A} := \frac{\hat{\delta} \exp \mathbf{A}}{\hat{\delta} \mathbf{A}}.$$

Thus, a combination of automatic differentiation and scalar generating function leads to stable, singularity-free and computationally efficient closed-form representation of matrix exponential and its derivative. Numerical tests show that automatic differentiation based formulation of matrix exponential gives machine precision accurate results and that is almost always numerically more efficient than the truncated series approximation of matrix exponential and its derivative. Presented automatic differentiation based formulation of elasto-plastic problems and matrix exponential is general and it can be used to derive numerically efficient elasto-plastic finite elements of arbitrary complexity. Moreover, as shown in [1] it can be easily extended to automatic differentiation based formulation of sensitivity analysis as a basis for gradient based nonlinear optimization.

References

[1] J. Korelc, *Automation of primal and sensitivity analysis of transient coupled problems*, Comput. mech. **44** (2009), 631-649.
[2] A. Logg, *Automating the Finite Element Method*, Archives of Computational Methods in Engineering **14** (2007) 93-138.
[3] J. Lu., *Exact expansions of arbitrary tensor functions $\boldsymbol{F(A)}$ and their derivatives*, Int. J. Sol. Struct. **41** (2004), 337–349.

Optimal Uncertainty Quantification

Michael Ortiz
(joint work with Michael McKerns, Houman Owhadi, Tim Sullivan, Clint Scovel)

The present work is concerned with the formulation of a rigorous theory of Uncertainty Quantification (UQ) within the framework of Quantification of Margins and Uncertainties (QMU) [1, 2, 3, 4], as well as with the formulation of efficient methods of solution and approximation thereof. For definiteness, we adopt throughout a certification viewpoint. Specifically, we consider a system with random inputs in a probability space $(\mathcal{X}, \mu)$, whose behavior is characterized by a response function $f : \mathcal{X} \to \mathbb{R}^n$. The values of f may be viewed as a collection of performance measures, and the safe behavior of the system requires f to take values within a safe or admissible set $A \subset \mathbb{R}^n$. The probability of failure (PoF) of the system is, then,

$$\text{PoF} = \mathbb{E}_\mu[\chi_{\{f \notin A\}}], \tag{1}$$

where, here and subsequently, χ_E denotes the indicator function of the set E. We say that the system is certified with probability at least $1 - \epsilon$ if

$$\text{PoF} \leq \epsilon, \tag{2}$$

where ϵ is a failure tolerance.

In practice, a number of difficulties prevent the direct evaluation of the probability of failure of a system. For instance, the input space is often of very high dimension and some of the input parameters are unknown (unknown unknowns). In addition, the probability distribution of the inputs is often not fully known. The

response of many systems is stochastic and it is only imperfectly characterized experimentally or otherwise. Physical and computational models of the system may exist, but often these models are only partially verified and validated. In some cases, some of the underlying physics may be unwittingly omitted from the models or may not be covered by existing theory. The situation is often compounded for systems whose performance cannot be fully tested, either because the operating conditions cannot be reproduced in the laboratory, or because the tests are costly, or subject to environmental or treaty restrictions, or some combination thereof. Often, legacy or archival data exists but is incomplete, or inconsistent, or noisy. Moreover, the mechanisms responsible for the failure of systems are often rare events and thus not directly accessible to simple Monte Carlo sampling. Finally, the failure of some systems is of great consequence, be it economic or in loss of life, and the tolerance for failure is correspondingly low.

Owing to these and other strictures, in practice the available information about a system is limited and suffices only to restrict its possible response functions f and its possible probability distributions μ of the inputs to some admissible or information set $\mathcal{A} \subseteq \mathcal{M}(\mathcal{X}) \times \mathcal{F}(\mathcal{X})$, where $\mathcal{F}(\mathcal{X})$ denotes the space of real-valued (Borel) measurable functions on $\mathcal{X}$ and $\mathcal{M}(\mathcal{X})$ denotes the set of Borel probability measures on $\mathcal{X}$. Thus, any pair $(\mu, f) \in \mathcal{A}$ represents a scenario consistent with all the information available on the system. Under these conditions,

$$\mathcal{L}(\mathcal{A}) \equiv \inf_{(\mu,f)\in\mathcal{A}} \mathbb{E}_\mu[\chi_{\{f\notin A\}}] \leq \mathrm{PoF} \leq \sup_{(\mu,f)\in\mathcal{A}} \mathbb{E}_\mu[\chi_{\{f\notin A\}}] \equiv \mathcal{U}(\mathcal{A}) \tag{3}$$

are the best, or tightest, upper and lower bounds on the PoF of the system, in the sense that, if p_L and p_U are respectively, *any* valid lower and upper bounds on PoF, it follows that, necessarily,

$$p_L \leq \mathcal{L}(\mathcal{A}) \leq \mathrm{PoF} \leq \mathcal{U}(\mathcal{A}) \leq p_U. \tag{4}$$

In general, (3) defines two exceedingly large global optimization problems over infinite dimensional spaces of functions and measures, which calls into question the computability of the optimal bounds $\mathcal{L}(\mathcal{A})$ and $\mathcal{U}(\mathcal{A})$. However, it has been shown by Owhadi *et al.* [5] that, under rather general conditions, these optimization problems can be reduced to finite dimensions, and that the resulting finite-dimensional problems are computable. In order to enunciate the main result, let

$$\Delta_k(\mathcal{X}) \equiv \left\{ \sum_{j=0}^{k} \alpha_j \delta_{x_j} \;\middle|\; x_j \in \mathcal{X}, \alpha_j \geq 0 \text{ for } j = 0, \ldots, k \text{ and } \sum_{j=0}^{k} \alpha_j = 1 \right\} \tag{5}$$

denote the set of $(k+1)$-fold convex combinations of Dirac masses. Then, the main reduction result is embodied in the following theorem [5].

Theorem 0.1. *Let $\mathcal{X}_i$, $i = 1, \ldots, m$, be Suslin spaces and $\mathcal{X} = \mathcal{X}_1 \times \cdots \times \mathcal{X}_m$. Suppose that the information set is of the form:*

$$\mathcal{A} = \left\{ (\mu, f) \;\middle|\; \begin{array}{c} f \in \mathcal{G} \subseteq \mathcal{F}(\mathcal{X}), \\ \mu = \mu_1 \otimes \cdots \otimes \mu_m, \\ \mathbb{E}_\mu[g_{0j}] \leq 0, j = 1, \ldots, n_0, \\ \mathbb{E}_{\mu_1}[g_{1j}] \leq 0, j = 1, \ldots, n_1, \\ \cdots \\ \mathbb{E}_{\mu_m}[g_{mj}] \leq 0, j = 1, \ldots, n_m, \end{array} \right\} \tag{6}$$

where $g_{0j} \colon \mathcal{X} \to \mathbb{R}$, $j = 1, \ldots, n_0$, and $g_{ij} \colon \mathcal{X}_i \to \mathbb{R}$, $j = 1, \ldots, n_i$, $i = 1, \ldots, m$ are measurable functions that may depend in an arbitrary way on f. Let

$$\mathcal{A}_{\mathrm{red}} = \left\{ (\mu, f) \in \mathcal{A} \;\middle|\; \mu \in \bigotimes_{i=1}^{m} \Delta_{n_0+n_i}(\mathcal{X}_i) \right\} \tag{7}$$

be a reduced information set consisting of convex combinations of Dirac masses. Then,

$$\mathcal{L}(\mathcal{A}) = \mathcal{L}(\mathcal{A}_{\mathrm{red}}) \tag{8a}$$

$$\mathcal{U}(\mathcal{A}) = \mathcal{U}(\mathcal{A}_{\mathrm{red}}) \tag{8b}$$

Linear moment constraints on the factor spaces $\mathcal{X}_i$ permit consideration of information sets with independent random variables $X_1, \ldots, X_m$ and weak constraints on their probability distribution. An example of such an admissible set is furnished by Bernstein inequalities [6], in which *a priori* bounds are given on the variances of the variables X_i. Other examples of information sets of practical relevance arise, e. g., when *a priori* bounds are known on the mean performance $\mathbb{E}_\mu[f]$ of the system or on the oscillation of the system response [5, 7, 8]. The optimal bounds delivered by OUQ in these cases improve on classical inequalities such as Hoeffding's [9] and McDiarmid's [10]. A different type of constraints on the information set arises when certain features of the response function f can be elucidated *a priori*, e. g., Lipschitz constants, and when legacy or archival experimental data is available [11]. Issues pertaining to the computability of the optimal bounds, and efficient algorithms for their computation thereof, are discussed in [5, 12, 13]. Applications of OUQ to terminal ballistics and seismic risk assessment may be found in [5, 7, 8].

References

[1] D. H. Sharp and M. M. Wood-Schultz. QMU and nuclear weapons certification: What's under the hood. *Los Alamos Science*, (28):47–53, 2003.

[2] D. Eardley and *et. al.* Quantification of margins and uncertainties (QMU). Technical Report JSR-04-330, The MITRE Corporation, 7515 Colshire Drive McLean, Virginia, 22102, March 2005.

[3] Committee on the Evaluation of Quantification of Margins and Uncertainties Methodology for Assessing and Certifying the Reliability of the Nuclear Stockpile. Evaluation of quantification of margins and uncertainties for assessing and certifying the reliability of the nuclear stockpile. Technical report, National Academy of Science/National Research Council (NAS/NRC), Washington, DC: National Academy Press, 2008.

[4] L. J. Lucas, H. Owhadi, and M. Ortiz. Rigorous verification, validation, uncertainty quantification and certification through concentration-of-measure inequalities. *Computer Methods in Applied Mechanics and Engineering*, 197:4591–4609, 2008.
[5] H. Owhadi, C. Scovel, T. J. Sullivan, M. McKerns, and M. Ortiz. Optimal uncertainty quantification. *arXiv:1009.0679*, 2010.
[6] S. N. Bernstein. *Collected Works*. Izdat. "Nauka", Moscow, 1964.
[7] A. A. Kidane, A. Lashgari, B. Li, M. McKerns, M. Ortiz, H. Owhadi, G. Ravichandran, M. Stalzer, and T. J. Sullivan. Rigorous Model-Based Uncertainty Quantification with Application to Terminal Ballistics - Part I. Systems with Controllable Inputs and Small Scatter. *Journal of the Mechanics and Physics of Solids* (in press) 2012.
[8] M. Adams, A. Lashgari, B. Li, M. McKerns, J. Mihaly, M. Ortiz, H. Owhadi, A. J. Rosakis, M. Stalzer, and T. J. Sullivan. Rigorous Model-Based Uncertainty Quantification with Application to Terminal Ballistics - Part II. Systems with Uncontrollable Inputs and Large Scatter. *Journal of the Mechanics and Physics of Solids* (in press) 2012.
[9] W. Hoeffding. Probability inequalities for sums of bounded random variables. *J. Amer. Statist. Assoc.*, 58:13–30, 1963.
[10] C. McDiarmid. On the method of bounded differences. In *Surveys in Combinatorics, 1989, vol. 141 of London Math. Soc. Lecture Note Ser.*, pages 148–188. Cambridge Univ. Press, 1989.
[11] T. J. Sullivan, M. McKerns, D. Meyer, F. Theil, H. Owhadi, and M. Ortiz. Optimal uncertainty quantification for legacy data observations of Lipschitz functions. *arXiv:1202.1928v1*, 2012.
[12] M. M. McKerns, L. Strand, T. J. Sullivan, A. Fang and M. A. G. Aivazis. Building a Framework for Predictive Science. *arXiv:1202.1056*, 2012.
[13] M. McKerns, H. Owhadi, C. Scovel, T. J. Sullivan and M. Ortiz. The Optimal Uncertainty Algorithm in the Mystic Framework. *arXiv:1202.1055*, 2012.

Conservative and monotone optimization–based transport

Pavel Bochev
(joint work with Denis Ridzal, Joseph Young)

1. Introduction

In [4, 11, 9], we formulate, apply and study computationally a new optimization-based framework for computational modeling. The framework uses optimization and control ideas to (i) assemble and decompose multiphysics operators and (ii) preserve their fundamental physical properties in the discretization process. It further develops the approach in [3, 2], which demonstrates an optimization-based synthesis of fast solvers. In this talk we develop an optimization-based algorithm for transport (OBT) of a positive scalar function, which is monotone and preserves local bounds and linear functions on arbitrary unstructured grids.

The OBT algorithm combines the incremental remap (constrained interpolation) strategy for transport in [6] with the reformulation of the remap step as an inequality constrained quadratic program (QP) [5]. The objective in this QP is to minimize the discrepancy between target high-order mass fluxes and the approximate mass fluxes subject to inequality constraints derived from physically motivated bounds on the primitive variable (density). The merger of these ideas

yields a new type of transport algorithms that can be applied to arbitrary unstructured grids and extended to higher than second-order accuracy by using suitably defined target fluxes.

Our approach differs substantially from the dominant methods for transport, which preserve the physical properties directly in the discretization process through monotonic reconstruction of the fields. The slope and flux limiters used for this purpose tie together preservation of physical properties with restrictions on the mesh geometry and/or the accuracy. As a result, many of them do not preserve linear functions on irregular grids [1], which impacts accuracy and robustness. An alternative is to use sophisticated "repair" procedures [7] or error compensation algorithms [8], which fix the out-of-bound values and maintain positivity on arbitrary unstructured grids. However, limiters and "repair" procedures obscure the sources of discretization errors, which complicates the analysis of the transport schemes, and their higher-order extensions on unstructured grids are very complex.

2. Application to transport problems

We present a new class of conservative, monotone and bounds preserving methods for the scalar transport equation

$$\partial_t \rho + \nabla \cdot \rho \mathbf{v} = 0 \quad \text{on } \Omega \times [0,T] \quad \text{and} \quad \rho(\mathbf{x},0) = \rho^0(\mathbf{x})\,, \tag{1}$$

where $T > 0$ is the final time, $\rho(\mathbf{x},t)$ is a positive density function (the primitive variable) on $\Omega \times [0,T]$ with initial distribution $\rho^0(\mathbf{x})$, and $\mathbf{v}$ is a velocity field. For simplicity, we assume that $\rho(\mathbf{x},t) = 0$ on $\partial\Omega \times [0,T]$. Let $K_h(\Omega)$ denote a partition of Ω into cells κ_i, $i = 1,\ldots,K$.

On each cell κ_i the degree of freedom ρ_i^n approximates the mean cell density

$$\int_{\kappa_i} \rho(\mathbf{x},t_n) dV \Big/ \int_{\kappa_i} dV$$

at time $t = t_n$. The approximate mass in cell κ_i at time t_n is $m_i^n = \rho_i^n \mathrm{vol}(\kappa_i)$.

To solve (1) we proceed as follows. Numerical integration of $\rho^0(\mathbf{x})$ on each grid cell κ_i yields the initial cell masses $\vec{m}^{\,0} = (m_1^0,\ldots,m_K^0)$ and the initial density distribution $\vec{\rho}^{\,0} = (\rho_1^0,\ldots,\rho_K^0)$ on $K_h(\Omega)$, where $\rho_i^0 = m_i^0/\mathrm{vol}(\kappa_i)$. Suppose that the approximate solution $\vec{\rho}^{\,n} = (\rho_1^n,\ldots,\rho_K^n)$ is known on $K_h(\Omega)$ at time $0 \le t_n < T$ and Δt_n is an admissible *explicit* time step. To find the approximate density distribution $\vec{\rho}^{\,n+1} = (\rho_1^{n+1},\ldots,\rho_K^{n+1})$ on $K_h(\Omega)$ at the new time step $t_{n+1} = t_n + \Delta t_n$, we apply the forward *incremental remapping* algorithm [6]. This algorithm advances the solution of (1) to the next time step using that the mass of a Lagrangian volume $V_L(t)$ is conserved along the trajectories $d\mathbf{x}/dt = \mathbf{v}$:

$$\int_{V_L(t_{n+1})} \rho dV = \int_{V_L(t_n)} \rho dV\,. \tag{2}$$

The incremental remap approach evolves $K_h(\Omega)$ into a grid $\widetilde{K}_h(\widetilde{\Omega})$ on the deformed region $\widetilde{\Omega}$ at t_{n+1}, computes the mean density on this grid and interpolates it

Algorithm 1 One forward step of incremental remapping

input: Density approximation $\vec{\rho}^{\,n} = (\rho_1^n, \ldots, \rho_K^n)$ at time t_n, time step Δt_n
output: Density approximation $\vec{\rho}^{\,n+1} = (\rho_1^{n+1}, \ldots, \rho_K^{n+1})$ at time t_{n+1}

Project grid:	$K_h(\Omega) \ni \mathbf{x}_p \mapsto \mathbf{x}_p + \Delta t_n \mathbf{v} = \widetilde{\mathbf{x}}_p \in \widetilde{K}_h(\widetilde{\Omega})$
Transport m and ρ:	$\forall \widetilde{\kappa}_i \in \widetilde{K}_h(\widetilde{\Omega})$ set $\widetilde{m}_i = m_i^n$ and $\widetilde{\rho}_i = \widetilde{m}_i / \mathrm{vol}(\widetilde{\kappa}_i)$
Remap density:	$\vec{\rho}^{\,n+1} = \mathcal{R}(\{\widetilde{\rho}_1, \ldots, \widetilde{\rho}_K\})$

back to $K_h(\Omega)$. Let $V_L(t_n) = \kappa_i$ then, from (2) the mass $\widetilde{m}_i$ in $V_L(t_{n+1})$ equals the mass m_i^n in $V_L(t_n)$ and the mean density on $V_L(t_{n+1})$ is $\widetilde{\rho}_i = m_i^n / \mathrm{vol}(V_L(t_{n+1}))$.

We approximate $V_L(t_{n+1})$ by evolving the vertices $\{\mathbf{x}_p\}$ of κ_i along the trajectories using time integrator. This yields a cell $\widetilde{\kappa}_i$ with vertices $\widetilde{\mathbf{x}}_p = \mathbf{x}_p + \Delta t_n \mathbf{v}$, which approximates $V_L(t_{n+1})$. The mass $\widetilde{m}_i$ and the mean density $\widetilde{\rho}_i$ on $\widetilde{\kappa}_i$ are

$$\widetilde{m}_i = m_i^n \quad \text{and} \quad \widetilde{\rho}_i = \frac{m_i^n}{\mathrm{vol}(\widetilde{\kappa}_i)}\,; \quad i = 1, \ldots, K\,.$$

Conservative interpolation (remap) of the mean density values $\widetilde{\rho}_i$ from the deformed mesh $\widetilde{K}_h(\widetilde{\Omega})$ onto the original mesh $K_h(\Omega)$ gives the approximate mean cell density $\vec{\rho}^{\,n+1} = (\rho_1^{n+1}, \ldots, \rho_K^{n+1})$ at the next time level; see Algorithm 1. The conservative interpolation (remap) operator $\mathcal{R}$ is the key ingredient of Algorithm 1. To state the requirements on $\mathcal{R}$ without going into unnecessary technical details, it is convenient to assume that $\mathbf{v} \cdot \mathbf{n} = 0$. In this case the original and deformed regions coincide: $\Omega = \widetilde{\Omega}$, and the mass is conserved at all times. Let $\widetilde{N}_i$, and N_i denote the neighborhoods of $\widetilde{\kappa}_i \in \widetilde{K}_h(\widetilde{\Omega})$, and $\kappa_i \in K_h(\Omega)$, resp., i.e., all cells that share vertex or an edge or a face with $\widetilde{\kappa}_i$ or κ_i. Define

$$\widetilde{\rho}_i^{\min} = \min_{j \in \widetilde{N}_i} \widetilde{\rho}_j\,; \qquad \widetilde{\rho}_i^{\max} = \max_{j \in \widetilde{N}_i} \widetilde{\rho}_j\,;$$

Under the assumptions stated above, $\mathcal{R}$ must satisfy the following requirements:

R.1 local bounds are preserved: $\widetilde{\rho}_i^{\min} \le \rho_i^{n+1} \le \widetilde{\rho}_i^{\max}$;

R.2 total mass is conserved: $\sum_{i=0}^K m_i^{n+1} = \sum_{i=0}^K \widetilde{m}_i = \sum_{i=0}^K m_i^n$;

R.3 linearity is preserved: $m_i^{n+1} = \int_{\kappa_i} \rho(\mathbf{x}, t_{n+1}) dV$ if $\rho(\mathbf{x}, t)$ is linear in $\mathbf{x}$.

The starting point in the construction of $\mathcal{R}$ is the flux-form formula for the cell masses on $K_h(\Omega)$ corresponding to the new time level:

$$m_i^{n+1} = \widetilde{m}_i + \sum_{\widetilde{\kappa}_j \in \widetilde{N}_i} \widetilde{F}_{ij}^h\,; \quad i = 1, \ldots, K\,. \tag{3}$$

The mass fluxes $\widetilde{F}_{ij}^h$ approximate the mass exchanges between the cells in the neighborhood $\widetilde{N}_i$ of $\widetilde{\kappa}_i$. The target fluxes are

$$\widetilde{F}_{ij}^T = \int_{\kappa_i \cap \widetilde{\kappa}_j} \widetilde{\rho}_j^{\,\ell}(\mathbf{x}) dV - \int_{\widetilde{\kappa}_i \cap \kappa_j} \widetilde{\rho}_i^{\,\ell}(\mathbf{x}) dV\,; \quad \widetilde{\kappa}_j \in \widetilde{N}_i\,; \kappa_j \in N_i$$

where $\widetilde{\rho}_i^{\ell}(\mathbf{x})$ is density reconstruction on cell $\widetilde{\kappa}_i$, which is exact for linear functions. Finally, from R.1 we obtain bounds for the mass on the new time level:

$$\widetilde{\rho}_i^{\min}\mathrm{vol}(\kappa_i) = m_i^{\min} \leq m_i^{n+1} \leq m_i^{\max} = \widetilde{\rho}_i^{\max}\mathrm{vol}(\kappa_i)$$

The following QP defines the constrained interpolation operator $\mathcal{R}$:

$$\underset{\widetilde{F}_{ij}^h}{\text{minimize}} \sum_{i=1}^{K} \sum_{\widetilde{\kappa}_j \in \widetilde{N}_i} (\widetilde{F}_{ij}^h - \widetilde{F}_{ij}^T)^2 \quad \text{subject to}$$

$$\text{(4)} \qquad \begin{cases} \widetilde{F}_{ij}^T = \displaystyle\int_{\kappa_i \cap \widetilde{\kappa}_j} \widetilde{\rho}_j^{\ell}(\mathbf{x})dV - \int_{\widetilde{\kappa}_i \cap \kappa_j} \widetilde{\rho}_i^{\ell}(\mathbf{x})dV \\ \widetilde{F}_{ij}^h = -\widetilde{F}_{ji}^h \\ m_i^{\min} \leq \widetilde{m}_i + \displaystyle\sum_{\widetilde{\kappa}_j \in \widetilde{N}_i} \widetilde{F}_{ij}^h \leq m_i^{\max} \end{cases} .$$

The optimization-based formulation (4) separates enforcement of the physical properties R.1 and R.2, which is done through the constraints, from the enforcement of the accuracy R.3, which is achieved through the objective functional. As a result, (4) is impervious to cell shapes and can be used on arbitrary grids.

In [5] we prove that (4) preserves linear densities if the barycenter of κ_i remains in the convex hull of the barycenters of the cells in $\widetilde{N}_i$ for all $1 \leq i \leq K$. This condition is less restrictive than the one required for linearity preservation by Van Leer limiting [10] and is valid for any unstructured grid. In summary, using Algorithm 1 in conjunction with an operator $\mathcal{R}$ defined by the QP (4), yields a conservative and monotone transport algorithm that is applicable to *arbitrary cell shapes*, including polygons and polyhedra.

References

[1] Marsha Berger, Scott M. Murman, and Michael J. Aftosmis. Analysis of slope limiters on irregular grids. In *Proceedings of the 43rd AIAA Aerospace Sciences Meeting*, number AIAA2005-0490, Reno, NV, January 10–13 2005. AIAA.

[2] P. Bochev and D. Ridzal. Additive operator decomposition and optimization–based reconnection with applications. In I. Lirkov, S. Margenov, and J. Wasniewski, editors, *Proceedings of LSSC 2009*, volume 5910 of *Springer Lecture Notes in Computer Science*, 2009.

[3] P. Bochev and D. Ridzal. An optimization-based approach for the design of PDE solution algorithms. *SIAM Journal on Numerical Analysis*, 47(5):3938–3955, 2009.

[4] P. Bochev, D. Ridzal, and D. Young. Optimization–based modeling with applications to transport. Part 1. Abstract formulation. In I. Lirkov, S. Margenov, and J. Wasniewski, editors, *Proceedings of LSSC 2011*, Springer Lecture Notes in Computer Science, Submitted 2011.

[5] Pavel Bochev, Denis Ridzal, Guglielmo Scovazzi, and Mikhail Shashkov. Formulation, analysis and numerical study of an optimization-based conservative interpolation (remap) of scalar fields for arbitrary lagrangian-eulerian methods. *Journal of Computational Physics*, 230(13):5199 – 5225, 2011.

[6] John K. Dukowicz and John R. Baumgardner. Incremental remapping as a transport/advection algorithm. *Journal of Computational Physics*, 160(1):318 – 335, 2000.

[7] Milan Kucharik, Mikhail Shashkov, and Burton Wendroff. An efficient linearity-and-bound-preserving remapping method. *Journal of Computational Physics*, 188(2):462 – 471, 2003.

[8] L. G. Margolin and Mikhail Shashkov. Second-order sign-preserving conservative interpolation (remapping) on general grids. *Journal of Computational Physics*, 184(1):266 – 298, 2003.

[9] D. Ridzal, P. Bochev, J. Young, and K. Peterson. Optimization–based modeling with applications to transport. Part 3. Implementation and computational studies. In I. Lirkov, S. Margenov, and J. Wasniewski, editors, *Proceedings of LSSC 2011*, Springer Lecture Notes in Computer Science, Submitted 2011.

[10] Blair Swartz. Good neighborhoods for multidimensional Van Leer limiting. *Journal of Computational Physics*, 154(1):237 – 241, 1999.

[11] J. Young, D. Ridzal, and P. Bochev. Optimization–based modeling with applications to transport. Part 2. Optimization algorithm. In I. Lirkov, S. Margenov, and J. Wasniewski, editors, *Proceedings of LSSC 2011*, Springer Lecture Notes in Computer Science, Submitted 2011.

Three-field mixed methods in elasticity: old and new

Daya Reddy

Mixed formulations are among the more popular approaches for constructing finite element methods for problems in elasticity and more generally in solid mechanics, which are stable in the incompressible limit. A particular objective has been that of developing methods that are stable when low-order elements are used. Some representative works include [1, 8].

Two- and three-field methods, first proposed more than 50 years ago [6, 7, 11], have been a particularly fertile basis from which to develop stable methods. Among computational specialists, an approach favoured is that in which the corresponding saddle-point problem takes the form, on a bounded domain $\Omega \subset R^d$,

$$
\begin{aligned}
(\boldsymbol{u}, \boldsymbol{d}, \boldsymbol{\sigma}) = &\quad \arg\ \min_{\boldsymbol{v},\boldsymbol{e}} \max_{\boldsymbol{\tau}} H_1(\boldsymbol{v}, \boldsymbol{e}; \boldsymbol{\tau}) \\
= &\quad \int_\Omega \left[\tfrac{1}{2}(\operatorname{tr} \boldsymbol{e})^2 + \mu |\boldsymbol{e}|^2 + (\boldsymbol{e} - \boldsymbol{\epsilon}(\boldsymbol{v})) : \boldsymbol{\tau} - \boldsymbol{f} \cdot \boldsymbol{v} \right] \, dx \, .
\end{aligned} \tag{1}
$$

Here $\boldsymbol{u}, \boldsymbol{d}, \boldsymbol{\sigma} \in [H_0^1(\Omega)]^d \times [L^2(\Omega)]_s^{d\times d} \times [L^2(\Omega)]_s^{d\times d}$ are respectively the displacement, symmetric strain and stress fields with corresponding arbitrary quantities $\boldsymbol{v}, \boldsymbol{e}, \boldsymbol{\tau}$, while λ and μ are the Lamé constants and $\boldsymbol{f}$ is the body force. The strain-dislacement relation is given by $\boldsymbol{\epsilon}(\boldsymbol{u}) = \frac{1}{2}(\nabla \boldsymbol{u} + (\nabla \boldsymbol{u})^T)$. The incompressible limit corresponds to $\lambda \to \infty$. This formulation is in contrast to those two-field formulations favoured by the mathematical community, in which $\boldsymbol{u}, \boldsymbol{d}, \boldsymbol{\sigma} \in [L^2(\Omega)]^d \times [H(\mathrm{div})(\Omega)]^{d\times d}$, with the symmetry of the stress possibly not imposed a priori.

A full analysis has been presented in [9] of a broad range of three-field finite element approaches based on (1). Special cases covered by the general analysis include the method of mixed enhanced strains [8] and the method of enhanced strains [10]. In order to carry out such an analysis it is essential to modify the functional (1) so that, for isotropic bodies, it takes the form

$$
\begin{aligned}
(\boldsymbol{u}, \boldsymbol{d}, \boldsymbol{\sigma}) &= \arg\ \min_{\boldsymbol{v},\boldsymbol{e}} \max_{\boldsymbol{\tau}} H_2(\boldsymbol{v}, \boldsymbol{e}; \boldsymbol{\tau}) \\
&= \int_\Omega \left[\mu |\boldsymbol{e}|^2 + (\boldsymbol{e} + (\operatorname{tr} \boldsymbol{e}) \boldsymbol{I} - \boldsymbol{\epsilon}(\boldsymbol{v})) : \boldsymbol{\tau} - \tfrac{1}{2}(\lambda/(d\lambda + 2\mu))|\boldsymbol{\tau}|^2 - \boldsymbol{f} \cdot \boldsymbol{v} \right] \, dx \, .
\end{aligned}
$$

This functional is in fact a special case of a modified formulation introduced in [9], in which a family of modified forms, parametrized by a scalar, is introduced. Conditions for the uniform convergence of finite element approximations are established, and applied to the case in which displacements are approximated by piecewise-bilinear functions in two dimensions.

In more recent work [4] the general conditions for convergence established in [9] are used as a basis for constructing new stable families. The starting point is a velocity-pressure pair that is stable for the Stokes problem: this defines the space of displacements which is the same as that for the velocities, while the pressure space serves to define a discrete space of stresses, and then of the stresses. A number of examples, based on the Mini, Crouzeix-Raviart and Taylor-Hood elements [3] is presented.

The final part of the presentation is concerned with the extension of the ideas in the linear theory to problems in finite-strain elasticity. The three-field form of the rate problem is

$$H_3(\boldsymbol{v}, \boldsymbol{e}; \boldsymbol{\tau}) = \int_\Omega \left[\tfrac{1}{2} \dot{\boldsymbol{F}} : \mathbb{A} \dot{\boldsymbol{F}} + (\dot{\boldsymbol{F}} - \nabla \dot{\boldsymbol{u}}) : \boldsymbol{P} - \boldsymbol{f} \cdot \dot{\boldsymbol{u}} \right] \, dx \,, \tag{2}$$

in which $\boldsymbol{F}$ is the deformation gradient, $\boldsymbol{P}$ the first Piola-Kirchhoff stress, and $\mathbb{A} = \partial^2 W / \partial \boldsymbol{F} \partial \boldsymbol{F}$ is the elasticity tensor, for a specified strain energy function W. Current work is concerned with establishing conditions for the stability of finite element approximations of the rate problem, borrowing from the framework for the linear problem.

References

[1] T. Belyscthko and W. Bachrach, *Efficient implementation of quadrilaterals with high coarse-mesh accuracy*, Computer Methods in Applied Mechanics and Engineering, **54** (1986), 279–301.

[2] D. Braess, C. Carstensen and B. D. Reddy, *Uniform convergence and a posteriori estimators for the enhanced strain finite element method*, Numerische Mathematik **96** (2004), 461–479.

[3] F. Brezzi and M. Fortin, *Mixed and Hybrid Finite Element Methods*, Springer-Verlag, New York, 1991.

[4] A. Chama and B. D. Reddy, *Some new stable finite elements based on the three-field formulation in elasticity*, 2012 (in preparation).

[5] J. K. Djoko, B. P. Lamichhane, B. D. Reddy and B. Wohlmuth, *Conditions for equivalence between the Hu-Washizu and related formulations, and computational behavior in the incompressible limit*, Computer Methods in Applied Mechanics and Engineering **195** (2006), 4161–4178.

[6] B. M. Fraeijs de Veubeke, *Diffusion des inconnues hyperstatiques dans les voilures á longeron couplés*, Bull. Serv. Technique de l'Aeronautique, Impremérie Marcel Hayez, Bruxelles (1951).

[7] H. Hu, *On some variational principles in the theory of elasticity and the theory of plasticity*, Scientia Sinica **4** (1955), 33–54.

[8] E. P. Kasper and R. L. Taylor, *A mixed-enhanced strain method. Part I: geometrically linear problems*, Computers and Structures **75** (2000), 237–250

[9] Lamichhane, B. P. and Reddy, B. D. and Wohlmuth, B. I., *Convergence in the incompressible limit of finite element approximation based on the Hu-Washizu formulation*, Numerische Mathematik **104** (2006), 151–175.

[10] J. C. Simo and M. S. Rifai, *A class of assumed strain methods and the method of incompatible modes*, International Journal for Numerical Methods in Engineering **29** (1990), 1595–1638.
[11] K. Washizu, *On the variational principles of elasticity and plasticity*, Report 25-18, Massachusetts Institute of Technology, 1955.

Multiscale modelling and approximation of incompressible reinforced materials

Patrick Le Tallec
(joint work with Éric Lignon)

Fiber reinforced layers are very popular in industry but are prone to structural instabilities. Such situations combine global inplane buckling of the reinforcing fibers and local shearing or compression of the filling material. Standards shell elements as described in [2] do not have the proper kinematics to treat such inplane instabilities. Our purpose is then to develop an enriched multiscale model, able to treat both aspects through an adequate kinematic and energetic description of the different components and their coupling at different scales. By a classical asymptotic analysis, it introduces in addition to the filling material a surface density of rods able to resist against in plane and out of plane bending. The result is implemented in a new finite element model developed at macroscopic level and validated in different asymptotic or postbuckling regimes [4].

The overall strategy is based on a two scale asymptotic expansion. The macroscopic scale is defined by the overall dimension L of the structure. A small scale ε is introduced to handle the thickness $t_\varepsilon = \varepsilon * t$ of the reinforcing layer, the radius $r_\varepsilon = \varepsilon * r$ of the reinforcing fibers, the distance $e_\varepsilon = \varepsilon * e$ between two fibers, and the rubber shear modulus $G_\varepsilon = \varepsilon^2 * G$ as compared to the fiber elastic modulus G. The idea is to find a local model independent of ε describing the microdeformations on the fiber reinforced plane at the limit when the small scale ε tends to 0. This is classically achieved as in [1] by using a two scale asymptotic expansion of the overall deformation inside the reinforced layer

$$\underline{x}_m(X_1, X_2 + \varepsilon Y_2, \varepsilon Y_3) = \underline{x}^0(X_1, X_2, Y_2, Y_3) + \varepsilon \underline{x}^1(X_1, X_2, Y_2, Y_3) + \dots$$

coupled to a smooth expansion of the same deformation outside the layer. Here X_1, X_2 are global coordinates in center plane, and $(Y_2, Y_3) = (X_1/\varepsilon, X_2/\varepsilon)$ are local normalized coordinates inside the representative volume element, describing the local variations of the solution at fiber scale.

The scale separation is specified by imposing on the solution at the reinforced layer a Y_2 periodicity condition and a P_0 mortar matching condition in Y_3

$$\frac{1}{e}\int \underline{x}_m(\dots, \varepsilon Y_2, \pm\varepsilon\frac{t}{2})dY_2 = \underline{x}_{U,D}(\dots, \pm\varepsilon\frac{t}{2})$$

which assumes slowly varying interface stresses. After matching independently the different powers of ε in the equilibrium equations and in the weak treatment

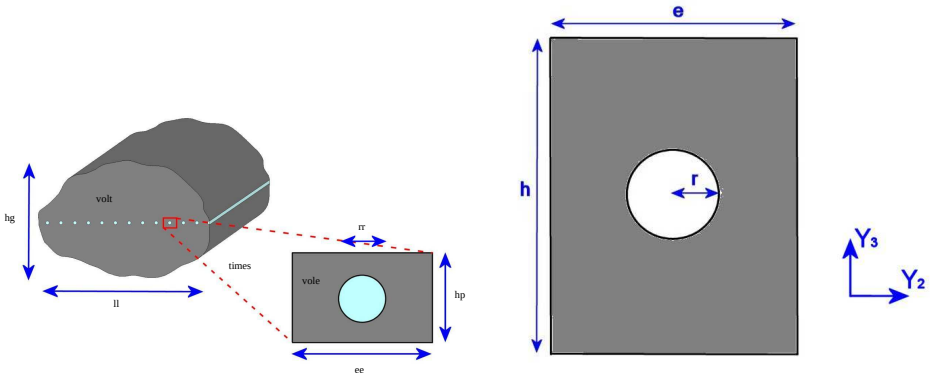

FIGURE 1. Two scale expansion, and resulting two dimensional representative volume element

of the local boundary conditions, it is proved that the zero order expansion is independent on Y, that the fibers at first order obey a Bernouilli kinematics

$$\underline{x}_{|\text{cab}} = \underline{r}(X_1, X_2) + Y_2\underline{d}_2(X_1, X_2) + Y_3\underline{d}_3(X_1, X_2),$$

with $(\dfrac{\partial \underline{r}}{\partial X_1}, \underline{d}_2, \underline{d}_3)$ orthonormal, and that the first order correction $\underline{x}^1(Y_2, Y_3)$ (with respect to center rod motion) in the membrane is obtained by locally minimizing

$$\int_{\Omega_Y} w \left(\frac{\partial \underline{r}}{\partial X_1} \otimes \underline{e}_1 + \left(\frac{\partial \underline{r}}{\partial X_2} + \frac{\partial \underline{x}^1}{\partial Y_2} \right) \otimes \underline{e}_2 + \frac{\partial \underline{x}^1}{\partial Y_3} \otimes \underline{e}_3 \right) d\Omega$$

at each macroscopic point (X_1, X_2) on the set of local fields $\underline{x}^1(Y_2, Y_3)$ respecting the specified local boundary conditions.

The resulting global model developed in [6] and implemented in [4] is a 3D continuous body with fibers, the filling material in the far field being governed by a standard smooth large deformation elastic model, the reinforcing fibers behaving like a continuous distributions of beams, the global rubber and fiber motion being coupled by the boundary conditions at local scale, and the local energy of the rubber next to the fibers being given by the solution of the above local energy minimisation problem.

On this model, it is then necessary to properly handle the incompressibility constraints which requires a triple action :

- Impose pointwise incompressibility of the rubber inside each local problem which is achieved by using mixed finite elements with discontinuous pressures on local problem.

- Ensure the well posedness of the local problem. In particular, global deformations imposed at local scale must verify a volume preserving restriction.

- Avoid numerical locking at global scale due to the volume preserving restriction to be imposed at local scale and to the incompressibility of the rubber at far field.

The last two issues are resolved by weakly imposing the incompressibility of the finite element solution at global level (Q_2 displacements with P_1 discontinuous pressures), by using reduced invariants for the far field energy, and by using a least

square correction of the boundary conditions at local level in order to satisfy the volume preserving condition. This strategy can be proved to be consistent and convergent for linear problems by following the steps of [5].

The remaining question is to properly choose the reference thickness t in the local problem. This affects the construction of the homogeneized energy and the definition of the region where the far field energy is to be used. The challenge is to avoid a region which will be too thin and hence where the interface stresses will not be smooth enough while forbidding any zero energy mode in cross bending. The second order strategy proposed in [3] cannot be directly applied. A practical choice has been implemented in [4], but must be further justified.

This work was largely supported by M.F.P. Michelin

References

[1] M. Brun, O. Lopez-Pamies, and P.P. Castaneda, *Homogenization estimates for fiber-reinforced elastomers with periodic microstructures*, International Journal for Solids and Structures, **44**, (2007), 5953–5979.

[2] M. Bischoff, W.A Wall, Bletzinger K.U, and E. Ramm. *Models and finite elements for thin walled structures,* In Encyclopedia of Computational Mechanics, Editors : Stein, E. and de Borst, R. and Hughes T.J.R, (2004).

[3] V. G. Kouznetsova, M. G. D. Geers, W. A. M. Brekelmans, and Ek. *Multi-scale second-order computational homogenization of multi-phase materials: a nested finite element solution strategy.* Computer Methods in Applied Mechanics and Engineering, **193** (48-51) (2004) 5525–5550.

[4] P. Le Tallec, R. Boussetta and E. Lignon, *An enriched model of fiber reinforced thin flexible structures with in plane buckling capabilities*, International Journal of Numerical Methods in Engineering (2012), to appear.

[5] P. Le Tallec, A. Patra, *Nonoverlapping domain decomposition methods for adaptive hp approximations of the Stokes problem with discontinuous pressure fields*, Comp Meth. Appl. Mech. and Eng., **145**, (1997) 361–379.

[6] E. Lignon. Modélisation multiéchelle d'une nappe fibrée en compression. PhD thesis, Ecole Polytechnique, (2011).

Medius Error Analysis of Discontinuous Galerkin Methods: Estimates under Minimal Regularity

Thirupathi Gudi

(joint work with S.C. Brenner, S. Gu, M. Neilan, and L. Y. Sung)

The standard *a priori* error analysis of discontinuous Galerkin methods requires additional regularity on the solution of the elliptic boundary value problem in order to justify the Galerkin orthogonality and to handle the normal derivative on element interfaces that appear in the discrete energy norm. Medius error analysis of discontinuous Galerkin methods is developed using only the H^k weak formulation of a boundary value problem of order $2k$. This is accomplished by constructing a suitable enriching map that connects the discontinuous finite element space to a conforming finite element space, by replacing the Galerkin orthogonality with estimates borrowed from *a posteriori* error analysis and by using a discrete energy

norm that is well defined for functions in H^k. The results lead up to some higher order terms the best approximation property in the discrete energy norm [4].

References

[1] T. Gudi, *A New error analysis for discontinuous finite element methods for linear elliptic problems*, Math. Comp., **79** (2010), 2169-2189.

[2] S.C. Brenner, S. Gu, T. Gudi and L.Y. Sung, *A quadratic C^0 interior penalty method for fourth order boundary value problems with boundary conditions of the Cahn-Hilliard type*, Preprint.

[3] T. Gudi and M. Neilan, *An interior penalty method for a sixth-order elliptic equation*, IMA J. Numer. Anal., **31** (2011), 1734–1753.

[4] C. Carstensen, D. Peterseim and M. Schedensack, *Comparision results of three first-order finite element methods for the Poisson model problem*, Preprint.

S. C. Brenner, Department of Mathematics and Center for Computation and Technology, 216 Johnston Hall, Louisiana State University, Baton Rouge, LA 70803. email: brenner@math.lsu.edu

Shiyuan Gu, Department of Mathematics, Louisiana State University, Baton Rouge, LA 70803. email: gshy@math.lsu.edu

Thirupathi Gudi, Department of Mathematics, Indian Institute of Science, Banglaore, India 560012. email: gudi@math.iisc.ernet.in

Michael J. Neilan, Department of Mathematics, University of Pittsburgh, 605 Thackeray Hall, Pittsburgh, PA 15260. email: neilan@pitt.edu

Li-yeng Sung, Department of Mathematics, Louisiana State University, Baton Rouge, LA 70803. email: sung@math.lsu.edu

Reporter: Carsten Carstensen

Participants

Prof. Olivier Allix
L.M.T. Cachan
61 Avenue du President Wilson
F-94235 Cachan

Prof. Dr. Ferdinando Auricchio
Dipt. di Meccanica Strutturale
Universita di Pavia
Via Ferrata 1
I-27100 Pavia

Dr. Daniel Balzani
Fakultät für Ingenieurwissenschaften
Universität Duisburg-Essen
Universitätsstr. 15
45141 Essen

Prof. Dr. Yuri Bazilevs
Department of Structural Engineering
University of California, San Diego
9500 Gilman Drive
La Jolla , CA 92093-0085
USA

Prof. Dr. Pavel B. Bochev
Sandia National Laboratories
Computational Mathematics and
Algorithms Department
MS 1320, P.O.Box 5800
Albuquerque , NM 87185-0378
USA

Prof. Dr. Daniele Boffi
Dipartimento di Matematica
Universita di Pavia
Via Ferrata, 1
I-27100 Pavia

Prof. Dr. Dietrich Braess
Fakultät für Mathematik
Ruhr Universität Bochum
Universitätsstr. 150
44780 Bochum

Prof. Dr. Susanne C. Brenner
Department of Mathematics
Louisiana State University
Baton Rouge LA 70803-4918
USA

Prof. Dr. Zhiqiang Cai
Department of Mathematics
Purdue University
West Lafayette , IN 47907-1395
USA

Prof. Dr. Carsten Carstensen
Fachbereich Mathematik
Humboldt Universität Berlin
Unter den Linden 6
10099 Berlin

Prof. Dr. Ludovic Chamoin
L.M.T. Cachan
61 Avenue du President Wilson
F-94235 Cachan

Prof. Dr. Pedro Diez
Universitat Politecnica de
Catalunya (UPC)
Jordi Girona 1-3
E-08034 Barcelona

Prof. Dr. Ricardo Duran
Depto. de Matematica - FCEYN
Universidad de Buenos Aires
Ciudad Universitaria
Pabellon 1
Buenos Aires C 1428 EGA
ARGENTINA

PD Dr.-Ing. Bernhard Eidel
Institut für Mechanik
Universität Duisburg-Essen
Universitätsstraße 2
45117 Essen

Dietmar Gallistl
Fachbereich Mathematik
Humboldt Universität Berlin
Unter den Linden 6
10099 Berlin

Prof. Dr. Lucia Gastaldi
Dipartimento di Matematica
Universita di Brescia
Via Valotti, 9
I-25133 Brescia

Dipl.-Math. Joscha Gedicke
Fachbereich Mathematik
Humboldt Universität Berlin
Unter den Linden 6
10099 Berlin

Prof. Dr. Jay Gopalakrishnan
Department of Mathematical Sciences
Portland State University
P.O. Box 751
Portland , OR 97207-0751
USA

Dr. Pierre Gosselet
L.M.T. Cachan
61 Avenue du President Wilson
F-94235 Cachan

Prof. Dr. Thirupathi Gudi
Department of Mathematics
Indian Institute of Science
Bangalore 560 012
INDIA

Prof. Dr. Dr.h.c. Wolfgang Hackbusch
Max-Planck-Institut für Mathematik
in den Naturwissenschaften
Inselstr. 22 - 26
04103 Leipzig

Prof. Dr. Antonio Huerta
Universitat Politecnica de
Catalunya (UPC)
Jordi Girona 1-3
E-08034 Barcelona

Dr. Jun Hu
School of Mathematical Sciences
Peking University
100 871 Beijing
P.R.CHINA

Prof. Dr. Mi-Young Kim
Department of Mathematics
Inha University
Incheon 402-751
SOUTH KOREA

Prof. Dr. Joze Korelc
University of Ljubljana
Faculty of Civil and Geodetic Eng.
Jamova 2
Ljubljana
SLOVENIA

Prof. Dr. Pierre Ladeveze
L.M.T. Cachan
61 Avenue du President Wilson
F-94235 Cachan

Prof. Dr. Rajco D. Lazarov
Department of Mathematics
Texas A & M University
College Station , TX 77843-3368
USA

Prof. Dr. Patrick Le Tallec
Laboratoire Mecanique des Solides
Ecole Polytechnique
F-91128 Palaiseau Cedex

Dr. Adrien Leygue
Laboratoire de Mecanique et Materiaux
Ecole Centrale de Nantes
1 Rue de la Noe
F-44321 Nantes

Dr. Stefan Löhnert
Institut für Kontinuumsmechanik
Leibniz Universität Hannover
Appelstr. 11
30167 Hannover

Prof. Dr. Peter Monk
Department of Mathematical Sciences
University of Delaware
501 Ewing Hall
Newark , DE 19716-2553
USA

Dana Müller-Hoeppe
Institut für Kontinuumsmechanik
Leibniz Universität Hannover
Appelstr. 11
30167 Hannover

Prof. Dr. Neela Nataraj
Department of Mathematics
Indian Institute of Technology Bombay
Powai, Mumbai 400 076
INDIA

Prof. Dr. Michael Ortiz
Division of Engineering and
Applied Sciences, MS 104-44
California Institute of Technology
Pasadena , CA 91125
USA

Prof. Dr. Eun-Jae Park
Computational Sciences & Engineering-WCU
Yonsei University
Seoul 120-749
KOREA

Dr. Daniel Peterseim
Fachbereich Mathematik
Humboldt Universität Berlin
Unter den Linden 6
10099 Berlin

Prof. Dr. Paulo Pimenta
Department of Structural and
Geotechnical Engineering, Polytechnic
School at University of Sao Paulo
Av. Prof. Almeida Prado, trav. 2, 83
Sao Paulo SP 05508-900
BRAZIL

Dipl.-Math. Hella Rabus
Fachbereich Mathematik
Humboldt Universität Berlin
Unter den Linden 6
10099 Berlin

Prof. Dr. B. Daya Reddy
Department of Mathematics and
Applied Mathematics
University of Cape Town
7701 Rondebosch
SOUTH AFRICA

Prof. Dr.-Ing. Stefanie Reese
Institut für Angewandte Mechanik
RWTH Aachen
Mies-van-der-Rohe-Str. 1
52074 Aachen

Prof. Dr. Christian Rey
L.M.T. Cachan
61 Avenue du President Wilson
F-94235 Cachan

Mira Schedensack
Fachbereich Mathematik
Humboldt Universität Berlin
Unter den Linden 6
10099 Berlin

Prof. Dr. Joachim Schöberl
Institut für Analysis und
Scientific Computing
Technische Universität Wien
Wiedner Hauptstr. 8 - 10
A-1040 Wien

Prof. Dr. Jörg Schröder
Institut für Mechanik
Universität Duisburg-Essen
45117 Essen

Prof. Dr. Andreas Schröder
Fachbereich Mathematik
Humboldt Universität Berlin
Unter den Linden 6
10099 Berlin

Dr. Alexander Schwarz
Institut für Mechanik
Universität Duisburg-Essen
45117 Essen

Prof. Dr. Gerhard Starke
Institut für Angewandte Mathematik
Leibniz Universität Hannover
Welfengarten 1
30167 Hannover

Prof. Dr. Dr.h.c. Erwin Stein
Institut für Baumechanik und
Numerische Mechanik
Leibniz Universität Hannover
Appelstr. 9A
30167 Hannover

Prof. Dr. Li-yeng Sung
Department of Mathematics
Louisiana State University
Baton Rouge LA 70803-4918
USA

Prof. Dr. Robert L. Taylor
Structural Eng., Mech. and Material
Dept. of Civil and Environ. Eng.
Univ. of California, Berkeley
714 Davis Hall
Berkeley CA 94720-1710
USA

Dr. Alexander Veit
Institut für Mathematik
Universität Zürich
Winterthurerstr. 190
CH-8057 Zürich

Prof. Dr.-Ing. Wolfgang A. Wall
Lehrstuhl für Numerische Mechanik
Technische Universität München
Boltzmannstraße 15
85748 Garching bei München

Prof. Dr. Tim C. Warburton
Department of Mathematics
Rice University
6100 Main Street
Houston , TX 77005-1892
USA

Prof. Dr. Peter Wriggers
Institut für Kontinuumsmechanik
Leibniz Universität Hannover
Appelstr. 11
30167 Hannover